

Title	Design of Membrane Surface of Self-Assembled Vesicles for Selective Alkylation Reaction in Aqueous Media
Author(s)	岩崎, 文彦
Citation	大阪大学, 2017, 博士論文
Version Type	VoR
URL	<a href="https://doi.org/10.18910/61807">https://doi.org/10.18910/61807</a>
rights	
Note	

*Osaka University Knowledge Archive : OUKA*

<https://ir.library.osaka-u.ac.jp/>

Osaka University

**Design of Membrane Surface of Self-Assembled Vesicles  
for Selective Alkylation Reaction in Aqueous Media**

**Fumihiko Iwasaki**

**MARCH 2017**

**Design of Membrane Surface of Self-Assembled Vesicles  
for Selective Alkylation Reaction in Aqueous Media**

**A dissertation submitted to**

**THE GRADUATE SCHOOL OF ENGINEERING SCIENCE**

**OSAKA UNIVERSITY**

**in partial fulfillment of the requirements for the degree of**

**DOCTOR OF PHILOSOPHY IN ENGINEERING**

**BY**

**Fumihiko Iwasaki**

**MARCH 2017**

## PREFACE

This dissertation work was conducted under the supervision of Professor Hiroshi Umakoshi at Division of Chemical Engineering, Graduate School of Engineering Science, Osaka University from 2012 to 2017.

The objective of this thesis is to establish the methodology to design the vesicle membranes for the enhancement of the selective alkylation reaction carried out in the vesicle suspension in aqueous media. The partitioning behavior of the reactants, the interaction between vesicles and reactants, and the reaction model are investigated, especially focusing on the influence of the physicochemical properties of vesicles in order to clarify the key factors for high yield and high selectivity.

The author hopes that this research would contribute to the design of the vesicle membrane for the application of chemical reaction processes. The methodology established in this study is expected to contribute to the regulation of the chemical reaction processes at the hydrophobic-hydrophilic interface.

Fumihiko Iwawasaki

Division of Chemical Engineering  
Graduate School of Engineering Science  
Osaka University  
Toyonaka, Osaka, 560-8531, Japan

## Abstract

Self-assembly system can provide hydrophobic region at nano-scale in aqueous environment, which can be utilized for chemical reactions in aqueous media. It has been recently reported that the functions of recognition and regulation of bio-molecules can be controlled by the physicochemical properties of phospholipid vesicle membrane if the surface of the self-assembly system could be utilized as a platform of both functions. In this study, the effect of the vesicle membrane properties on the selective alkylation reaction was investigated in order to establish the design of vesicle membranes for the reaction with high yield and high selectivity.

In chapter 1, the micro-environments of lipid vesicles and partitioning behavior of the substrates were systematically characterized. The variations in the micro-membrane properties was found to lead to the regulation of the partitioning behaviors of substrates. After the partitioning of the substrates, the variation of the micro-membrane properties, especially the polarities, was observed suggesting that the dehydration of vesicle membranes occurred by the partitioning of hydrophobic molecules. Based on the results, the interaction model and the possible design of vesicles to regulate the partitioning of substrates were finally proposed.

In chapter 2, the 1,3-dipolar cycloaddition of BNO (benzonitrile oxide) and EMI (*N*-ethylmaleimide) in bulk system and self-assembly system was selected as a case study to model the chemical reaction on the different platforms. In the bulk system, the reaction rate linearly decreased with the increase of relative dielectric constant, while self-assembly system indicated maximum reaction rate at the certain value of relative dielectric constant. For the optimization of the self-assembly system, the regulation of the hydration environment around the substrates was found to be an important factor.

In chapter 3, the selective alkylation of the amino acid derivative was carried out. The racemic product was obtained in two-solvent system or micellar system, while the enantio-selective product was obtained with phospholipid vesicles. In addition, the same enantiomer was produced regardless of the chirality of phospholipid. Based on the results, the interaction mechanism to explain the enantioselectivity was finally proposed.

In chapter 4, the vesicles composed of non-natural (synthetic) surfactants was characterized in order to show more variety on the vesicle membrane properties. It was shown that the DDAB (dilauryldimethylammonium bromide) vesicle, DDAB vesicle could provide a polar environment as compared to the conventional phospholipid vesicles. By the modification of cholesterol, DDAB vesicle was found to represent the unique characteristics which could contribute to the design of platform for chemical reactions.

In chapter 5, the alkylation reaction employed in chapter 3 was performed by selecting DDAB vesicle membrane as the platform. By comparing to the reaction in micelle and phospholipid vesicle systems, the distribution ratio of reactants, conversion, and enantio-selectivity were strongly related to the environment which the self-assembly forms. From these findings, the important factors for the design of interface was clarified after the plausible reaction mechanism was proposed.

Based on the findings obtained in this study, the efficient and selective reaction enhanced by self-assembly system can be improved by the understanding of the interaction mechanism and reaction mechanism on the membrane surface, indicating the importance in the design of hydrophilic-hydrophobic interface of self-assembly systems

# Contents

<b>General Introduction</b>	1
<b>Chapter 1</b>	
<b>Variations in the Membrane Properties Induced by the Partitioning of Reaction Substrates</b>	
<b>1. Introduction</b>	13
<b>2. Materials and Methods</b>	16
<b>3. Results and Discussion</b>	
<b>3.1 Partitioning behaviors of BO and BNO onto liposome membranes</b>	19
<b>3.2 Variations of the polar environment of liposome membranes in the presence of substrates</b>	20
<b>3.3 Variations in the micro-viscosity of lipid vesicle membranes in the presence of substrates</b>	21
<b>4. Summary</b>	24
<b>Chapter 2</b>	
<b>Interfacial Reactions on the Surface of Model-Biomembrane Regulated by the Membrane Polarity</b>	
<b>1. Introduction</b>	25
<b>2. Materials and Methods</b>	28
<b>3. Results and Discussion</b>	
<b>3.1 Characterization of lipid vesicles by relative dielectric constant (<math>\epsilon'</math>)</b>	32
<b>3.2 Effect of lipid vesicles on 1,3-dipolarcycloaddition</b>	35
<b>3.3 Accumulation of BNO and EMI in lipid vesicle membranes</b>	37
<b>3.4 Estimation of the localization of reactants in lipid vesicle membranes</b>	38
<b>3.5 Estimation of the reaction rate constants occurring at the surface of lipid vesicles</b>	41
<b>4. Summary</b>	44

## **Chapter 3**

### **Enantioselective C-C Bond Formation Reaction with Model-Biomembrane**

<b>1. Introduction</b>	45
<b>2. Materials and Methods</b>	48
<b>3. Results and Discussion</b>	
<b>3.1 Alkylation of DMGBE with benzyl bromide in aqueous media</b>	51
<b>3.2 Reaction site at the membrane interface</b>	53
<b>3.3 Evaluation of the polar environment constructed on the membrane surface</b>	56
<b>3.4 Discussion for the enantioselective of the reaction mechanism in the presence of lipid vesicles</b>	58
<b>4. Summary</b>	61

## **Chapter 4**

### **Characterization and Evaluation of the Self-Assembly Systems Composed of Fully-Synthetic Amphiphiles**

<b>1. Introduction</b>	65
<b>2. Materials and Methods</b>	68
<b>3. Results and Discussion</b>	
<b>3.1 Formation of DDAB/cholesterol vesicles and the characterization by Laurdan</b>	71
<b>3.2 The interaction model of surfactants and additives</b>	76
<b>4. Summary</b>	81

## **Chapter 5**

### **Selective Alkylation Reaction with Vesicles Composed of Fully-Synthetic Surfactants and Comparison to Other Self-Assemblies**

<b>1. Introduction</b>	82
<b>2. Materials and Methods</b>	84
<b>3. Results and Discussion</b>	

<b>3.1 Evaluation of the alkylation reaction with DDAB and DDAB/cholesterol vesicles</b>	88
<b>3.2 The effects of the membrane polarities on the reaction system</b>	90
<b>3.3 Plausible reaction model of the reaction with DDAB vesicle and comparison to the reaction with phospholipid vesicles</b>	94
<b>4. Summary</b>	97
<b>General Conclusions</b>	99
<b>Suggestions for Future Works</b>	103
<b>Nomenclatures</b>	105
<b>List of Abbreviations</b>	106
<b>References</b>	108
<b>List of Publications</b>	121
<b>Acknowledgement</b>	123



## General Introduction

Our daily life has been improved together with the development of chemistry, where the organic synthesis has contributed to the production of new materials, such as pharmaceutical molecules, etc. Among the possible trends in the organic synthesis, the C-C bond formation reaction is fundamental and convenient technique for producing worthwhile molecules [Stephen *et al.*, 2000, Jia *et al.*, 2000, Frantz *et al.*, 2000]. In most of the organic synthesis processes, catalysts play a key role for achieving high yield and high selectivity of the desirable products [Demir *et al.*, 2002, Souillart *et al.*, 2014, Thankachan *et al.*, 2015]. Many catalysts and catalytic processes have been developed within a several decades, which showed the incredibly-high yield as compared to the stoichiometric reaction. One example of the most famous and high-impact catalytic process was developed in 1900s by Haber and Bosch; it is the well-known method to produce ammonium from nitrogen and hydrogen. There was a huge impact that this catalytic process allowed us to produce food from the air and water, which changed our life significantly. Other famous catalytic processes are also shown in **Table 1**. Other famous catalytic reactions developed in the 1950s, such as Ziegler-Natta Catalysis and

**Table 1** List of the examples of catalytic process

Catalytic Process	Catalyst	Reaction (Product)
Habor-Bosch process	Fe	$\text{N}_2 + 3\text{H}_2 \rightarrow 2\text{NH}_3$
Ziegler-Natta catalyst	$(\text{C}_2\text{H}_5)_3\text{Al-TiCl}_4$	Polymerization of olefins
Wacker oxidation	$\text{PdCl}_2, \text{CuCl}_2$	$2\text{C}_2\text{H}_4 + \text{O}_2 \rightarrow 2\text{CH}_3\text{CHO}$
Mizoroki-Heck reaction	$\text{Pd}^0$	modification of alkene
Negishi Coupling	R-Zn, Pd	C-C coupling
Suzuki-Miraura coupling	R-B, Pd	C-C coupling
Asymmetric synthesis	Rh-BINAP, etc.	(-)-menthol, etc.

Wacker Oxidation. These catalytic processes were effective on the industrial application that large amount and high yield of the production was achieved. The further developments of these catalytic process were followed by other scientists around 1980s and still improved. At the same time, the effective C-C coupling reaction processes were developed in order to solve the demand of fine chemicals. The catalyst composed of palladium, rhodium, or ruthenium showed the positive effect on the formation of C-C bonds. These processes are still used in these days to improve our daily life. In addition, to produce more complex molecules such as pharmaceutical materials, the catalysts for asymmetric synthesis have been developed. One of the most famous catalysts for asymmetric synthesis is BINAP catalysts, which compose 2,2'-bis(diphenylphosphino)-1,1'-binaphthyl structure. The example of this process is the production of (-)-menthol by Rh-BINAP catalyst. The asymmetric synthesis processes utilizing BINAP catalysts are still used and developed in these days to produce new materials which makes our daily life better.

As a part of the “Green Chemistry”, not only the catalytic reactions but also the whole reaction process including the recovery of the product should be concerned. Recently, “flow fine synthesis” has been developed so that the separation of the products from catalysts becomes easier, which indicates less energy would be required as a whole reaction process [Kirshning *et al.*, 2006, Soldi *et al.*, 2008, Kobayashi, 2016]. Considering the separation process, the polar organic solvents, such as dimethylsulfoxide and dimethylformamide, have a disadvantage in the recovery of the reaction products due to their high boiling points. More energy might be required for the separation (evaporation), and even after the separation, polar organic solvents are not environmentally-friendly that the additional energy and process would be necessary to dispose appropriately. However, these polar organic solvents were used in the conventional organic synthesis due to its ability of the solvation of many reactants. Nonpolar organic solvents with lower boiling points, e.g., hexane and toluene, could not enhance the organic synthesis because one of the reactants is usually water-soluble while another is water-insoluble. To avoid

the use of polar organic solvents as reaction media, phase transfer catalysis (PTC) has been proposed (**Table 2, Fig. 1**). PTC reaction involves aqueous phase (usually alkali aqueous solution) and organic phase (organic solvent with lower boiling points), so that both of water-soluble and water-insoluble reactants can be dissolved in the system. Phase transfer catalysts can work at the hydrophilic-hydrophobic interface, wherein PTC transports water-soluble reactants to organic phase to promote the reaction. In addition, PTC can be designed to restrict the interaction with reactant (or reaction intermediate): as an example, Maruoka catalyst has been developed to bind Si-face of DMGBE intermediate, then it can promote the enantioselective alkylation [Kitamura *et al.*, 2005]. Conventionally, metal catalyst and inorganic

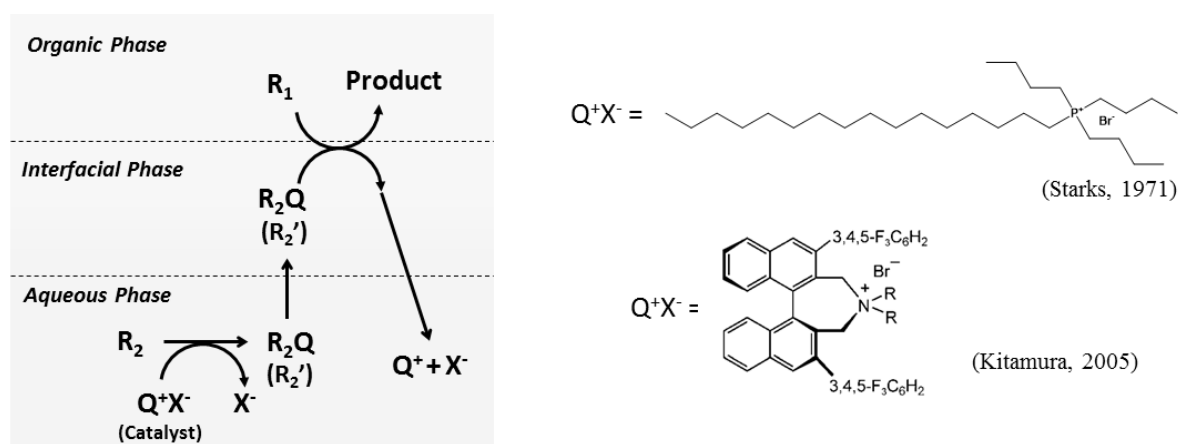


**Figure 1** Graphical Scheme of phase transfer catalysis (PTC)

**Table 2** List of heavy metal-free catalyst systems

Reference	Catalyst	Reaction (Product)
Starks 1971	quaternary phosphine	hydrolysis
O'Donnell <i>et al.</i> 2004	cinchona alkaloid	amino acid derivatives
Maruoka <i>et al.</i> 2005	BINAP-PTC	amino acid derivatives
List <i>et al.</i> 2000	L-Proline	Aldol reaction
Najera <i>et al.</i> 2005	L-Pro derivative	cycloaddition
Jousseau <i>et al.</i> 2011	NHC (carbene)	amino acid derivatives

catalyst have been utilized for stereoselective organic synthesis. However, heavy metals, such as Rhodium, Ruthenium, etc., are harmful materials to our body, they must be removed completely from the products especially foods or medicines. In contrast, organic catalysts including phase transfer catalysts have an advantage in the viewpoint of Green Chemistry, and they have been utilized. Phase transfer catalysts are examples of organic catalysts. Starks have reported that quaternary ammonium or quaternary phosphate group can work as a catalytic center to some reactions, and they can be utilized them as phase transfer catalysts. Maruoka *et al.* have reported quinine and other molecules which contain quaternary ammonium moiety as PTC. Other scientists have reported that L-proline and its derivatives can work as organic catalysts, and they also achieved with high yield and high enantioselectivity for enantioselective aldol reaction and Michael addition. For example, List *et al.* have reported that L-proline could be used to catalyze the aldol reaction, and Najera *et al.* represented L-pro derivatives still showed the high activity as a catalyst [List *et al.*, 2009, Najera *et al.*, 2005].

Despite an advantage of heavy metal-free process, the above-mentioned reaction systems still require organic solvent as media. It has recently reported that some organic synthesis processes could avoid from the use of any organic solvents while they could use only water as a reaction medium. Water is the most ideal solvent as a reaction medium from a viewpoint of environmental load. Water is quite stable, non-flammable, and environmentally-friendly. However, to utilize water as a reaction medium, there are still some problems: one

**Table 3** List of organic synthesis conducted in water

Reference	Catalyst	Reaction (Product)
Kokubo <i>et al.</i> 2008	Sc (Lewis acid)	hydroxy methylation
Li <i>et al.</i> 2012	Rh within micelles	chiral reduction of ketone
Hayashi <i>et al.</i> 2006	L-Pro derivative	aldol reaction
Mase <i>et al.</i> 2009	L-Pro derivative	chiral aldol reaction
Pan <i>et al.</i> 2014	PEG-supported aminoalcohol	chiral Michael addition

problem is that the reactants for organic synthesis are usually water-insoluble, and even if reactants can be dissolved in aqueous medium, the reactivity is low in highly polar environment most of the time. The catalytic reaction would be the solution for the low reactivity, but conventional metal catalyst cannot show the effective enhancement in water because of the deformation of the catalysts by hydrolysis. Although the adversities of the organic synthesis in aqueous media, some catalysts which can act effectively in water were developed recently (**Table 3**). Kokubo *et al.* have reported that the Lewis-acid can be utilized for the effective reaction in the aqueous media [Kokubo *et al.*, 2008]. Li *et al.* have shown the possibility of using metal catalysis in aqueous media by modifying the catalyst to be amphiphilic [Li *et al.*, 2012]. Some of the organic catalysts (L-proline derivatives) have also shown its possibility to be used in water and still achieved reasonable yield and selectivity [Hayashi *et al.*, 2006]. The reaction in water have developed recently, so further improvements are expected to be studied by many scientists.

From another point of view, most of chemical synthesis in biological systems are conducted in water. In the biological system (e.g., inside the biological cell), many chemical reactions are achieved in aqueous media, which are usually catalyzed by enzyme. Enzymes and the substrates are often referred as “lock” and “key” that a certain enzyme can interact with only one substrate, which leads to the extremely high selectivity of the substrate and product, even in a crowding condition in cell. Enzymes could also be utilized for organic synthesis

**Table 4** List of organic synthesis in biological systems

Reference	Catalyst	Reaction (Product)
Hirose <i>et al.</i> 1995	Lipase AH, PS	Enantioselective hydrolysis
Glueck <i>et al.</i> 2005	<i>Lactobacillus</i>	Deracemization
Keinan <i>et al.</i> 1986	Alcohol dehydrogenase	Reduction of ketones
Kawano <i>et al.</i> 2003	Microbe ( <i>Candida maris</i> )	Chiral pyridineethanol
Wang <i>et al.</i> 2012	DNA-based catalyst	Diels-Alder Reaction

process outside of our body (**Table 4**). For example, Kawano *et al.* have reported that the enantioselective reaction could be conducted by using certain type of cells [Kawano *et al.*, 2003]. The usefulness of enzymes was shown as the materials which represent the similar properties as enzymes. These “artificial enzymes” were studied and started to be reported from around 1970 by many scientists [Breslow *et al.*, 1970, Makino *et al.*, 1972] (**Fig. 2**). Breslow *et al.* reported that the reaction rate increased significantly by combining the metal catalytic center and hydrophobic moieties around catalytic center. The reports about artificial enzymes were published continuously and showed their advantages to be used in the chemical processes. For example, de Vries *et al.* reported the artificial enzyme synthesized by the modification of papain to achieve asymmetric hydrogenation [de Vries *et al.*, 2006]. Breslow represented his continuous research on the methodologies to design the catalytic center and the cavity of artificial enzymes [Breslow, 1995]. Lin *et al.* introduced the Au-nanoparticle supported catalyst which showed the enzymatic activity that the cascade reaction, oxidations of glucose and 3,3,5,5-tetramethylbenzidine at the same time, were achieved [Lin *et al.*, 2013]. Some scientists have prepared the artificial catalysts by the self-assembly of complex molecules such as dendrimers and supramolecular encapsulated catalyst assembly [Marlau *et al.*, 2001, Kofoed *et al.*, 2005, Darbre *et al.*, 2006]. Since enzymes have complex structures, the design of artificial

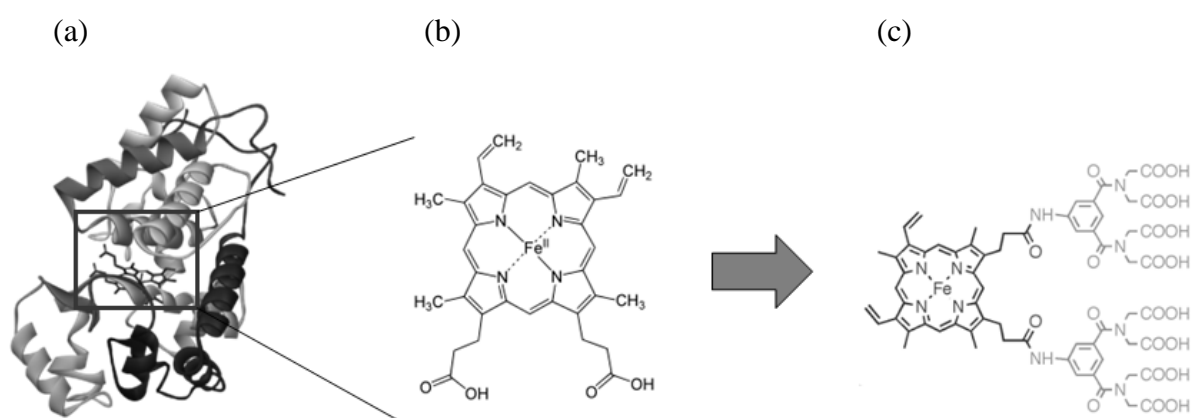


**Figure 2** (a) Illustration of the enzyme (peroxidase), (b) catalytic center of peroxidase, (c) one example of catalytic center of artificial enzyme [Hayashi *et al.*, 2002]

enzymes was also approached by the computational experiments [Nanda *et al.*, 2010]. In addition to the enzymatic reactions, some of organic reactions (*e.g.*, Michael addition reaction, Diels-Alder reaction, and so on) have been reported to happen in biological systems. Wherein, a hydrophobic environment, such as the lipid membrane surface, would provide a reaction site at which less polar compounds can be localized. It is suggested that the biologically happened environment could be utilized as a functional platform to achieve organic synthesis.

Inspired from biological membranes, the nano-ordered self-assembly systems including micelles, vesicles can be formed. They have also attracted much attention as a reaction platform (**Fig. 3, Table 5**). Nano-ordered self-assemblies are generated from the amphiphilic molecules by noncovalent interactions such as hydrophobic interaction (van der Waals interaction).

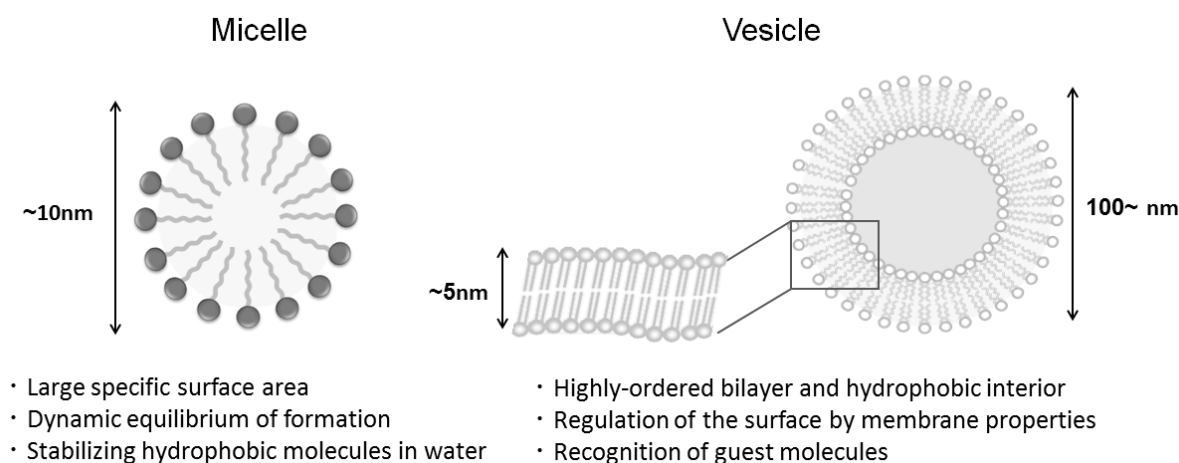


**Figure 3** Illustration of micelle and vesicle about specific features

**Table 5** List of self-assembly assisted organic synthesis

Reference	Catalyst	Reaction (Product)
Hamasaka <i>et al.</i> , 2014	Pd within vesicles	Cyclization
Kunishima <i>et al.</i> , 2005	Micelle with fatty acid salts	Dehydrocondensation
Kumar <i>et al.</i> , 2013	SDS micelle	Mannich reaction
Wang <i>et al.</i> , 2016	Polymer micelle	H <sub>2</sub> production
Manabe <i>et al.</i> , 2002	o/w emulsion formed by DBSA	Dehydration

Therefore, hydrophobic substrates are able to be dispersed in the aqueous media by the help of self-assembly systems. Engberts *et al.* have studied about the effect of the environment which self-assembly systems can form on Diels-Alder and Diels-Alder-like reactions [Engberts *et al.*, 2006]. Kunishima *et al.* employed the enrichment effect of substrates by the interaction between micelles and substrates to improve the reactivity [Kunishima *et al.*, 2005]. Self-assembly system can represent additional effects; Manabe *et al.* have reported that the dehydration can be achieved in the interior of oil-in-water emulsion that the water produced by the dehydration reaction would be excluded to outside of the O/W emulsion, so that the reaction equilibrium shifted to the product [Manabe *et al.*, 2002]. Some catalytic reactions also proceeded with self-assembly system. Hamasaka *et al.* have reported the catalyst which could form vesicle can work in water and enantioselective reaction was achieved [Hamasaka *et al.*, 2014]. Junker *et al.* have reported the formation of polyaniline by enzymatic reaction utilizing vesicle as a template [Junker *et al.*, 2014]. The interfacial reaction utilizing the interface of self-assembly system is showing the possibility to be utilized as a platform for the new chemical reaction process, although the mechanisms and parameters to be widely used were not clarified yet.

The reaction system with high yield and selectivity should include three essential factors: (i) catalytic center – where governs the conversion reaction, (ii) ordered structure around the catalytic center – where governs the selectivity of the reaction, and (iii) the reaction environment – where affect the solvation of the reactants and catalysts. For example, the enzymes possess the metal complex as a catalytic center which can be used as a powerful tool to enhance the reaction. The ordered structure formed by polypeptide surrounding the catalytic center of enzymes is unique and highly ordered that only one substrate can be recognized by a certain type of enzyme. Since enzymatic reactions are highly selective and effective, the reaction environment is selected not to denature the enzymes. These three factors are also key to the effective reaction utilizing the self-assembly system as a platform. The head group of amphiphiles (component of self-assembly system) such as quaternary ammonium moieties can



work as a reaction center. The regulation of the membrane properties can lead to the regulation of the (ii) ordered structure around the catalytic center and (iii) reaction environment. Therefore, it is important to regulate the physicochemical properties of the self-assembly system and clarify the relationship between membrane properties and the reactivity.

The final purpose of this thesis is to reveal the mechanism of selective chemical reactions and clarify the important parameters for the reactions, especially at the hydrophilic-hydrophobic interface of the self-assembly. The catalytic reactions (including PTC) usually require organic solvents, strong acid/base, or metals but show very high yield and high selectivity. To achieve the high yield and high selectivity in water, the physicochemical properties of the self-assembly systems should be regulated in detail as mentioned in former paragraph. The framework and flow chart of the present study are schematically shown in **Figure 4** and **5**, respectively.

In chapter 1, the physicochemical properties of model-biomembrane (natural lipid vesicles) were investigated by fluorescent probe method. The partitioning behavior of reaction substrate (benzonitrile oxide; BNO) and the precursor (benzaldoxime; BO) onto lipid vesicles were analyzed. By the distribution of these substrates, the micro-environment (micro-polarity, micro-viscosity, etc.) inside the lipid vesicles were varied, and interaction between vesicles and substrates were discussed.

In chapter 2, the interfacial reaction at the hydrophilic-hydrophobic interface of lipid vesicles was investigated. As a model case, 1,3-dipolar cycloaddition of BNO and EMI (*N*-ethylmaleimide) was carried out in water/dioxane system, micellar system, and lipid vesicular systems with the variation of relative dielectric constant  $\epsilon$ . Based on the partitioning behavior discussed in chapter 1, the reaction was considered to proceed in water and at the interface in parallel to investigate the reaction more deeply. This analysis could lead to the plausible reaction model in the lipid vesicle suspension, and represented the possible design of hydrophilic-hydrophobic interface to be used as a platform for chemical reaction.

In chapter 3, another reaction system which requires the enantioselectivity was carried out in water-dichloromethane system, CTAB micellar system, and lipid vesicular systems. Based on the reaction behavior, the highly-ordered interface which vesicle forms was required for the enantioselective reaction, and the possible interaction model to produce the one type of enantiomer was proposed. The strategy to design the vesicle membrane surface as a platform for the reaction was also discussed based on the results obtained in chapter 1 through chapter 3, showing that the membrane properties of the self-assemblies and the variations in membrane properties by the addition of the substrates are important factors on the reaction carried out at the surface of the self-assembly system.

In chapter 4, non-natural surfactant were used to prepare vesicles in order to make more variations in physicochemical properties of hydrophilic-hydrophobic interface of vesicles. Cationic surfactant, DDAB (dilauryldimethylammonium bromide), and anionic surfactant, AOT (sodium bis(2-ethylhexyl) sulfosuccinate), were employed, and vesicles composed of these surfactants were analysed. The variation in the physicochemical properties of these surfactant vesicles by the addition of modifier such as cholesterol was investigated and compared to that of phospholipid vesicles.

In chapter 5, the enantioselective alkylation discussed in chapter 3 was carried out with cationic surfactant vesicle. Finally, the effect of self-assembly system on the chemical reaction was discussed by the comparison of self-assemblies with the variations in the physicochemical properties. Based on the results obtained, the interaction model of the reaction was also compared to each other, and the regulation of the reaction by focusing on the physicochemical properties of hydrophilic-hydrophobic interface was proposed.

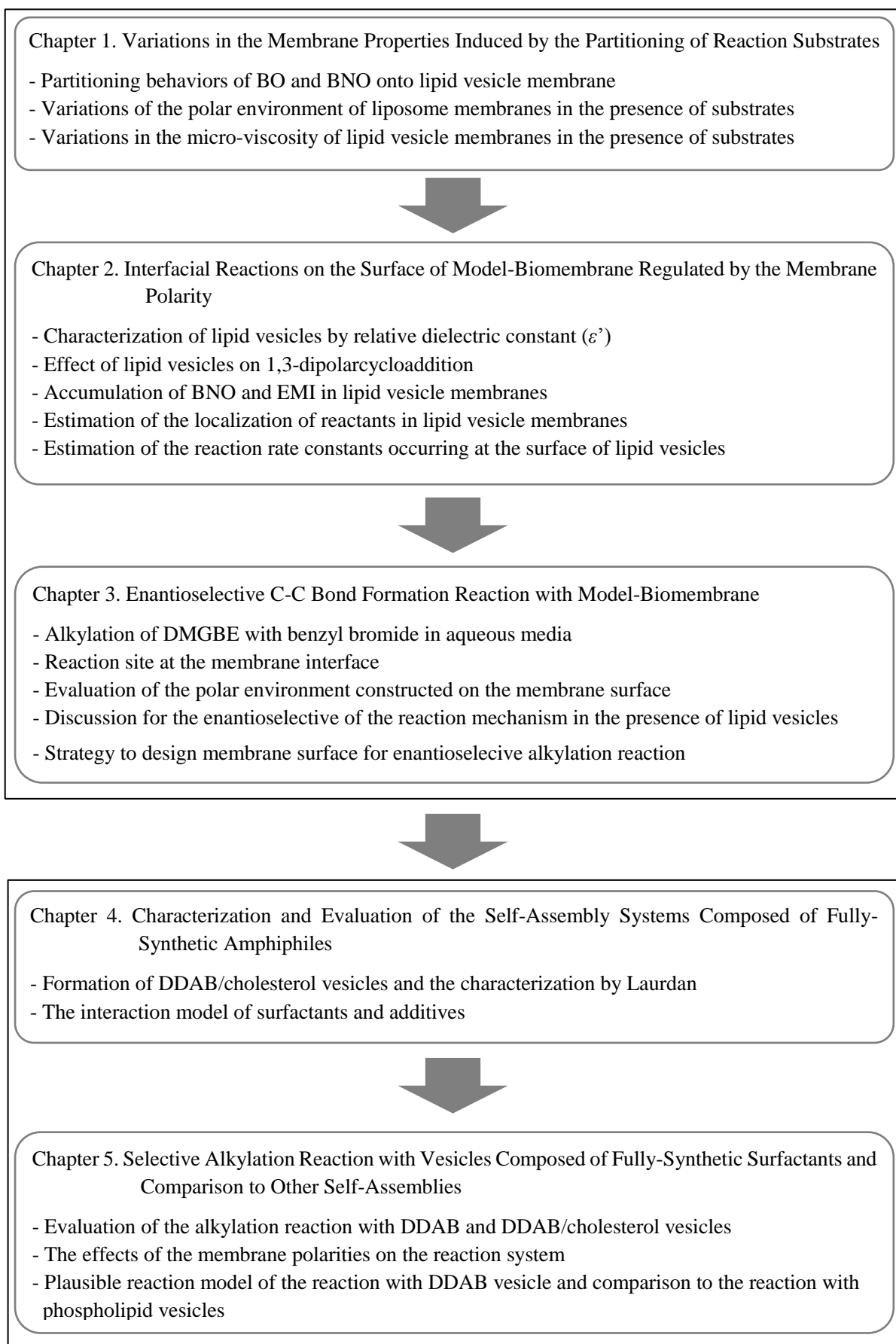


**Figure 4** Framework of the present study



# Chapter 1

## Variations in the Membrane Properties Induced by the Partitioning of Reaction Substrates

### 1. Introduction

Partitioning behaviors of the substrates are the very important factor in extraction, chromatography, and interfacial reaction processes comprising two or more phases in one system. The partitioning behaviors can be varied by the following factors: (i) chemical properties and structure of the target molecules, (ii) physicochemical properties of the surrounding environment (solvent), and (iii) properties of the interface formed between the multiple phases. In the simple extraction in liquid-liquid system, the factors (i), (ii), and the (physico)chemical properties of the solute and the solvent, are dominant factors. For example, the extraction of RNA by using two-solvent system have been reported [Chomczynski *et al.*, 1987]. The extraction behavior of a chemical is expectable based on the hydrophobicity (Log  $P$  value) of the target molecule. In addition, the polarity (relative dielectric constant  $\epsilon$ ) can predict the approximate distribution ratio of the target chemical. On the other hand, the extraction process including amphiphilic molecules, such as the extraction systems with micelle and reverse micelle, requires the design of the physicochemical properties of the interface. These processes can separate substrates beyond the simple properties such as Log  $P$  and  $\epsilon$ , which is necessary for effective extraction. Pires *et al.* and other scientists reported that the liquid-liquid extraction of proteins could be enhanced by utilizing reversal micelles [Pires *et al.*, 1996, Krei *et al.*, 1992, Ruiz *et al.*, 2007]. However, the property design of the interface has not fully revealed the extraction behaviors of molecules, thereby each extraction system has been

practically designed and applied in chemical process. Further investigation would be required to reveal the mechanism of interfacial partitioning behaviors.

The concept of extraction is applied to the chemical reaction occurring at the interface of two solvents. For example, Phase Transfer Catalysis (PTC) contains the catalysts which can act at the interface of aqueous and organic solvent, and achieves high yield in the reaction of water-soluble reactant and water-insoluble reactant (Fig. 1 in General Introduction) [Kitamura *et al.*, 2005, *etc.*]. Finally, PTC migrates the reactant into organic phase, where another reactant exists. PTC have shown its effectiveness for more environmentally-friendly process and high yield, wherein the reactions are considered to occur at the interface. The physicochemical properties such as polarity and viscosity of the interface are important rather than those of each solvent to regulate the reaction, nevertheless the properties of the interface is unclear. The achievement of the high yield is strongly dependent on the design of the catalysts. The problem of being dependent on the highly designed catalysts is that the producing catalysts requires many steps of synthesis, which requires a lot of costs and produces many by-products. Instead, by regulating the properties of the interface, the catalysts could be more simple.

As compared to the interface of liquid-liquid two phase, the self-assembly interface can be designable and tunable. In recent years, there have been some reports about the extraction/distribution process with liposome suspension [Tang *et al.*, 2013, Okamoto *et al.*, 2016]. Liposome also represents the hydrophilic-hydrophobic interface in aqueous phase. The greatest advantage of the liposomal system is that the hydrophilic-hydrophobic interface can be varied by changing its membrane properties such as phase state and fluidity. The adsorption of amino acids and proteins onto various liposome membranes have been reported [Litt *et al.*, 2009, Ishigami *et al.*, 2015], and the differences were discussed. The liposome membrane has also been used for the regulation of biological molecules such as RNAs [Suga *et al.* 2011, Tuan *et al.*, 2008]. Now, liposome is expected to be used as a platform for the regulation of non-biological molecules and processes.

There are some chemical reactions that are conducted at hydrophobic-hydrophilic interfaces. The cycloaddition reaction of benzonitrile oxide and ethylmaleimide is a type of Diels-Alder reaction [Rispens, *et al.*, 2003], which is conducted by the contact of each reactant. BNO is less soluble to water while EMI is water soluble. By using self-assembly interfaces, the reaction of BNO and EMI is expected to be improved. Therefore, the characteristics of the self-assembly interface and its effect on the molecular partitioning behavior should be clarified.

In this chapter, the partitioning behavior of non-biological molecules onto liposome membrane was investigated, expecting to utilize liposome membrane as a platform for the chemical reaction (**Fig.1-1**). The various liposomes which show different characteristics in membrane polarity, membrane fluidity, and surface charge were prepared to reveal the appropriate physicochemical properties of hydrophilic-hydrophobic interface for the distribution of the molecules. In addition, the variations in the micro-environment inside of the liposome membrane before and after the addition of partitioning molecules were analysed to achieve further regulation of the interface between bulk and liposome membrane.

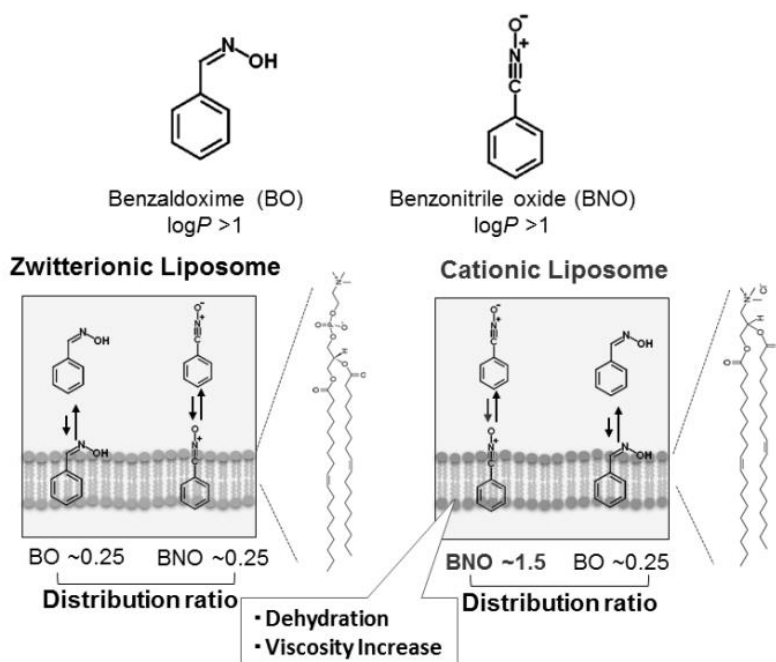


**Figure 1-1** Schematic illustration of the study in this chapter.

## **2. Materials and Methods**

### **2.1 Materials.**

1,2-Dioleoyl-*sn*-glycero-3-phosphocholine (DOPC) and 1,2-dioleoyl-3-trimethylammonium-propane (DOTAP) were purchased from Avanti Polar Lipids, Inc. (Alabaster, AL, USA). Benzaldoxime (BO), 1,6-diphenyl-1,3,5-hexatrien (DPH) and 6-lauroyl-2-dimethylaminonaphthalene (Laurdan) were purchased from Sigma-Aldrich (St. Louis, MO, USA). Other chemicals were purchased from Wako Pure Chemical (Osaka, Japan) and were used without further purification.

The benzonitrile oxide (BNO) was prepared as the following [Rispen *et al.*, 2003]: 21.6  $\mu$ L of benzaldehyde oxime was dissolved in the 2 mL of NaClO(aq)/1-propanol solution (50:50). 0.36 g of NaCl was added to this solution to separate it to two phases. After the upper phase was taken and diluted by 1-propanol, 25 mM benzonitrile oxide solution was obtained. The formation of BNO was determined by UV-vis spectroscopy (UV-1800; Shimadzu, Kyoto, Japan), where the conversion of BO was >85 %. The obtained solution was used as the BNO solution. The prepared BNO solution was stable for at least 3 h, and the experiments were performed soon after the BNO was prepared.

### **2.2 Preparation of Liposomes.**

A solution of lipids in chloroform was dried in a round-bottom flask by rotary evaporation under vacuum. The obtained lipid thin film was kept under high vacuum for at least 3 h, and then hydrated with distilled water at room temperature. The obtained liposome suspension was frozen at -80 °C and then thawed at 50 °C; this freeze-thaw cycle was repeated 5 times. A large unilamellar vesicle was obtained by extruding the vesicle suspension 11 times through 2 layers of a polycarbonate membrane with a mean pore diameter of 100 nm using an extruding device (Liposofast; Avestin Inc., Ottawa, Canada).



### 2.3 Adsorption of reactants onto liposome.

The distribution ratios ( $D$ ) of the substrates in the liposome membranes were evaluated by using the ultrafiltration method. Each substrate was incubated with the liposome solution for 30 min at room temperature, and the liposome and substrates distributed in the membrane were removed with the ultrafiltration unit USY-5 (molecular weight cutoff: 50,000, Advantec Toyo, Ltd., Tokyo, Japan). The distribution ratios of substrates on the filtration membranes were lower than 0.05, and the fraction of each substrate was calculated with the corrected concentration of the substrates. The  $D$  values of the substrates were calculated as follows:

$$D = C_m / C_w$$

where  $C_m$  and  $C_w$  are the concentrations of the substrate in the membrane and in the water solution, respectively. The concentration of the reactant in the eluted solution was measured by UV-vis spectroscopy.

### 2.4 Evaluation of membrane polarities.

The fluorescence spectra of Laurdan and DPH were measured by using a fluorescence spectrophotometer (FP-8500; Jasco, Tokyo, Japan). The excitation wavelength of Laurdan was 340 nm, measured with a 10 mm path length quartz cell. The fluorescence intensity of Laurdan was normalized with the spectrum of each liposome without substrates. The fluorescence anisotropy ( $r$ ) of DPH was calculated based on the previous report. A fluorescent probe DPH was added to the liposome suspension with a molar ratio of lipid/DPH of 250/1; the final concentrations of lipid and DPH were 100 and 0.4  $\mu\text{M}$ , respectively. The fluorescence polarization of DPH (Ex = 360 nm, Em = 430 nm) was measured after incubation at room temperature for 30 min. The sample was excited with vertically polarized light (360 nm), and emission intensities both perpendicular ( $I_{\perp}$ ) and parallel ( $I_{\parallel}$ ) to the excited light were recorded at 430 nm. The anisotropy ( $r$ ) of DPH was then calculated using the following equations [Kepczynski *et al.*, 2011]:

$$r = (I_{\parallel} - GI_{\perp}) / (I_{\parallel} + 2GI_{\perp}) \quad (2)$$

$$G = i_{\perp} / i_{\parallel} \quad (3)$$

where  $i_{\perp}$  and  $i_{\parallel}$  are the emission intensities, perpendicular and parallel to the horizontally polarized light, respectively, and  $G$  is the correction factor. Based on the previous report [Kepczynski *et al.*, 2011], the micro-viscosity ( $\eta_{\text{DPH}}$ ) was calculated using the following equation:

$$\eta_{\text{DPH}} = 2.4r / (0.362 - r) \quad (4)$$

The  $\eta_{\text{DPH}}$  values of the oleic acid vesicles in the literature [Kepczynski *et al.*, 2011] and in our study were 59 cP and 39 cP, respectively, indicating that this method could estimate the micro-viscosity of lipid membranes.

### 3. Results and Discussion

#### 3.1 Partitioning behaviors of BO and BNO onto liposome membranes

The  $\log P$  values of BO and BNO were calculated via both computational and experimental methods (**Table 1-1**). The results indicated that BO and BNO were hydrophobic, implying that they can be accumulated in the hydrophobic regions of liposome membranes. **Figure 1-2** shows the distribution ratios ( $D$ ) of BO and BNO onto DOPC and DOTAP liposomes. In the case of the DOPC liposome, the  $D$  values of BO and BNO were almost the same (Figure 2(a)), suggesting that the partitioning of hydrophobic molecules onto the zwitterionic liposome could be driven by hydrophobic interaction. In contrast, the  $D$  values of BNO onto the cationic DOTAP liposome were higher than those of BO (**Figure 1-2(b)**). Despite the difference in the

**Table 1-1**  $\log P$  values of BO and BNO.

	$Mw$	$\log P_{cal}^{*1}$	$\log P_{cal}^{*2}$	$\log P_{ex}^{*3}$
BO	121.14	1.9	1.91	1.29
BNO	119.12	1.1	1.82	>1

\*<sup>1</sup> Referred by PubChem database: <http://pubchem.ncbi.nlm.nih.gov/> \*<sup>2</sup> Referred by ChemSpider database: <http://www.chemspider.com/> \*<sup>3</sup> Determined by partitioning coefficient in water/1-octanol two-phase system.

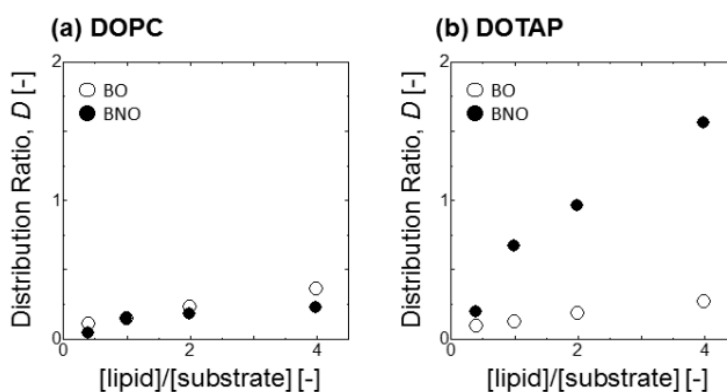


**Figure 1-2.** Distribution ratios of BO (open circle) and BNO (closed circle) in liposomes. BO or BNO (250  $\mu M$ ) was incubated with the liposome solution at room temperature, and the distributed substrates were separated by ultra-filtration.

partitioning behaviors in liposome membrane systems, the partitioning behaviors of BO and BNO in liquid-liquid two phase systems (i.e. water/1-octanol system) were not significantly different (**Table 1-1**). It was therefore found that the DOTAP liposome could accumulate BNO, suggesting that there exists multiple interactive forces, i.e. hydrophobic and electrostatic interaction. Because BNO is one of the substrates in 1,3-dipolar cycloaddition reactions [Engberts *et al.*, 2002, Rispens *et al.*, 2003], it is expected that the DOTAP liposome membrane surface can be utilized as a platform for the 1,3-dipolar cycloaddition reaction. It has been reported that the interaction between liposomes and target molecules can induce the dehydration of the membrane surfaces. The solvent polarity and viscosity are key factors in regulating the yield and stereoselectivity in the Diels-Alder reaction [Rispens *et al.*, 2005]. It is therefore important to investigate the microscopic polarity and viscosity of the liposome membranes with the localization of hydrophobic molecules.

### **3.2 Variation of the polar environment of liposome membranes in the presence of substrates**

It has been previously reported that the micro-polarity of the liposome membrane surface can be monitored by Laurdan [Parasassi *et al.*, 1991, Suga *et al.*, 2013]. The fluorescent probe Laurdan, embedded in the hydrophilic- hydrophobic interface region of liposome membranes, is sensitive to the polarity around itself, which reflects the surface polarity of lipid membranes to be determined. In liposome membranes, Laurdan shows a peak at around 440 nm in the gel phase (ordered phase), where the lipid molecules are tightly-packed in membranes. On the other hand, Laurdan shows a peak at around 490 nm in the fluid phase (disordered phase), where the lipid molecules laterally diffuse in the membranes. The fluorescence spectra of Laurdan in the presence of BO and BNO were investigated (**Figure 1-3**). By adding BNO, a decrease of fluorescence intensity and a blue-shifted peak around 440 nm were observed. In our previous report, the blue-shifted peak was evidence of the “ordered” phase, and such ordered phases are

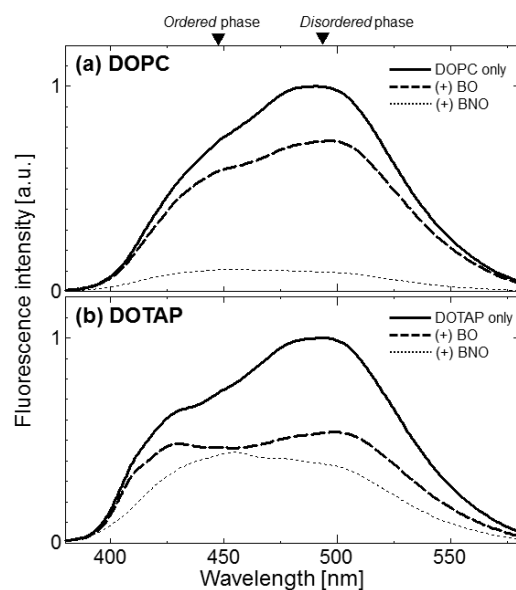


**Figure 1-3.** Fluorescence spectra of Laurdan in liposomes. (a) DOPC, and (b) DOTAP. Lines indicate in the absence of substrates (*bold line*), in the presence of BO (*dashed line*), and BNO (*dotted line*). The total concentrations of the lipid, Laurdan, and the substrate were 0.5 mM, 20  $\mu$ M, and 5 mM, respectively.

dehydrated, as compared with disordered phases. The blue-shifted peak was also observed in the presence of the anionic polynucleotides [Suga *et al.* 2013]. This indicates that the liposome membrane surface is dehydrated in the presence of BNO. The fluidity (viscosity) of liposome membranes also relates to the variations in the Laurdan spectra. In addition, the viscosity of the solvent is one of the factors that affect the behavior of fluorescent probes. Our results suggest that the micro-viscosity of the liposome membrane can vary with the localization of BNO [Uchiyama *et al.*, 2003, Shiraishi *et al.*, 2010, Stsiapura *et al.*, 2008].

### 3.3 Variations in the micro-viscosity of liposome membranes in the presence of substrates

The micro-viscosity of the self-assembly systems has been studied by using fluorescent probes: the C<sub>12</sub>TAB micelle, 11.9 cP [Pramanik *et al.*, 2000]; the polymer assembly 30-70 cP [Shiraishi *et al.*, 2010]; the oleic acid vesicle, 59 cP [Kepczynski *et al.*, 2011]. The micro-

viscosities ( $\eta_{DPH}$ ) of the liposome membranes could be evaluated by using DPH. **Figure 1-4** shows the  $\eta_{DPH}$  values of the liposomes in the presence of BO and BNO. The  $\eta_{DPH}$  values of DOPC and DOTAP liposomes were 64.7 cP and 48.4 cP, respectively. It was found that the DOPC and DOTAP liposomes, in disordered phases, showed the lower micro-viscosities, while the liposomes in ordered phases showed much higher micro-viscosities: DPPC, 783 cP (26.1 °C); DOPC/cholesterol=1:1, 177 cP (26.1 °C); DODAB vesicles, 805 cP [Kepczynski *et al.*, 2011]. It is therefore suggested that the micro-viscosity of the liposome is relating to its phase state. In the presence of BNO, the  $\eta_{DPH}$  values of the DOTAP liposomes increased, on the other hand, those of the DOPC did not increase much, indicating that the interaction between BNO and DOTAP liposomes could affect both the micro-polarity (**Figure 1-3**) and the micro-

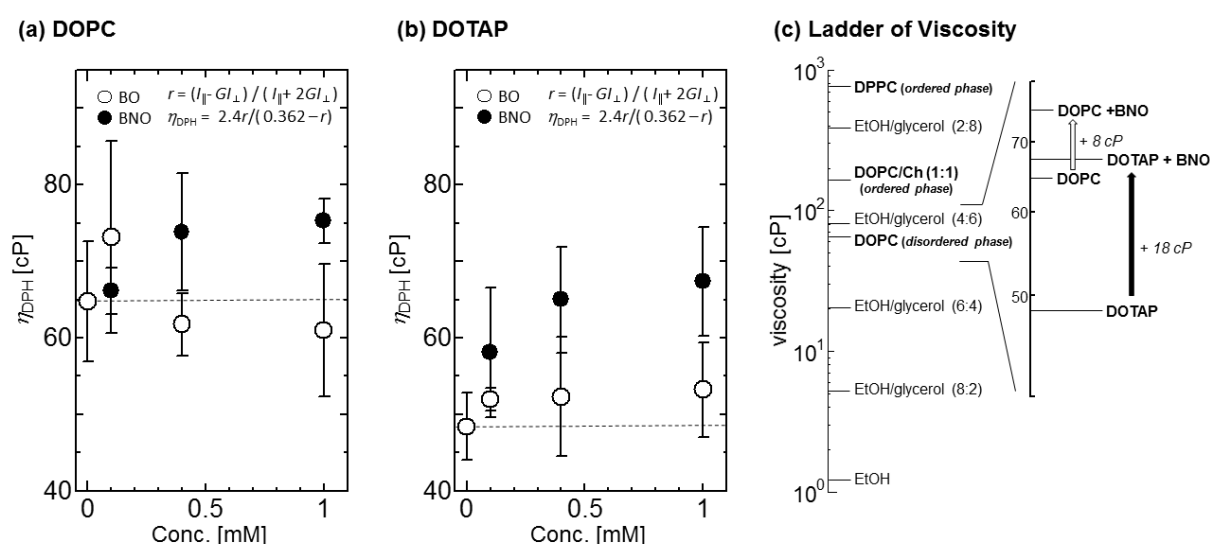


**Figure 1-4.** Analysis of the micro-viscosity of liposome membranes by using DPH. (a) DOPC and (b) DOTAP. Symbols indicate BO (*open circle*) and BNO (*closed circle*), respectively. Each dotted line indicates the  $\eta_{DPH}$  value in the absence of substrates. The values of the DPH anisotropy ( $r$ ) and the micro-viscosity ( $\eta_{DPH}$ ) were calculated based on previous the report. The total concentrations of lipid and DPH were 0.1 mM and 0.4  $\mu$ M, respectively. (c) Ladder chart of viscosity. The viscosity of ethanol/glycerol systems was reported previously [Alkindi *et al.*, 2008]. Open and closed arrows indicate the increased  $\eta_{DPH}$  value of DOPC and DOTAP in the presence of BNO, respectively.

viscosity (**Figure 1-4**). It has been reported that the solvent relaxation time of the DOTAP liposome was increased in the presence of zwitterionic DOPC [Jurkiewicz *et al.*, 2006], which suggests that the dipolar interaction between lipid molecules can stabilize the lipid membranes. It is therefore found that the localization of BNO in the DOTAP liposome could induce the stabilization of the membrane with the variation of the membrane surface state (disordered phase to ordered phase). These results suggest that the BNO can be localized on the DOTAP liposome and, furthermore, BNO and lipid molecules are tightly packed within the dehydrated membrane surface.

#### **4. Summary**

The micro-environment of the lipid bilayer was successfully evaluated. The fluorescent probe Laurdan represented the micro-polarity in the lipid bilayer, and the fluorescent probe DPH could represent the micro-viscosity of the vesicle membrane. By comparing to lipid vesicles, DOPC and DOTAP, the distribution ratio of BNO was higher in DOTAP vesicle than that in DOPC vesicle. The significant changes in micro-polarity of vesicles was induced after the BNO addition, indicating that the partitioning of hydrophobic molecules could lead to the dehydration of vesicles. The micro-viscosity of the vesicles was also influenced by the addition of BNO while the changes were small compared to the micro-polarities. It was found that vesicles could be designed by the partitioning of molecules as in DOTAP and BNO that the vesicle membrane became more dehydrated and viscous.

Because the environmental properties around the reaction substrates are always important factors to regulate the reaction and sometimes selectivity, the properties of vesicles, which forms the surrounding environment of reaction substrates, are key factors for the interfacial reaction to be carried out at the surface of vesicles. Based on the findings about the partitioning behavior of substrates and changes in the environment after the partitioning of the substrates, the reaction process would be discussed in the following chapter 2.



# Chapter 2

## Interfacial Reactions on the Surface of Model-Biomembrane

### Regulated by the Membrane Polarity

#### 1. Introduction

Chemical reactions in aqueous media have been in the huge demand for several decades in the aspect of green sustainable chemistry. Before 2000s, conventional organic synthesis mostly required organic solvents and some non-environmentally-friendly additives although the short time of the reaction, high yield, and high selectivity were achieved. Many catalysts and processes have been developed for several decades, while most of them worked only in hydrophobic environment. One of the major problems in applying the chemical reaction process to aqueous environment is that the (metal-)catalysts are deformed by the hydration. To overcome the problem, some scientists have reported the new catalysts which can work in the aqueous media. Kokubo *et al.* reported that the Lewis acid can work as a catalyst for hydroxymethylation [Kokubo *et al.*, 2008]. For another method, Li *et al.* have reported about the amphiphilic catalyst that can self-assemble into micelles and work properly in water [Li *et al.*, 2012]. Hamasaka *et al.* even represented that the catalyst could also self-assemble into vesicles and achieved the enantioselective reaction in aqueous media [Hamasaka *et al.*, 2014]. Phase transfer catalysis (PTC) can reduce the use of organic solvents by designing the catalysts, while the PTC process still requires nonpolar organic phase (e.g., hexane) [Kitamura *et al.*, 2005]. Such developments in catalysts and process design will contribute to green sustainable chemistry that the organic solvents are not required for the organic synthesis.

In general, organic synthesis reactions (e.g., alkylation reaction) are conducted in the organic solvent because most of the reactants are hydrophobic and not dissolved into aqueous media. PTC can solve this problem: the hydrophobic molecules can be dissolved in the organic phase and reaction can proceed. The hydrophobic molecules can even be dispersed in aqueous media by interacting with self-assemblies such as micelles, O/W emulsions, or vesicles. For example, some micellar aggregates have been reported to promote Diels–Alder reactions [Rispen *et al.*, 2003, Engberts *et al.*, 2006, Chatterjee *et al.*, 2003]. Micellar suspensions can provide a hydrophilic–hydrophobic interphase between the bulk solution and hydrophobic interior of the assembly. It has been reported that the pseudo-phase model [Viparelli *et al.*, 1999] can be applied to the aldol reaction and Diels–Alder reaction in micellar or emulsion systems. Meanwhile, 1,3-dipolar cycloadditions, which are similar to the Diels–Alder reaction, can be influenced by the degree of solvation as well as the frontier molecular orbitals (FMOs) of the reactants [Khursan *et al.*, 2010, Benchouk *et al.*, 2011]. In homogeneous solution systems, it is assumed that the relative dielectric constant ( $\epsilon'$ ) and proticity of the reaction media play important roles on the reaction. Although the reaction mechanism might be different in micelle

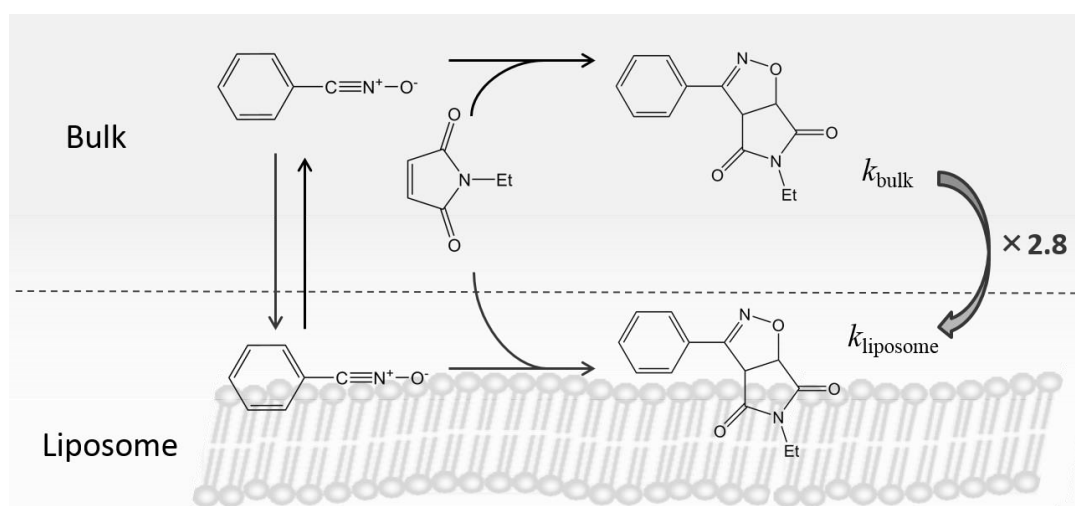


**Figure 2-1** Schematic illustration of the study in this chapter.

solution, the properties of the hydrophilic–hydrophobic environment around the reactants may also regulate the reactions.

In this chapter, the reaction at the surface of liposome membrane was carried out in aqueous medium based on the membrane properties of liposomes and partitioning behavior of reaction substrates as discussed in chapter 1. As a model reaction, 1,3-dipolar cycloaddition of benzonitrile oxide (BNO) and *N*-ethylmaleimide (EMI) was selected (**Fig.2-1**). First, the reaction in the bulk system, micellar system, and liposomal system were compared, suggesting that the relative dielectric constant ( $\epsilon'$ ) was the important factor to increase/decrease the reaction rates and conversion. The interfacial reaction was further discussed by the relationship between reaction rate and relative dielectric constant or distribution ratio. Based on the relationship between them, the reaction model was investigated and the possible regulation of the interfacial reaction by changing the membrane properties was proposed.

## 2. Materials and Methods

### 2.1 Materials.

1-Palmitoyl-2-oleoyl-*sn*-glycero-3-phosphocholine (POPC), 1,2-distearoyl-*sn*-glycero-3-phosphocholine (DSPC), 1,2-dioleoyl-3-trimethylammonium-propane (DOTAP), and 1,2-dipalmitoyl-3-trimethylammonium-propane (DPTAP) were purchased from Avanti Polar Lipid (Alabaster, AL, USA). 6-Lauroyl-2-dimethylaminonaphthalene (Laurdan) and 6-(*p*-toluidino)-2-naphthalenesulfonic acid sodium salt (TNS) were purchased from Sigma-Aldrich (St. Louis, MO, USA). Benzaldehyde oxime and sodium hypochlorite solution (NaClO(aq)) were purchased from Kanto Chemical (Tokyo, Japan). Other chemicals were purchased from Wako Pure Chemical (Osaka, Japan). These chemicals were used without further purification.

Benzonitrile oxide (BNO) was prepared as following [Rispiens *et al.*, 2003]: 21.6  $\mu$ L of benzaldehyde oxime was dissolved in the 2 mL of NaClO(aq)/1-propanol solution (50:50). 0.36 g of NaCl was added to this solution to separate it to two phases. After the upper phase was taken and diluted by 1-propanol, 25 mM benzonitrile oxide solution was obtained. The formation of BNO was determined by UV-vis spectroscopy (UV-1800; Shimadzu, Kyoto, Japan) and high resolution double-focusing magnetic sector mass spectrometer (JMS700; JOEL, Tokyo, Japan), where the conversion of BO was >85 %. The prepared BNO solution was stable for at least 3h, and the experiments were performed soon after the BNO was prepared.

### 2.2 Preparation of Liposomes.

A chloroform solution with lipids was dried in a round-bottom flask by evaporation under a vacuum. The obtained lipid thin film was dissolved in chloroform again, and the solvent was evaporated. The lipid thin film was kept under a high vacuum for at least 3 hours, and was then hydrated with distilled water at room temperature. The liposome suspension was frozen at -80 °C and thawed at 50 °C to enhance the transformation of small vesicles into larger multi-lamellar vesicles (MLVs). This freeze-thaw cycles were performed five times. MLVs were used

to prepare the LUVs by extruding the MLV suspension 11 times through two layers of polycarbonate membranes with mean pore diameters of 100 nm using an extruding device (Liposofast; Avestin Inc., Ottawa, Canada).

### 2.3 Evaluation of membrane polarities.

Laurdan is sensitive to the polarity around the molecule itself, and its fluorescence properties enable to evaluate the surface polarity of lipid membranes. The Laurdan emission spectra exhibit a red shift caused by dielectric relaxation. The emission spectra were measured with an excitation wavelength of 340 nm, and the general polarization ( $GP_{340}$ ), the membrane polarity, was calculated as follows [Suga *et al.*, 2013]:

$$GP_{340} = (I_{440} - I_{490}) / (I_{440} + I_{490})$$

where  $I_{440}$  and  $I_{490}$  represent the fluorescence intensity of Laurdan at 440 nm and 490 nm, respectively. To compare the polar environment of liposome or micelle surface and solvent, the apparent polarity of liposome,  $\varepsilon'$ , was calculated. The values of  $NF_{340}$  were calculated to evaluate  $\varepsilon'$  as follows:

$$NF_{340} = (I_{\max} - I_{510}) / (I_{\max} + I_{510})$$

where  $I_{\max}$  and  $I_{510}$  represent the maximum peak intensity of Laurdan fluorescence between the wavelength from 400 nm to 500 nm and the peak intensity at 510 nm, respectively.

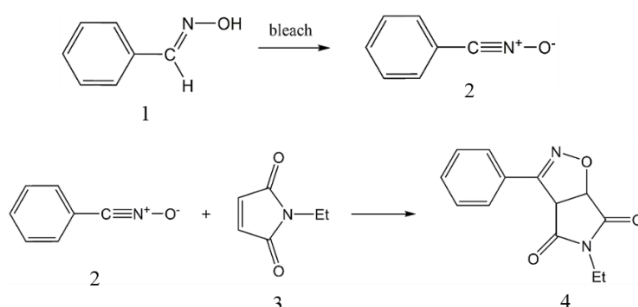
The total concentrations of lipid and Laurdan were 100 and 1  $\mu$ M, respectively.

For measuring membrane polarity by TNS, a TNS/ethanol solution (100  $\mu$ M) was used instead of a Laurdan/ethanol solution and the rest of the process is same as the measurement using Laurdan.

### 2.4 1,3-Dipolar cycloaddition of BNO and EMI (Scheme 2-1).

10  $\mu$ L of BNO solution (25 mM in 1-propanol) was mixed with 1 mL of sample solution, composed of dioxane/water mixture, liposome suspension (lipid concentration = 0.25 mM), or

micelle solution (lipid conc. = 250  $\mu\text{M}$ ). The sample solution was incubated for 30 min at room temperature, then, 5  $\mu\text{L}$  of EMI solution (200 mM in 1-propanol) was added to initiate the 1,3-dipolar cycloaddition. The total concentrations of BNO and EMI were 250  $\mu\text{M}$  and 1 mM, respectively.



**Scheme 2-1.** 1,3-Dipolar cycloaddition of benzonitrile oxide (BNO) and *N*-ethylmaleimide (EMI). 1. benzaldoxime, 2. benzonitrile oxide, 3. *N*-ethylmaleimide, 4. Product

## 2.5 Kinetics measurement of UV absorbance.

The UV absorbance spectra of sample solution was analyzed from 500 nm to 200 nm, using UV Spectrophotometer (UV-1800; Shimadzu, Kyoto, Japan). The UV absorbance at 278 nm is originated from product [Rispen *et al.*, 2003, Gothelf *et al.*, 1998], that is distinguishable from the peak of BNO (258 nm) or EMI (300 nm). The reaction was started in a quartz cuvette, and a time-course of the UV absorbance at 278 nm was measured for 15 min at room temperature. The reaction rate constant was analyzed as a pseudo-first-order kinetics, because of the excess of EMI (4-fold), which is calculated as follows:

$$-\ln\left(1 - \frac{A_{278}}{A_{278,e}}\right) = kt$$

where  $A_{278}$  and  $A_{278,e}$  represent the UV absorbance at 278 nm at any moment  $t$  in the reaction and that at 15 min (end of the reaction), respectively.  $k$  is the reaction rate constant, and  $t$  is the time. The concentrations of reactants were 0.25 mM for BNO and 1.0 mM for EMI. The

concentration of lipid was 0.25 mM. The relative reaction constant,  $k_{\text{rel}}$ , was calculated as follows:

$$k_{\text{rel}} = k / k_{\text{water}} ,$$

where  $k_{\text{water}}$  represents the reaction rate constant in water.

## 2.6 Adsorption of reactants onto liposome.

The adsorption amounts of reactants were also evaluated by UV spectrophotometer. 10  $\mu\text{L}$  of BNO solution (25 mM in 1-propanol) was mixed with 1 mL of liposome suspension (lipid concentration = 0.25 mM) and incubated for 30 min at the room temperature for measuring the adsorption of benzonitrileoxide. For measuring the adsorption of *N*-ethylmaleimide, 5  $\mu\text{L}$  of *N*-ethylmaleimide solution (200 mM in 1-propanol) was mixed with 1 mL of liposome suspension (lipid concentration = 0.25 mM) and incubated for 30 min at the room temperature. After the incubation, the liposome and reactants adsorbed on the membrane were removed with the ultrafiltration unit USY-20 (molecular weight cut-off: 200,000, Advantec Toyo, Ltd., Tokyo, Japan). The adsorption percentages were calculated from the difference in UV absorbance of the solution before and after the filtration:

$$\text{Adsorption percentage} = (A_{\text{initial}} - A_{\text{filtrated}}) / (A_{\text{initial}}) \times 100,$$

where  $A_{\text{initial}}$  and  $A_{\text{filtrated}}$  represent the absorbance of the reactant (BNO or EMI) in the solution before ultrafiltration and after ultrafiltration, respectively.

### 3. Results and Discussion

#### 3.1 Characterization of liposomes by relative dielectric constant ( $\epsilon'$ )

Pseudo-interphase reactions constitute an important group in chemical reactions in self-assembled systems. Notably, the polarity and proticity of solvents can regulate the partitioning of reactants; the microscopic environment of the liposome surface can also regulate the 1,3-dipolar cycloaddition reaction, as evaluated in this study. In order to investigate the membrane properties of the liposomes, the general polarization ( $GP_{340}$ ) was estimated using Laurdan. The  $GP_{340}$  values varied with the acyl chain length and surface charge of the lipid molecules that comprised the liposome membranes (**Table 2-1**). POPC and DOTAP liposomes showed lower  $GP_{340}$  values ( $GP_{340} < -0.2$ ), indicating that they were in the liquid-disordered phases [Suga *et al.*, 2011]. In contrast, DSPC and DPTAP showed higher  $GP_{340}$  values at room temperature. Because the phase transition temperatures of DSPC and DPTAP are 55°C and 45 °C, respectively, DSPC and DPTAP were in the solid-ordered phases. Because Laurdan peak shifts are dependent on environmental hydrophobicity,  $GP_{340}$  values can indicate the hydrophobicity as well as the relative dielectric constants. To investigate the relative dielectric constant, the nonpolarity factor ( $NF_{340}$ ) was examined;  $NF_{340}$  values reveal the degree of nonpolarity of the solvents and were applied to characterize the liposomes. The  $NF_{340}$  values were calculated using the ratio of the fluorescence intensities of Laurdan in organic solvents and water (**Fig. 2-2**). The relative dielectric constant,  $\epsilon'$ , can be calculated from  $NF_{340}$  values, suggesting that the approximate amount of water at the liposome membrane surface can be estimated by analyzing the  $GP_{340}$  values (**Fig. 2-2**). Liposomes in the liquid-disordered phases showed high  $\epsilon'$  values ( $\epsilon' = 20-25$ ), while low  $\epsilon'$  values ( $\epsilon' = 3-5$ ) were observed in liposomes in the solid-ordered phases. CTAB micelles also showed a higher  $\epsilon'$  value, implying that the membrane surface of CTAB micelles is similar to that of liposomes in liquid-disordered phases. It is known that the permeability of small molecules across liposome membranes can be influenced by the phase states of the liposomes [Anyarambhatla *et al.*, 1999]. Furthermore, it has been reported that the



distribution of BNO in positively-charged DOTAP liposomes is higher than that in zwitterionic DOPC liposomes. It is therefore expected that the reactants can accumulate at the surface of liposomes and the reaction can occur at the pseudo-interphase of the liposomes.

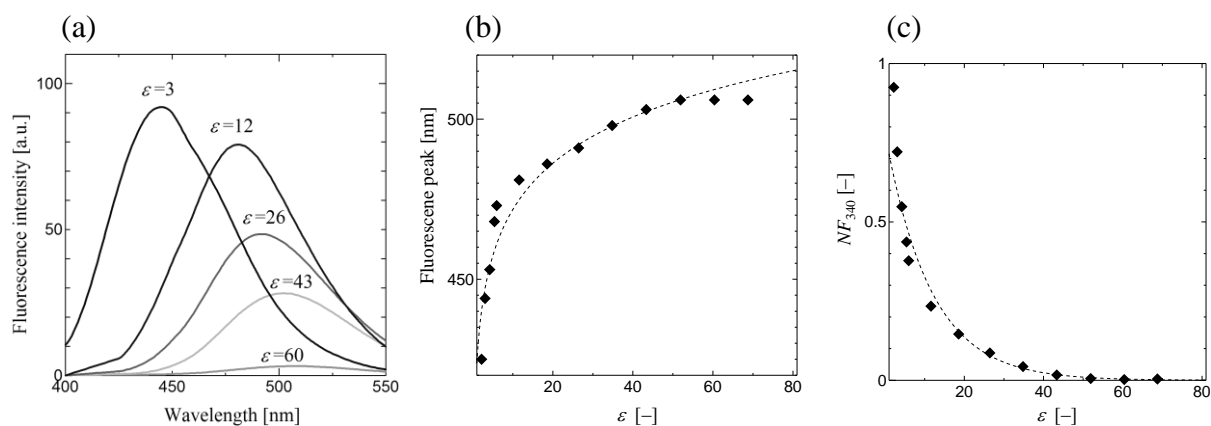


**Figure 2-1.** The calculation of relative dielectric constant. (a) Fluorescent spectra of Laurdan in each relative dielectric constant of water/1,4-dioxane media. (b) The relationship between  $\epsilon$  and fluorescence peak wavelength of Laurdan. Mediums which have various relative dielectric constant values were prepared from mixture of dioxane and water. The wavelength of fluorescence peak of Laurdan is known to be red-shifted when Laurdan is in polar environment. The relationship in the figure shows that fluorescent peak of Laurdan in water ( $\epsilon^2 \sim 78$ ) would be at 510 nm. (c) The relationship between  $\epsilon$  and  $NF_{340}$  values. This relationship was used to calculate  $\epsilon^2$  of liposomes and micelles.

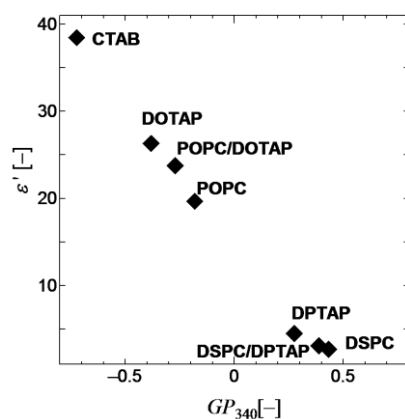


**Figure 2-2.** Characteristics of liposome. Membrane polarity ( $GP_{340}$ ) was measured from the experiment using Laurdan, and relative dielectric constant ( $\epsilon'$ ) was calculated by the fitting equation from **Fig. 2-1**.

**Table 2-1** Membrane properties of the vesicles and micelles

Lipid	$GP_{340}$ [-]	Zeta Potential* [mV]
POPC	-0.181	+ 2.3
DSPC	0.433	- 4.0
DOTAP	-0.381	+ 49.0
DPTAP	0.275	+40.7
CTAB (micelle)	-0.723	+90

\*Zeta potentials are from previous reports [Kecpczynski *et al.*, 2012, Makino *et al.*, 1991, Ma *et al.*, 2011, Barnier Quer *et al.*, 2012, Wojciechowski *et al.*, 2011].

**Table 2-2** values of  $\varepsilon'$  and comparison of the solvents and self-assembly systems

Solvent*	$\varepsilon'$ [-]	Self-assembly	$\varepsilon'$ [-]
Water	81.1	SDS (micelle)	45.4
Formic acid	58.5	CTAB (micelle)	38.5
Dimethylsulfoxide	46.7	DOTAP (liposome)	26.3
Acetonitrile	37.5	POPC/DOTAP (liposome)	23.8
Methanol	32.7	DOPC (liposome)	23.3
Ethanol	24.6	POPG (liposome)	21.3
1-Propanol	20.3	POPC (liposome)	19.7
Dichloromethane	9.1	DPTAP (liposome)	4.5
1,4-Dioxane	2.3	DPPC (liposome)	3.2
<i>n</i> -hexane	1.9	DSPC (liposome)	2.7

\*: The  $\varepsilon'$  values of solvents are referred to the Chemistry Handbook (The Chemical Society of Japan)

### 3.2 Effect of liposomes on 1,3-dipolar cycloaddition

In the 1,3-dipolar cycloaddition of BNO and EMI, the surrounding dielectric environment is a key factor [Van Mersbergen *et al.*, 1998]. Notably, the reaction between BNO and EMI was carried out in water (**Fig. 2-3**). In order to estimate the effects of the reaction media on the 1,3-dipolar cycloaddition between BNO and EMI, the relative dielectric constant  $\epsilon'$  and the relative reaction constant,  $k_{\text{rel}}$ , were plotted (**Fig. 2-3**, open circle). With the 1,4-dioxane/water systems, the  $k_{\text{rel}}$  values became higher with a decrease in the relative dielectric constant of the solvent. The relative reaction rate constant in 1,4-dioxane ( $\epsilon = 2.2$ ) was 1.6 times higher than that in water ( $\epsilon = 78$ ), indicating that the hydrophobic environment could promote the 1,3-dipolar cycloaddition. BNO is hydrophobic and thus prefers hydrophobic environments. Because 1,4-dioxane is an

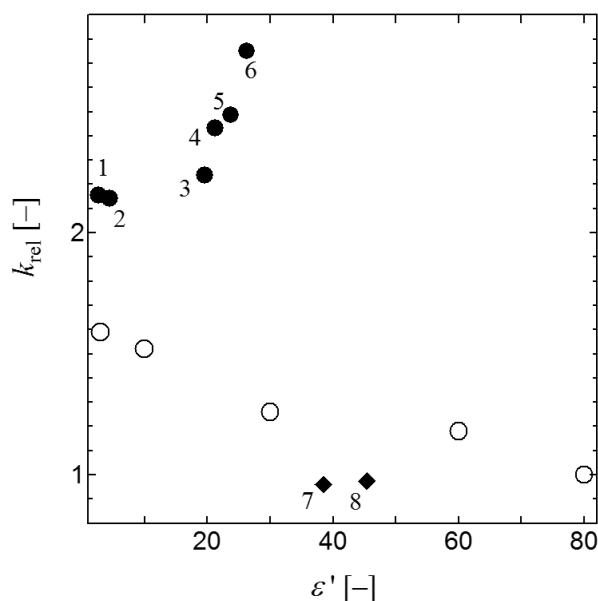


**Figure 2-3.** Reaction rate constant in various condition. The reaction of BNO (0.25 mM) and EMI (1.0 mM) was carried out in water at 25°C. The reaction was initiated after 30 min incubation of BNO with the medium. For 1,4-dioxane/water system (open circle), 1,4-dioxane/water was used as the medium to vary the relative dielectric constant. For liposome (closed circle), liposome suspensions (0.25 mM) were used as the reaction medium, and 5 mM micelle solutions were used for micelle (closed diamond). Each points indicates the followings: 1. DSPC, 2. DPTAP, 3. POPG, 4. POPC, 5. POPC/DOTAP, 6. DOTAP, 7. CTAB, 8. SDS. Rate constant values are relative values compared to the reaction conducted in water ( $\epsilon' = 78$ ).

aprotic solvent, the reaction between BNO and EMI in 1,4-dioxane/water systems would be dependent on the solvation of the reactants. With the micellar suspensions, a non-promotion effect was observed even though the surface of the micelles was hydrophobic ( $\epsilon' = 35\sim 45$ ). This result indicated that the reactants could not accumulate on the surface of the micelle aggregates. In the case of the liposomes, the  $k_{rel}$  values increased by 2.2-2.8 times as compared to the water solution, depending on the characteristics of the liposomes. Specifically, the reaction was more promoted in liposomes in the liquid-disordered phases ( $\epsilon' = 20\sim 25$ ) as compared to that in liposomes in the solid-ordered phases. Among the liposomes used in the present study, DOTAP liposome showed the highest promotion effect on the reaction, indicating that DOTAP liposome could provide a better environment for the reaction. Rispens and coworkers reported that 1-propanol containing 40 M of water was the best medium for the 1,3-dipolar cycloaddition between BNO and EMI.

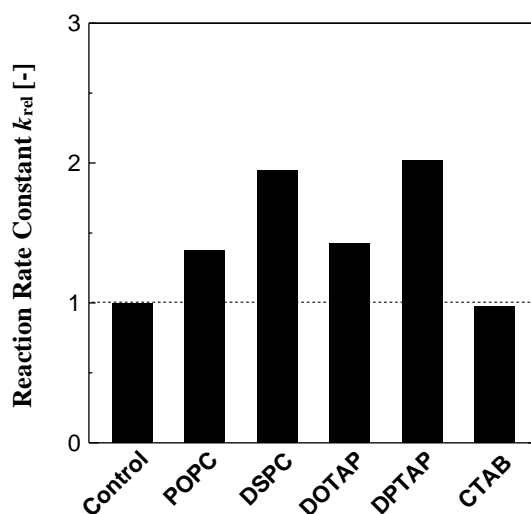


**Figure 2-4.** Reaction rate constant in various condition. The control reaction of BNO (0.25 mM) and MI (1.0 mM) was carried out in water at 25°C. The reaction was initiated by MI addition to the BNO solution (without 30 min incubation). For CTAB, CTAB solutions (5 mM) was used, and liposome solutions (0.25 mM) were used for POPC, DSPC, DOTAP, and DPTAP instead of water. Rate constant values are relative values compared to Control. Reaction rate constants without incubation are smaller than the ones with 30 min incubation. This result also indicates the importance of BNO distribution for the reaction.

Although the surface charge densities of liposomes or micelles differed (**Table 2-1**), no relationship was obtained between the surface charge density and the promotion of reaction. It is notable that the  $k_{rel}$  values were not so high just after the mixing of the reactants at each medium (**Fig. 2-4**). To find the better environment and to promote this reaction in liposome systems, the condensation of the reactants should be concerned.

### 3.3 Accumulation of BNO and EMI in liposome membranes

The local concentrations of the reactants were estimated based on the ultrafiltration method. The accumulation of the reactants on the liposome membranes could be critical to the enhancement of the 1,3-dipolar cycloaddition reaction between BNO and EMI at the DOTAP liposome membrane. **Figure 2-5** shows the amount of BNO and EMI distributed on each liposome. DPTAP, the cationic liposome in the solid-ordered phase, did not significantly promote the distribution of BNO as compared to DOTAP, while the distribution of BNO on DPTAP at 60 °C increased to 34%, when DPTAP was in the liquid-disordered phase. The BNO

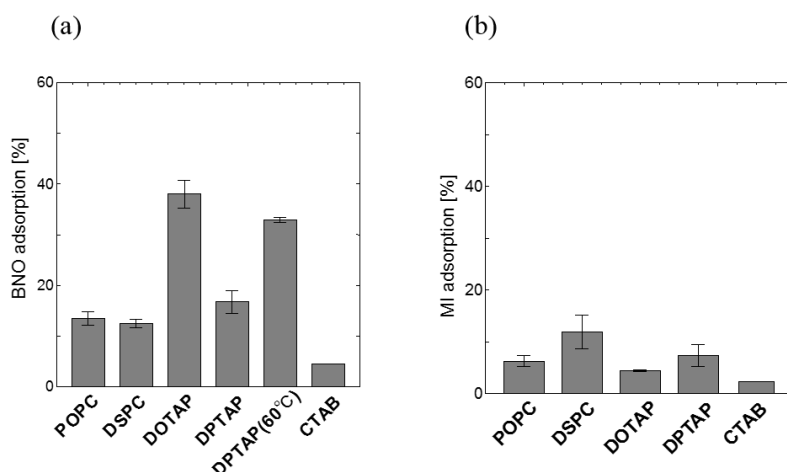


**Figure 2-5.** Adsorption Behavior of Substrate Molecules on Liposome Membrane. Each reactant (BNO: 0.25 mM and EMI: 1.0 mM) was incubated with liposome suspension (0.25 mM) in water for 30 min. Adsorption percentage was calculated from the difference of the absorbance before and after filtration (adsorption percentage =  $(A_{initial} - A_{filtered}) / (A_{initial})$ ). The absorbance was measured at 25 °C unless notified. (a) BNO adsorption, (b) EMI adsorption.

distribution analysis indicated that BNO was distributed on the DOTAP liposome not only because of the positive charge, but also because of the phase state. Only a small amount of BNO was distributed in the CTAB micelle. In contrast, BNO molecules could accumulate in the membrane. DOTAP, the cationic liposome in the liquid-disordered phase, formed a suitable environment for BNO accumulation. In the case of EMI, the distribution ratio was not much higher than that of BNO, and the adsorption percentage values were almost similar within the liposomes. EMI is more hydrophilic than BNO: the calculated  $\log P$  values for BNO and EMI were 1.82 and -0.18, respectively [Pence *et al.*, 2010]. Although the distributed amount of EMI was smaller than that of BNO, it was assumed that EMI preferred to be distributed on the solid-ordered membranes, such as DSPC and DPTAP. In general, 1,3-dipolar cycloadditions are concerted reactions [Huisgen *et al.*, 1976]. Thus, both reactants must accumulate at the pseudo-interphase region simultaneously if the reaction occurs around the surface of the liposome membrane. This indicates that strong interactions between reactants and liposome membranes might inhibit the reaction. In the case of the micelle solutions, the mismatched localization of reactants would inhibit the 1,3-dipolar cycloaddition. It is therefore important to estimate the co-localization of BNO and EMI at the surface of the liposomes.

### **3.4 Estimation of the localization of reactants in liposome membranes**

The distributions of the reactants in the DOTAP liposome membrane were investigated. Based on the hierarchic binding of the fluorescent probes, the localization behaviors of BNO and EMI were analyzed. TNS and Laurdan exist in the hydrophobic-hydrophilic interface region. After these fluorescent probes were embedded in the liposome membranes, BNO and EMI were added to each sample, and variations in the membrane properties were evaluated (**Fig. 2-6**). After BNO was added, the fluorescence intensity of TNS decreased and the  $GP_{340}$  values increased, indicating that BNO could be localized in the regions where TNS and Laurdan were embedded. It was therefore determined that BNO could be localized at the hydrophobic-hydrophilic interface of the DOTAP liposome. On the other hand, the Laurdan signals were not

significantly altered in the presence of EMI. The fluorescence intensity of TNS decreased after addition of EMI, indicating that EMI could be localized at the hydrophilic membrane surface region of the liposomes. From these results, it can be assumed that these two reactants were enclosed at the surface of the DOTAP liposome (**Fig. 2-7**), and the 1,3-dipolar cycloaddition would occur in the hydrophilic region of the membrane (not in the hydrophobic interior region). It is therefore expected that the accumulation of reactants in the DOTAP liposome can promote Diels-Alder reactions and 1,3-dipolar cycloadditions.

The polar environment of the liposome membrane was monitored by analyzing the variations in  $GP_{340}$  values before and after BNO distribution (**Fig. 2-8**). The  $\Delta GP_{340}$  value of DOTAP was highest among the liposomes used in this study, although the change in the  $GP_{340}$  value of DOTAP was not as significant as compared to the phase transition from the liquid-disordered phase to the solid-ordered phase. BNO could be embedded in the hydrophobic-hydrophilic interface region where water molecules bind, and could replace the water molecules,

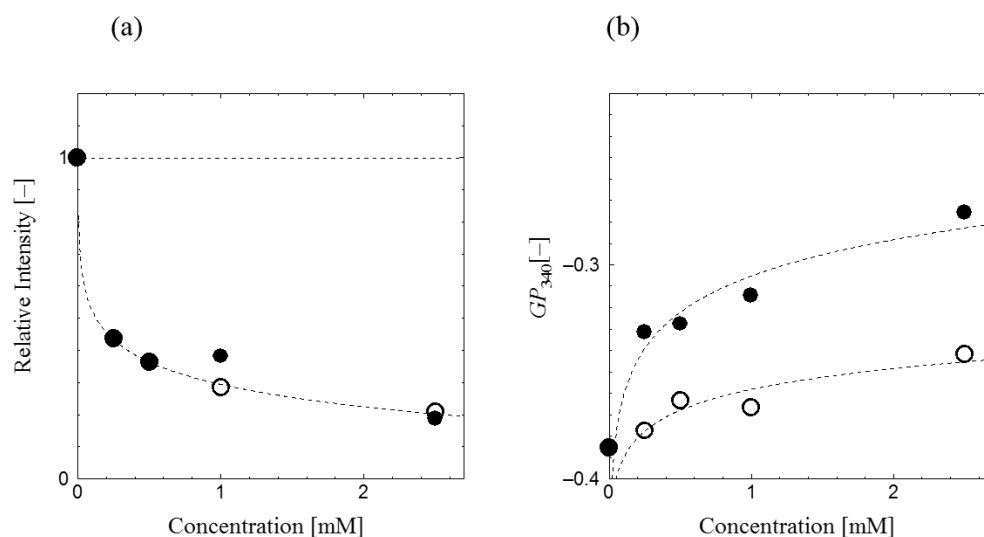


**Figure 2-6.** Change in values of fluorescent probes. (a) Intensity of TNS fluorescence was measured. TNS (1.0  $\mu\text{M}$ ), DOTAP liposome (100  $\mu\text{M}$ ), and optional amount of substrates were incubated for 30 min before measurement. (b) Fluorescent spectrum of Laurdan was obtained. Laurdan (1.0  $\mu\text{M}$ ), DOTAP liposome (100  $\mu\text{M}$ ), and optional amount of substrates were incubated for 30 min before measurement.  $GP_{340}$  values were calculated as written in methods section.

resulting in the dehydration of the membrane surface (i.e., an increase in the  $GP_{340}$  value). Here, a few percent of water was excluded from the liposome membrane (the relative dielectric constant  $\epsilon'$  varied to 25.0 from 26.3, see below). In the presence of BNO, the dehydration degree of DOTAP liposome was most significant. Based on the above results, the reactants were distributed in the water-rich environment on the surface of the DOTAP liposome (pseudo-interphase), and the reaction was promoted due to the enclosure of the two reactants.

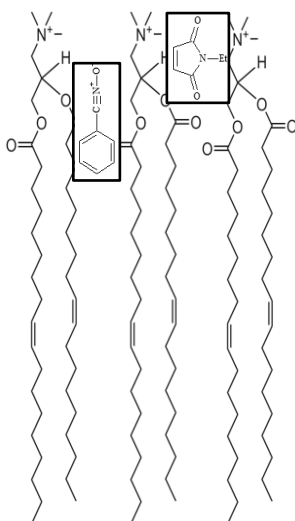


**Figure 2-7** Location of reactants in DOTAP liposome membrane

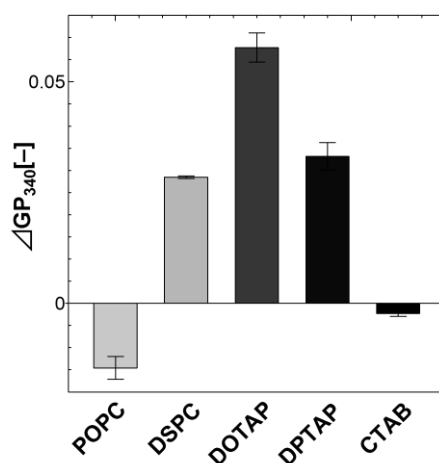


**Figure 2-8** Variations in  $GP_{340}$  values of liposomes or micelle after BNO addition. Fluorescent spectrum of Laurdan was obtained; Laurdan (1.0  $\mu\text{M}$ ), liposome (100 $\mu\text{M}$ ), and BNO (100 $\mu\text{M}$ ) were incubated for 30 min before measurement.  $GP_{340}$  values were calculated as written in methods section.



### 3.5 Estimation of the reaction rate constants occurring at the liposome surface

In this study, pseudo-first-order kinetics were applied to calculate the reaction rate constant of BNO and EMI in different media. Since the reaction rate constant of the 1,3-dipolar cycloaddition could depend on the degree of solvation and FMO of the reactants, the relative dielectric constant,  $\epsilon'$ , is helpful to understand the effects of the reaction media. In a homogeneous solution of 1,4-dioxane/water, a linear relationship between  $k_{\text{rel}}$  and  $\epsilon'$  was approximately obtained, indicating that the solvation of the reactants is critical to promote the reaction. In the case of the micelle solutions, the  $k_{\text{rel}}$  values were almost the same as those in water. The result shown in **Fig. 2-5** reveals that small amounts of BNO (4.5%) and EMI (2.3%) were distributed on the micelle membrane, where a non-promoting effect was observed on the surface of micelle aggregates. On the contrary, 2.1-to-2.8-fold higher  $k_{\text{rel}}$  values were obtained in liposome suspensions. However, the apparent reaction rate constant can be divided into two types of reactions: in bulk water and at the pseudo-interphase of the liposome (**Fig. 2-9**). In this way, the calculated reaction rate  $k_{\text{cal}}$  can be written as:

$$(\text{reaction rate}) = k[\text{BNO}]_{\text{total}} = k_{\text{W}}[\text{BNO}]_{\text{W}} + k_{\text{L}}[\text{BNO}]_{\text{L}}$$

where  $k_{\text{W}}$  is the reaction rate constant for the reaction occurring in the bulk water phase and  $k_{\text{L}}$  is the reaction rate for the reaction occurring at the pseudo-interphase of the liposome;  $[\text{BNO}]_{\text{W}}$  and  $[\text{BNO}]_{\text{L}}$  are the concentration of BNO in bulk water and at the pseudo-interphase of the liposome, respectively. The calculated values of  $(k_{\text{L}}/k_{\text{W}})$  are shown in **Table 2-3**. The reaction rates at the pseudo-interphase of the liposome were much higher than those in water or micellar solutions. The increase in reaction rate in liposome systems might be because of hydrated water at the liposome surface. Because EMI is localized at the surface of the liposome due to its hydrophilicity, the reaction was considered to take place at the surface of the liposome, where hydrated water molecules exist. It has been reported that an increase in the amount of water also increases the reaction rate; therefore, hydrated water molecules at the liposome surface can play an important role in the 1,3-dipolar cycloaddition. On the other hand, the reaction rates

decreased in 1,4-dioxane/water systems with increasing amounts of water. This is possibly because of the solvation of BNO in aqueous media; since BNO is a hydrophobic molecule, BNO might not be solvated in the bulk aqueous phase. However, when BNO is at the pseudo-interphase, BNO can be stabilized and solvated by water. Therefore, the solvation of the reactants by water molecules could be critical in forming the activated state and promoting the reaction.

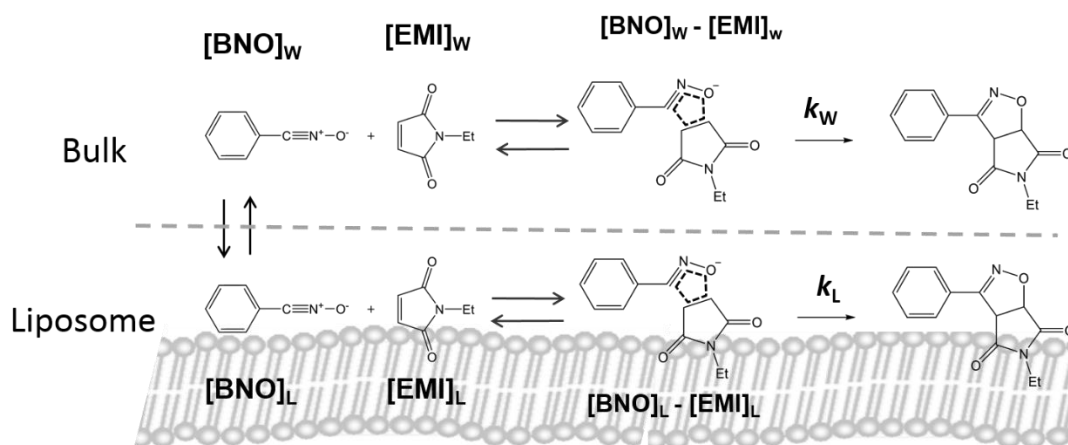


**Figure 2-9.** Scheme of the reaction at the interface of liposome membrane.

**Table 2-3** The values of the reaction rate with liposomes and micelle.

	$\varepsilon'$ [-]	$k_{rel} (=k/k_w)$ [-]	BNO ads. [%]	$k_L / k_w$ [-]
POPC	19.7	2.24	13.4	10.25
DSPC	2.69	2.15	12.4	10.27
DOTAP	26.3	2.75	38.0	5.61
DPTAP	4.52	2.14	16.7	7.83
CTAB	38.5	0.96	4.5	0.11

From **Table 2-3**, it can also be seen that the  $k_L$  values in DOTAP and DPTAP liposome systems were smaller than those in POPC and DSPC liposomes. This result shows that adsorption of BNO was not directly related to the value of  $k_L$ . Rather, it is indicated that the strong electrostatic interaction between BNO and liposomes can inhibit the reaction. A high adsorption of BNO might make BNO more solvated by water molecules, but a high affinity towards the reactants also influences the reaction, possibly because of the restriction imposed on the reactive moiety.

#### 4. Summary

The reaction rate of 1,3-dipolar cycloaddition with BNO and EMI could be discussed with the relative dielectric constant  $\epsilon'$ . The relative dielectric constants of vesicles were distributed from very low (similar to hydrocarbon such as hexane) to medium (similar to ethanol). The reaction rate was dependent on  $\epsilon'$ ; in the water/1,4-dioxane system, the reaction rate decreased linearly with the increase in the value of  $\epsilon'$  while the maximum reaction rate was found at the certain  $\epsilon'$  values in the self-assembly system. The maximum reaction rate was obtained with DOTAP vesicles, where adsorption experiment that more BNO was adsorbed onto DOTAP vesicle than that other vesicles, showing that more reactants were in a favorable environment for the reaction. The accumulation of BNO also contribute to the enrichment of the reactants, which suggest the larger reaction rate constant. The observed reaction rate could be considered as the sum of the reaction in the bulk water and the reaction at the pseudo-interphase of vesicles. By applying this evaluation method to the reaction conducted, zwitterionic phospholipid vesicles such as POPC and DSPC showed the highest reaction rate at the pseudo-interphase as compared to other self-assembly systems. These results suggest that the reaction itself proceeded better at the pseudo-interphase of zwitterionic phospholipid vesicles.

As a conclusion of this chapter, the reaction at the pseudo-interphase of vesicles can enhance the reaction rate due to the enrichment effect by the localization of two reactants within the lipid bilayer. However, the degree of the enhancement effect of vesicles is dependent on the environment vesicle forms, which can be characterized by  $\epsilon'$ . The conclusion became difficult to understand, when the interaction between reactants and vesicles are in consideration. The strong interaction such as electrostatic interaction stables the reaction intermediate, which negatively affect the intermediate to be reacted into the product. In the design of vesicles as a platform for the reaction, it is important to clarify the dominant factor in the reaction (enrichment, interaction, formation of the intermediate, etc.) to achieve the efficient reaction system.

# Chapter 3

## Enantioselective C-C Bond Formation Reaction with Model-Biomembrane

### 1. Introduction

In last few decades, the field of organic synthesis has been developed, focusing on the improvement in enantioselectivity [O'Donnell, *et al.* 1989, Kitamura *et al.*, 2003]. Such fine chemicals are preferable in pharmaceutical intermediates, coating materials, or other functional materials. These materials are required to be highly regulated. For example, only one of the enantiomer can show the medical effect in pharmaceutical materials. To achieve the highly-selective enantioselective synthesis, not only catalysts but also catalytic processes have been developed, and some of them are still widely used even in recent years. Kitamura *et al.* have presented the well-known BINAP catalyst which has the structure of bi-naphthyl as an enantioselective unit, and the BINAP catalysts are one of the most popular catalysts for the enantioselective reaction due to its high versatility [Kitamura *et al.*, 2003]. The designs and developments of BINAP catalysts were attempted by the wide variety of scientists, and many BINAP-derivatives were produced for the variety of reaction [Hashimoto *et al.*, 2007]. However, none of them was aimed to be used in the aqueous media. Since bi-naphthyl structure is composed of hydrophobic moiety, it is not suitable to work in water, suggesting that the enantioselective reaction process can be improved by finding the catalyst which can work in the aqueous media.

According to the previous reports [Kokubo *et al.*, 2008, Li *et al.*, 2012, etc.] and my study mentioned in chapter 2, the chemical reaction processes in aqueous media could be achieved

by utilizing the ideas of self-assembly system. One of the major solution for chiral catalysts being dissolved and active in water is to attach the alkyl chain and hydrophilic moiety to the catalysts, so that the catalytic complex can self-assemble into micelles or vesicles in aqueous media [Li *et al.*, 2012]. Hamasaka *et al.* has reported that self-assembled catalysts can be dispersed and work properly in aqueous media, and the enantioselective reaction in aqueous media could be achieved in part (it has been very difficult to achieve the high enantiomeric excess values) [Hamasaka *et al.*, 2014].

After avoiding from the organic solvents, one would also like to avoid the use of metals since excess amount of metals in fine chemicals might lead to the toxicity in our body. Organocatalyst can be also used for the enantioselective reaction without using any metals. The enantioselective reaction processes with organocatalyst have been reported, e.g., phase transfer catalyst (PTC) [O'Donnell *et al.*, 2004, Kitamura *et al.*, 2005, Shirakawa *et al.*, 2013, etc.] and the process including proline-derivative catalyst [Nájera *et al.*, 2003, Hayashi *et al.*, 2006, etc.]. Advantages in the use of PTC are high yield and enantioselectivity, and PTC can be applied to synthesize both natural and unnatural amino acids (**Scheme 3-1**) [O'Donnell *et al.*, 1989, Ooi *et al.*, 1999]. As an example of enantioselective alkylation of a prochiral glycine derivative *N*-(diphenylmethylene)glycine tert-butyl ester (1) and benzyl bromide (2), designed PTCs resulted in both products of (*S*)-product (3*S*) [O'Donnell *et al.*, 1989] and (*R*)-product (3*R*) [Ooi *et al.*, 1999, Kitamura *et al.*, 2005]. In this reaction, (i) the inorganic base (e.g., NaOH) promotes the deprotonation of 1 at organic-water interface; (ii) the ion pair formation migrates 1-intermediate to organic phase; (iii) alkylation has been conducted (**Figure 3-1**). Due to poor solubility of 1 and PTC, the reaction requires organic phase (e.g., toluene, CH<sub>2</sub>Cl<sub>2</sub>). Toward a development of green sustainable chemical process, metal-free, base/acid-free, and organic solvent-free systems are desired. However, highly selective reactions have rarely been succeeded [Kumar *et al.*, 1996]. Inspired from PTC, the selective reaction may be achieved by using the quaternary ammonium moiety and regulating the hydrophilic-hydrophobic interface.

In this chapter, the quaternary ammonium moiety in the lipid membrane and the hydrophilic-hydrophobic interface that lipid bilayer forms were attempted to be used as a catalyst and the platform for the reaction, respectively. The alkylation of glycine derivative was carried out as a model case to investigate the possibility of enantioselective reaction with lipid bilayer as a platform. After the reaction was carried out, plausible reaction model was also considered to suggest the method for the regulation of interfacial selective reaction in general.

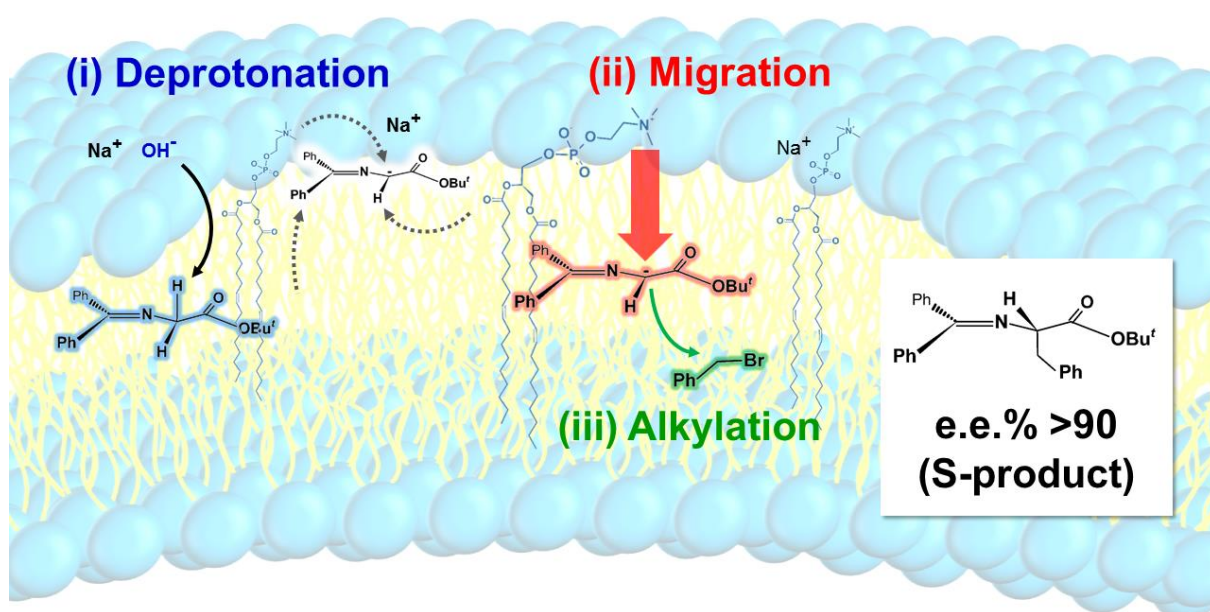


**Figure 3-1** Schematic illustration of the study in this chapter

## **2. Materials and methods**

### **2-1 Materials.**

1,2-Dipalmitoyl-*sn*-glycero-3-phosphocholine (DPPC) and 1,2-dioleoyl-*sn*-glycero-3-phosphocholine (DOPC) were purchased from Avanti Polar Lipid (Alabaster, AL, USA). Hexadecyltrimethylammonium bromide (CTAB), sodium hydroxide, and benzyl bromide were purchased from Wako Pure Chemicals (Osaka, Japan). Dilauryldimethylammonium bromide (DDAB), tetrabutylammonium hydrogensulfate (TBAH), and *N*-(diphenylmethylene)glycine *tert*-butyl ester (DMGBE) were purchased from Tokyo Chemical Industries (Tokyo, Japan). These chemicals were used without further purification.

### **2.2 Preparation of Liposomes.**

A chloroform solution containing lipids was dried in a round-bottom flask by evaporation under a vacuum. The obtained lipid thin film was dissolved in chloroform again, and the solvent was evaporated. The lipid thin film was kept under a high vacuum for at least 3 hours, and was then hydrated with distilled water at room temperature. The liposome suspension was frozen at -80 °C and thawed at 50 °C to enhance the transformation of small vesicles into larger multilamellar vesicles (MLVs). This freeze-thaw cycles were performed five times. MLVs were used to prepare the large unilamellar vesicles (LUVs) by extruding the MLV suspension 11 times through two layers of polycarbonate membranes with mean pore diameters of 100 nm using an extruding device (Liposofast; Avestin Inc., Ottawa, Canada).

### **2.3 Evaluation of membrane polarities.**

Laurdan is sensitive to the polarity around the molecule itself, and its fluorescence properties enable to evaluate the surface polarity of lipid membranes. The Laurdan emission spectra exhibit a red shift caused by dielectric relaxation. The emission spectra were measured



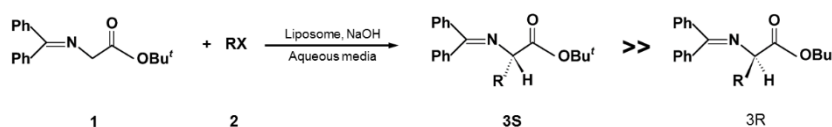
with an excitation wavelength of 340 nm, and the general polarization ( $GP_{340}$ ), the membrane polarity, was calculated as follows:

$$GP_{340} = (I_{440} - I_{490}) / (I_{440} + I_{490}),$$

where  $I_{440}$  and  $I_{490}$  represent the fluorescence intensity of Laurdan at 440 nm and 490 nm, respectively. The total concentrations of lipid and Laurdan were 100 and 1  $\mu$ M, respectively. The fluorescence spectrum of Laurdan was deconvoluted into two spectra by using the software Peakfit (Systat Software Inc., CA, USA): one originates from the localization of Laurdan in an ordered membrane (ordered phase), and the other originates from the localization of Laurdan in a disordered membrane (disordered phase). By calculating the area below the spectrum originating from the ordered phase ( $A_o$ ) and the area below the spectrum originating from the disordered phase ( $A_d$ ), the area ratio of ordered phase to disordered phase in the actual vesicle sample ( $A_o/A_d$ ) was determined.

## 2.4 Alkylation of DMGBE with benzyl bromide.

0.3 mg (1.0  $\mu$ mol) of DMGBE was dissolved in pure water, and then the water solution was mixed with liposome suspension and NaOH aqueous solution (10%) to obtain 1 mL of reaction solution. 1.5  $\mu$ L (12  $\mu$ mol) of benzyl bromide was finally added to initiate the reaction (**Scheme 3-1**). The reaction solution was stirred at 500 rpm in room temperature for 24 h. The total concentrations were DMGBE = 1.0 mM, benzyl bromide = 12 mM, lipid = 10 mM, NaOH = 0.3 M. In the case of surfactant (CTAB, TBAH, etc.) instead of liposomes, the aqueous solution of surfactant was added instead of liposome suspension. The total concentrations were fixed to the same value to the condition of the reaction with liposomes.



**Scheme 3-1** The alkylation of amino acid derivative (1) with alkyl halide (2)

## 2.5 HPLC measurements of reaction solution.

After the reaction was finished (24 h after the initiation of the reaction), the product (and reactant) were extracted to the organic solvent by using Bligh-Dyer method. In brief, the 1 mL of reaction solution was mixed with 2 mL methanol and 1 mL chloroform, resulting in homogeneous, colorless, and transparent liquid. Then 1 mL of chloroform and 1 mL pure water were added to the solution to lead to the phase separation. The centrifugation was performed (1400 rpm, 5 min) to complete the phase separation by a Tabletop Centrifuge KUBOTA 5200 (Kubota, Tokyo, Japan).

After the extraction, the organic phase was moved into round-bottom flask and chloroform was removed by evaporation. 1 mL of diethyl ether was added to the flask, and 10  $\mu$ L was taken and dissolved in 1 mL of mobile phase for HPLC analysis (Daicel Chiralpak IA, mobile phase was hexane:2-propanol = 99:1, flow rate = 0.5 mL/min). HPLC analysis was done by Waters 1515 Isocratic HPLC Pump and Waters 2489 UV/Visible Detector (Waters, Massachusetts, US) to evaluate the conversion of the reaction and the enantiomeric excess (*e.e.*).

### 3. Results and Discussion

#### 3.1 Alkylation of DMGBE with benzyl bromide in aqueous media.

In the alkylation of **1** with **2** using PTC, inorganic bases (NaOH, KOH) have been used to promote the deprotonation of **1** [Lipkowitz *et al.*, 1991]. In the presence of amphiphile assemblies and NaOH, the alkylation reactions of **1** with **2** were conducted (**Table 3-1**, **Figure 3-2**, **3-3**). In the presence of tetrabutylammonium hydrogensulfate (TBAH) in CH<sub>2</sub>Cl<sub>2</sub>-water solvent: entry I) and CTAB (micelle in water: entry III), the product **3** was obtained with higher conversion but small enantioselectivity (**Table 3-1**). The values of both conversion and *e.e.* values of the reaction with TBAH in water were very low (entry II), clearly suggesting that organic solvent-water interface is necessary for this reaction. In the presence of CTAB micelle, the hydrophobic environment of the self-assembly can be utilized as an alternate of organic solvent, wherein the value of *e.e.* was very low (*e.e.*% <10). In contrast, the reaction conducted with DOPC liposome resulted in high enantioselectivity (**3S**, *e.e.*% >90: entry IV). Such differences in conversion and *e.e.* values could be provided by the membrane structure: CTAB as micelle, DOPC as lipid bilayer.

**Table 3-1.** Conversion and *e.e.* of the alkylation reaction of **1** with **2** in the presence of self-assemblies.

Entry	Amphiphile (assembly)	Medium	Conv.%	<i>e.e.</i> % (S-R)
I	TBAH	water/CH <sub>2</sub> Cl <sub>2</sub>	94 ±2	-3 ±3
II <sup>a</sup>	TBAH	water	17 ±6	-6 ±7
III	CTAB (micelle)	water	95 ±2	5 ±3
IV	DOPC (liposome)	water	62 ±5	97 ±1

Unless otherwise notified, all reactions were carried out in water, in room temperature for 24 h. [1] = 1.0 mM, [2] = 12 mM, [amphiphiles] = 10 mM, and [NaOH] = 0.3 M. <sup>a</sup>TBAH in water does not form any particular assembly. At least 3 time-independent experiments were conducted to calculate conversion and *e.e.* values.

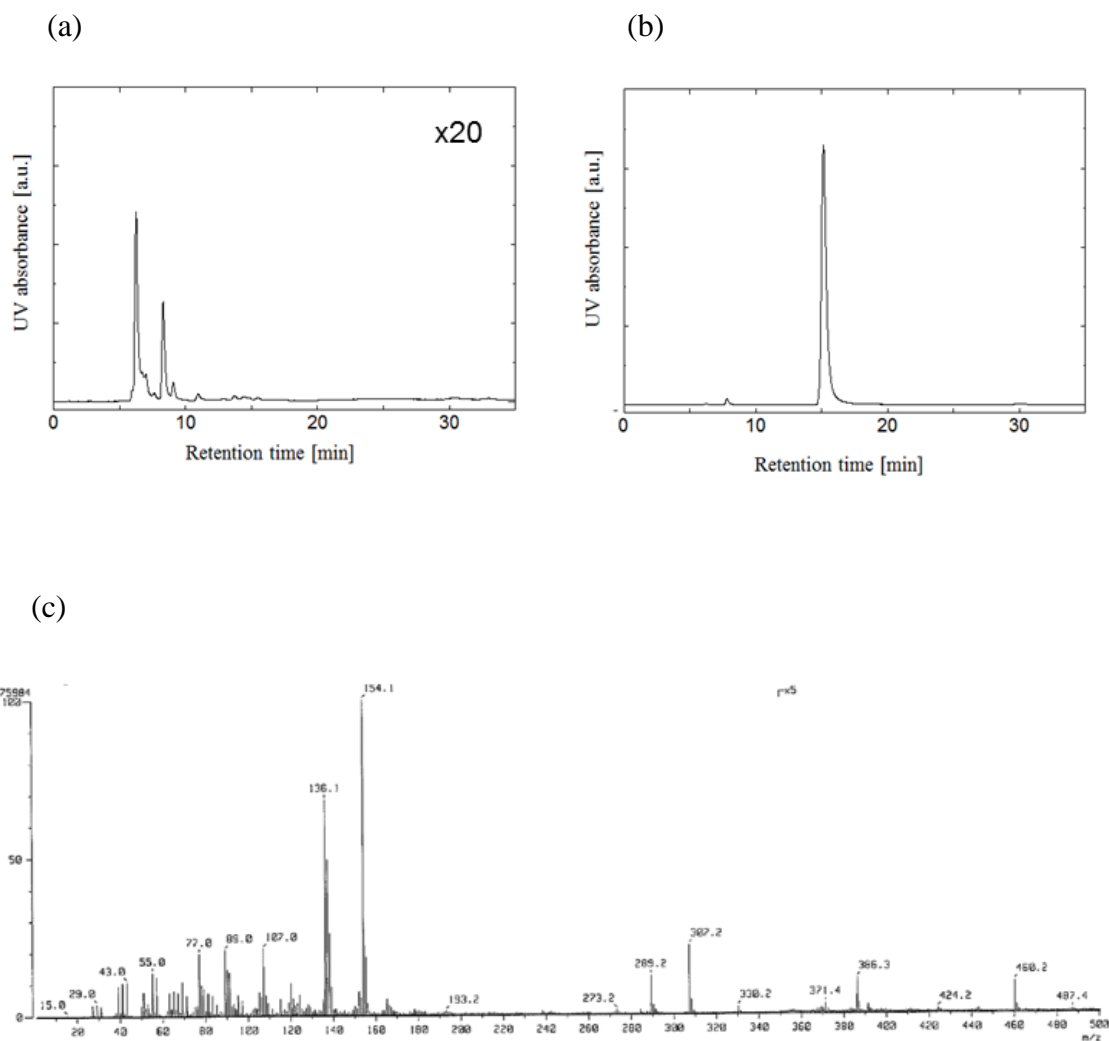


**Figure 3-2** HPLC chart of (a) **2** and (b) **1**, in the presence of DOPC liposome and NaOH. The retention times of **2** and **1** were 6.3-7.9 min and 14.9 min, respectively. For the products, the retention times of the **3R** and **3S** were 9.5 min and 24.5 min, respectively. Detection was carried out at  $\lambda = 255$  nm; mobile phase = hexane:isopropyl alcohol (99:1); flow rate = 0.5 mL/min; HPLC column: Chiralpak IA (Daicel, Japan). (c) Mass spectrum of the reaction solution. The reaction solution was obtained after 24 h mixing of **1** and **2**, in the presence of CTAB (micelle). The product was extracted by the Blich-Dyer method, and the organic phase was evaporated to obtain the product. The product was observed at  $m/z = 386.3$ .

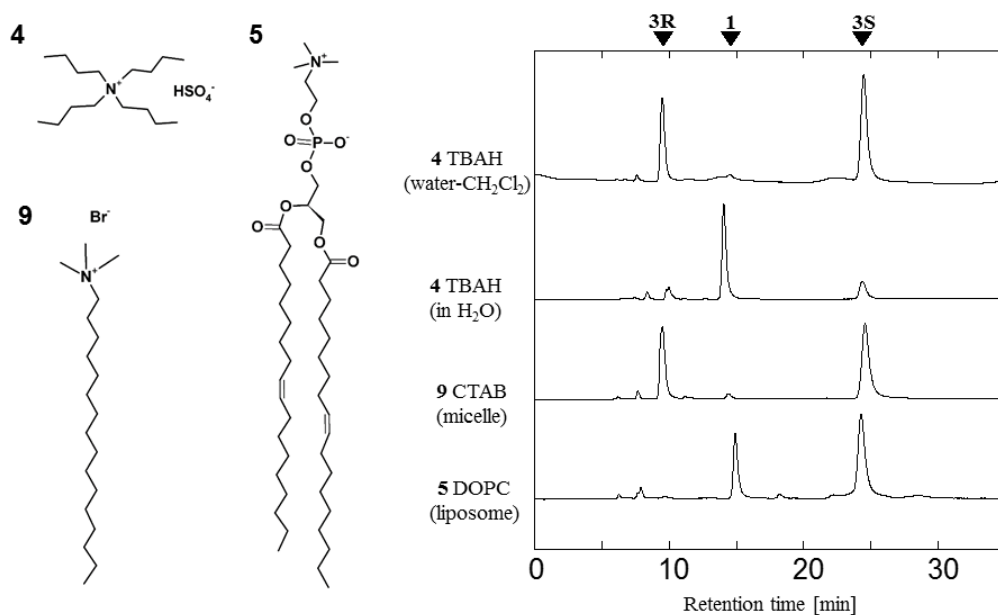


**Figure 3-3.** Chemical structures of amphiphiles: **4**, TBAH; **5**, DOPC; **9**, CTAB (bromide salt). HPLC chromatogram for the reaction in the presence of **4** (water-CH<sub>2</sub>Cl<sub>2</sub>, water), **9** (micelle), and **5** (liposome). Detection was carried out at  $\lambda = 255$  nm; mobile phase = hexane:isopropyl alcohol (99:1); flow rate = 0.5 mL/min; HPLC column: Chiralpak IA (Daicel, Japan). For retention time of **1**, **2**, **3R**, and **3S**, see supporting information Figure 3-3 and reference.

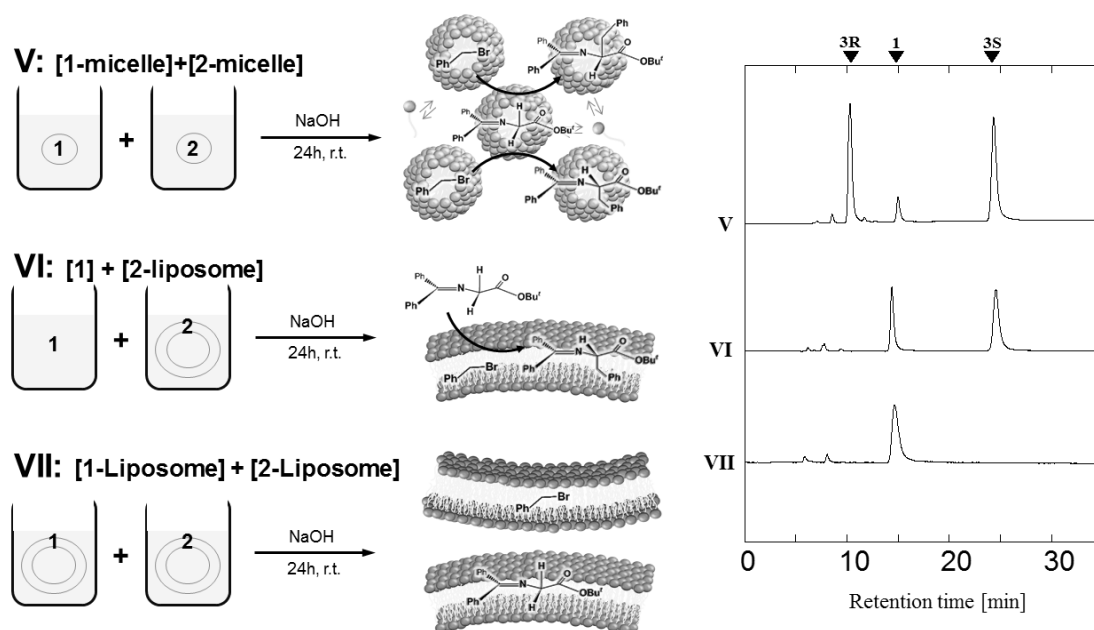
### 3.2 Reaction site at the membrane interface.

To estimate possible reaction site in the liposome, **1** and **2** were independently incorporated into self-assemblies, and then the suspensions were mixed to initiate the reaction (Table 3-2, see also Figure 3-4). For the case of DOPC liposome, negligible amount of **3** was obtained, suggesting that both of **1** and **2** isolated by each membrane, and the reaction at membrane-membrane interface hardly happened (entry VII). In contrast, a mixing of **1** and **2**-preadsorbed DOPC liposome provided **3S**, indicating that the hydrophobic-hydrophilic interface of the liposome can act as the reaction site of this (entry VI). In the case of CTAB

**Table 3-2.** Reaction at the membrane interior or at inter membrane.

Entry	Amphiphile(assembly)	Medium	Conv.%	<i>e.e.</i> %(S-R)
V <sup>a</sup>	CTAB (micelle)	water	92 ±4	4 ±2
VI <sup>b</sup>	DOPC (liposome)	water	56 ±8	92 ±2
VII <sup>c</sup>	DOPC	water	<2	n.d. <sup>e</sup>
VIII <sup>d</sup>	DOPC	water	11 ±2	>90

<sup>a</sup> **1**-adsorbed CTAB micelle and **2**-adsorbed CTAB micelle suspensions were mixed to initiate reaction. <sup>b</sup> **1** was added to **2**-adsorbed DOPC liposome suspension to initiate reaction. <sup>c</sup> **1**-adsorbed DOPC liposome and **2**-adsorbed DOPC liposome suspensions were mixed to initiate reaction. <sup>d</sup> The reaction was conducted for 9 h at r.t.. <sup>e</sup> not detected.

**Figure 3-4** Schematic illustration of the alkylation of **1** with **2** at self-assembly interface in aqueous media. Based on the HPLC chart, conversion and *e.e.* values were calculated.

micelle system, a mixing of **1** and **2**, which were independently pre-adsorbed into CTAB micelles, successfully conducted the reaction, although the *e.e.* value was quite low (entry V). Because of low CAC value of CTAB, the membrane surface of its micelle could show dynamic nature, wherein CTAB molecules continuously associate and dissociate with each other and the entrapped reactants can then be in contact with the micellar interface. Such dynamic nature of CTAB micelle leads the racemic products, as well as TBAH in organic solvent-water system. On the contrary, the liposome membrane itself showed an advantage in enantioselectivity. **Table 3-3** shows the comparison of enantioselectivity in the alkylation of **1** with **2**, in the presence of reported PTCs [Ooi *et al.*, 1999, Kitamura *et al.*, 2005]. As tendency, the PTC possessing rigid structure shows high enantioselectivity (PTC-1, PTC-2, PTC-4, and PTC-5). Although self-assembled materials are classified as soft matter, we demonstrated the enantioselective alkylation of **1** with **2** by using liposome membranes as soft interface. High *e.e.* value was obtained at earlier stage of the reaction in the presence of DOPC liposome (entry

**Table 3-3.** Yield and *e.e.* of the alkylation of **1** with **2** in the presence of PTC.

Entry	Catalyst <sup>e</sup>	Medium	Yield (%)	<i>e.e.</i> % (S-R)
IX <sup>a</sup>	TBAH	water/CH <sub>2</sub> Cl <sub>2</sub>	78	-
X <sup>b</sup>	PTC-1	water/hexane	75	-66
XII <sup>b</sup>	PTC-2	water/hexane	85	64
XIII <sup>c</sup>	PTC-3	water/hexane	34	-21
XIV <sup>c</sup>	PTC-4	water/hexane	73	-79
XV <sup>d</sup>	PTC-5	water/hexane	98	-99

<sup>a</sup> See reference for detailed information [O'Donnell *et al.*, 1978]. <sup>b</sup> See reference for detailed information [O'Donnell *et al.*, 1989]. <sup>c</sup> See reference for detailed information [Kitamura *et al.*, 2005]. <sup>d</sup> See reference for detailed information [Ooi *et al.*, 1999]. <sup>e</sup> See Figure 3-3 for chemical structures.

VIII). Particularly, zwitterionic DOPC assemblies showed high *e.e.* values, indicating that the migration of reaction intermediate (step (ii)) into the interior of liposome was assisted by the interaction of it with lipid headgroup, which restrict  $\alpha$ -carbon of **1** attack to **2** existing in the membrane.

### 3.3 Evaluation of the polar environment constructed on the membrane surface.

Liposomes (DOPC, DPPC, and DOTAP) were found to give the higher enantioselectivity than CTAB micelle (**Table 3-2**). The enhancement of the reaction at the surface of liposome membrane can be related to the microscopic environment. Particularly, the membrane polarity, evaluated by Laurdan [Parrasassi *et al.*, 1991, Suga *et al.*, 2013], could be key parameter to understand surroundings of **1** and **2**. In brief, a spectrum of Laurdan includes multiple emission peaks depending on its surrounding, and the obtained spectrum can be deconvoluted to understand the balance of existing hydrophobic and hydrophilic environments. As shown in **Figure 3-5**, one is from Laurdan embedded in the hydrophilic area (green lines: membrane in disordered phase) and the other is from the hydrophobic area (blue lines: membrane in ordered phase). DOPC contains unsaturated alkyl chains (fluid phase at r.t.), showing the disordered phase as dominant (**Fig 3-5 (a)**). On the other hand, the fluorescence spectrum of DPPC (**Fig. 3-5(b)**), which only contains saturated alkyl chains (gel phase at r.t.), showed that the ordered phase was dominant. The phase states can be revealed by calculating  $GP_{340}$  values; The lower  $GP_{340}$  values ( $GP_{340} < -0.2$ , **Fig. 3-5(d)**) indicated the liquid-disordered ( $l_d$ ) phase, while higher  $GP_{340}$  values ( $GP_{340} > 0.3$ ) indicated the presence of solid-ordered ( $s_o$ ) phase. Our previous report also revealed that the hydrophobic molecules could adsorb onto disordered phase liposomes (e.g., DOPC liposome), indicating that the interaction between the hydrophobic reactants and the liposomes was stronger with DOPC than with DPPC. In the presence of the DPPC liposome, the conversion value was lower than other liposomes (entry XVI, **Table 3-4**). Un-adsorbed reactants (in aqueous phase) were less reactive in the bulk aqueous solution (*c.f.*,



**Table 3-4.** Conversion and *e.e.* values in the presence of self-assemblies in aqueous media.

Entry	Amphiphile (assembly)	Medium	Conv. (%)	<i>e.e.</i> % (S-R)
XVI	DPPC (liposome)	water	45 ±7	94 ±1
XVII	DOPC:CTAB=90:10 (liposome)	water	66 ±5	96 ±1
XVIII	DOPC:DDAB=90:10 (liposome)	water	54 ±7	96 ±2
XIX	DOTAP (liposome)	water	61 ±3	97 ±2

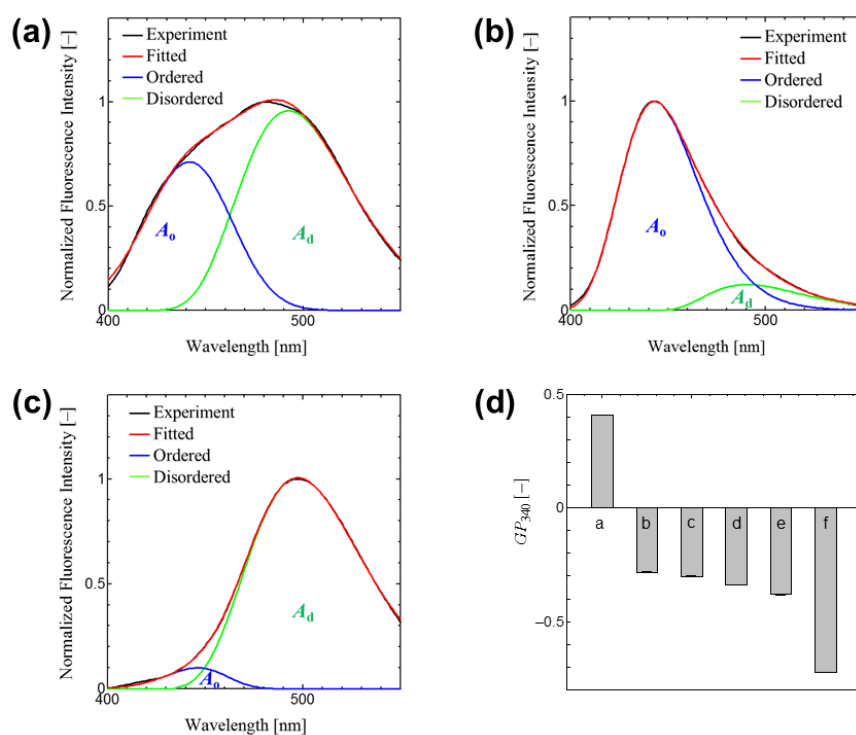


**Figure 3-5.** Fluorescence spectra of Laurdan in each self-assembly. (a) DOPC liposome, (b) DPPC liposome, (c) CTAB micelle. (d)  $GP_{340}$  values of each self-assembly. a. DPPC liposome, b. DOPC liposome, c. DOPC:CTAB=90:10 liposome, d. DOPC:DDAB =90:10 liposome, e. DOTAP liposome, f. CTAB micelle.

entry II). The effect on the membrane properties and the phase state of the liposome by the addition of CTAB and DDAB were also investigated. The DOPC liposome modified with CTAB and DDAB showed slight changes in the  $GP_{340}$  values, wherein the liposomes modified with CTAB and DDAB resulted in similar values of conversion and of *e.e.* (entries XVII and XVIII). Importantly, the analysis of Laurdan can distinguish the vesicles and micelles. Micelles show lower  $GP_{340}$  value ( $GP_{340} < -0.7$ ), and less hydrophobic environment of micelles could not produce enantioselectivity.

### 3.4 Discussion for the enantioselectivity of the reaction mechanism in the presence of liposomes.

According to Kitamura *et al.*, one successful strategy for the design of PTC is as follows: 1) quaternary ammonium, 2) rigid binaphthyl group, 3) flexible alkyl chain (PTC-5). Particularly, flexible alkyl chains increase polarity around ammonium group, which enables enolate to access the reaction pocket (see ref. [Ooi *et al.*, 1999] and **Figure 3-6**). A series of works by Maruoka *et al.* have reported the PTCs that can provide **3R**. Considering these previous findings, it is assumed that the interaction face of **1** (or deprotonated intermediate) with PTC is a key to gain the selectivity and the “active” plane of the alkylation can then be controlled. Considering the polarity of the carbanion intermediate of **1**, it could be located at the membrane surface. As a case study of asymmetric epoxidation, Kumar and Bhakuni reported that the specific interactions between the lipid and the guest molecule in liposomal configurations restrict the orientation of guest molecule at a specific sites, which has been exploited in stereospecific synthesis [Kumar *et al.*, 1996]. It is thus assumed that the controlled localization of reactants can provide stereospecificity of the product. In our case, one hypothesis is that the organized structure of lipid membranes has an advantage in the preference binding of **1** (or intermediate), thereby the reaction face (*Si* face (bottom side), *Re* face (top side), see **Figure 3-1**) can be restricted. The ionized lipid headgroup faces to bulk water while

hydrocarbon tails associate with neighboring lipid molecules in liposome membrane. Herein, possible interaction models for lipid molecule and **1** (carbanion) at the membrane were considered.

**3.4-1 Lipid chirality.** To verify the hypothesis, D-DPPC (enantiomer of L-DPPC (1,2-dipalmitoyl-*sn*-glycero-3-phosphocholine)) was used to form a liposome. As a result, no difference in conversion and *e.e.* values (**Table 3-5**). In general, a chiral selectivity is generated by the molecular chirality of catalyst. However, our result indicates that the enantioselectivity of the reaction rather generated by the platform (self-assembled lipid bilayer), independent of lipid chirality. The reaction intermediate of **1** is expected to be a planer structure after deprotonation of  $\alpha$ -carbon. Possible factors to promote the enantioselective reaction can herewith be described as follows: the quaternary ammonium group stabilizes anionic group of **1** intermediate (carbanion ( $\alpha$ -carbon) or enolate), hydrophobic interior attracts phenyl group of **1**, and hydrogen bond formation between the proton ( $\delta^+$ ) at  $\alpha$ -carbon of **1** intermediate and carbonyl group or phosphate group. At the liposome membrane, the orientation of lipid molecules is restricted irrelevantly to lipid chirality, revealing the less contribution of lipid chirality. To induce a chirality in product, at least “3-point” interaction between **1** and lipid molecules is necessary. Considering the laterally-organized structure of liposome, multiple lipid molecules could contribute to a stereospecific interaction with the intermediate. As a result, the *Re* face of **1** intermediate can be masked with lipid headgroup, then the alkylation was conducted mainly at *Si* face.

**Table 3-5.** Comparison of lipid chirality on enantioselectivity.

Entry	Amphiphile (assembly)	Medium	Conv. (%)	<i>e.e.</i> % (S-R)
XXI	D-DPPC (liposome)	water	39 $\pm$ 8	93 $\pm$ 1
XXII <sup>a</sup>	D-DPPC (liposome)	water	44 $\pm$ 7	90 $\pm$ 3

<sup>a</sup> **1** was added to **2**-adsorbed DOPC liposome suspension to initiate reaction.

**3.4-2 Phosphate group.** Phospholipids (DOPC, DPPC) are zwitterionic molecules, while DOTAP and CTAB are in alkylammonium salt form in self-assembly. By using DOTAP liposome, the effect of phosphate group can be discussed. As shown in **Table 3-6**, DOTAP liposome also provided **3S** with higher *e.e.* value, as well as DOPC liposome. The carbonyl group can be act as hydrogen bond donor, thus the speculated interaction between **1** and DOTAP molecules are electrostatic (at headgroup), hydrophobic (at membrane interior), and hydrogen bond (at carbonyl group) interactions. It is assumed that the counter ion (chloride) of DOTAP molecule forms ion pair with sodium cation at the reaction step (i), thereby the ion pair formed **1** intermediate could be migrated into the interior of the membrane at step (ii).

As summary, a supposed interaction mechanism of the reaction in the presence of DOPC liposome is shown in Figure e. In this study, although excess amount of amphiphiles was used as compared to reactants, we demonstrated that the liposome conducted the alkylation of **1** with **2** in aqueous media (without any organic solvent), and then obtained high enantioselectivity.

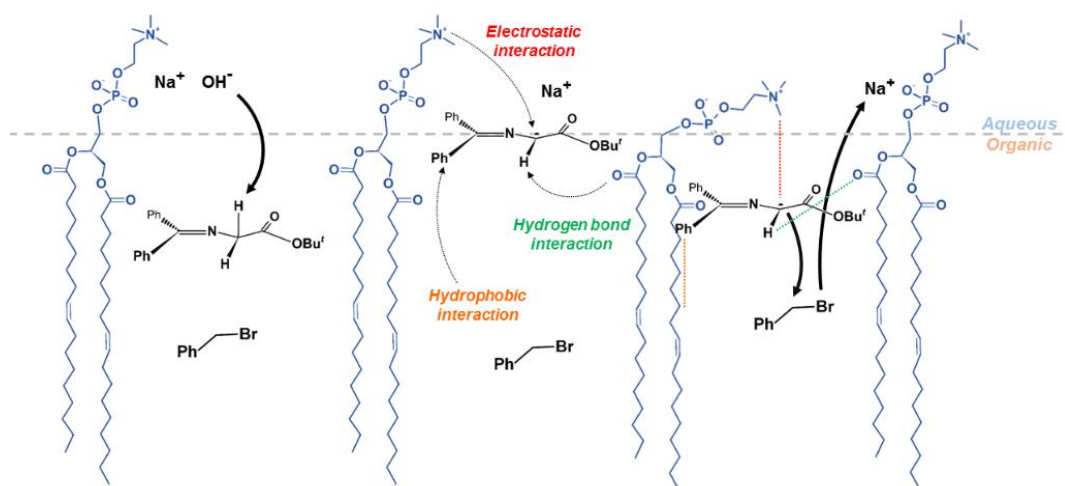


**Figure 3-6.** Plausible mechanism of the alkylation of **1** with **2** at DOPC liposome interface.

#### 4. Summary

Phospholipid vesicles were found to be utilized as a platform for selective alkylation reaction of amino acid derivatives. While the racemic products were obtained in water/dichloromethane system and CTAB micelle system, the reaction in the phospholipid vesicle suspension resulted in the formation of only one type of enantiomer as a product. The conversion of the reaction was influenced by the environment which vesicle formed, but the enantioselectivity was always high regardless of the chemical structure and the chirality of vesicle components. This finding indicated that the localization of the reactants was the important factor for regulating the reaction and its selectivity. The gradient in the dielectric constant of the bilayer in the vesicle membrane and the multiple interaction (electrostatic interaction, hydrogen bond, hydrophobic interaction, etc.) may cause the reactants to align in the favorable position for the selective reaction.

As a summary of chapter 1 through chapter 3, a strategy for the design of the membrane surface of the self-assembly was finally proposed (**Fig. 3-7**). Based on the results in chapter 2, the reaction rate was found to become larger with the solid-ordered lipid vesicles than that of liquid-disordered lipid vesicles. The difference among them was caused by the micro-environment at the surface of the lipid self-assembly formed. The lipid vesicles at solid-ordered phase formed the hydrophobic environment ( $\epsilon' \sim 3$ ), which is advantageous for the reaction including hydrophobic molecules. However, since lipids are packed closely in the solid-ordered vesicle, the amount of the adsorbed reactants and the yield of the reaction were relatively low as compared with those of liquid-disordered vesicles. Therefore, the best platform for the reaction is that the vesicle should first be in liquid-disordered phase and the adsorption of hydrophobic reactants should then change the membrane platform to be more ordered (form hydrophobic environment), so that the enhanced reactivity can be achieved. Based on the results from chapter 1, the micro-polarity and micro-viscosity of the vesicle membrane could be varied

by the addition of hydrophobic molecules. This finding indicates the important factor to design the vesicle as a platform for the reaction; the degree of the change in the membrane properties by the interaction between lipids and reactants can be the parameter to evaluate the interfacial reaction at the pseudo-interphase of lipid vesicles. For example, DOTAP vesicle represented the notable change in the membrane properties to be more ordered vesicle membrane after the addition of BNO, which probably contributes to the highest observed reaction rate.

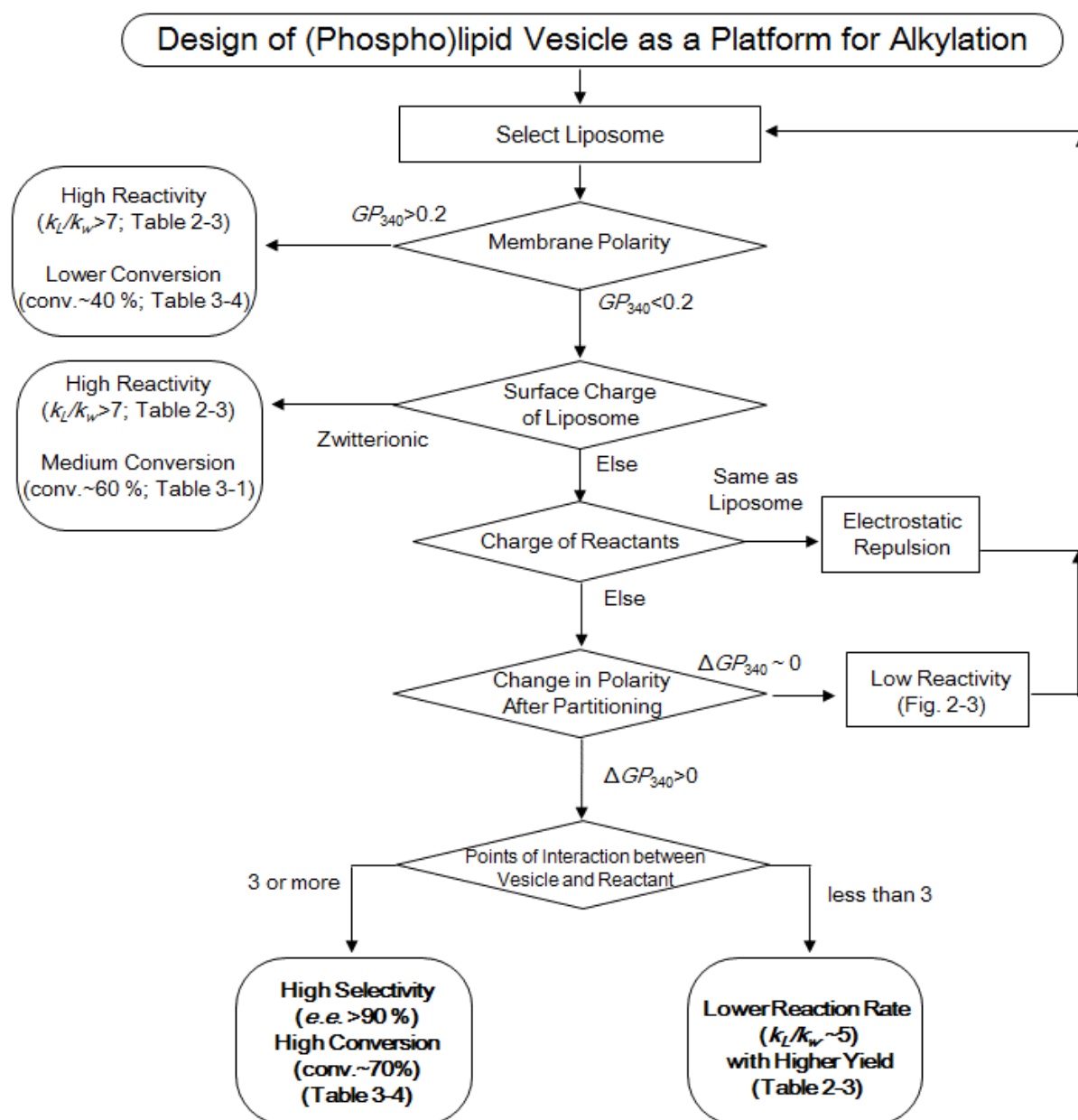


**Figure 3-7.** Scheme for the design of lipid vesicles as a platform for alkylation.

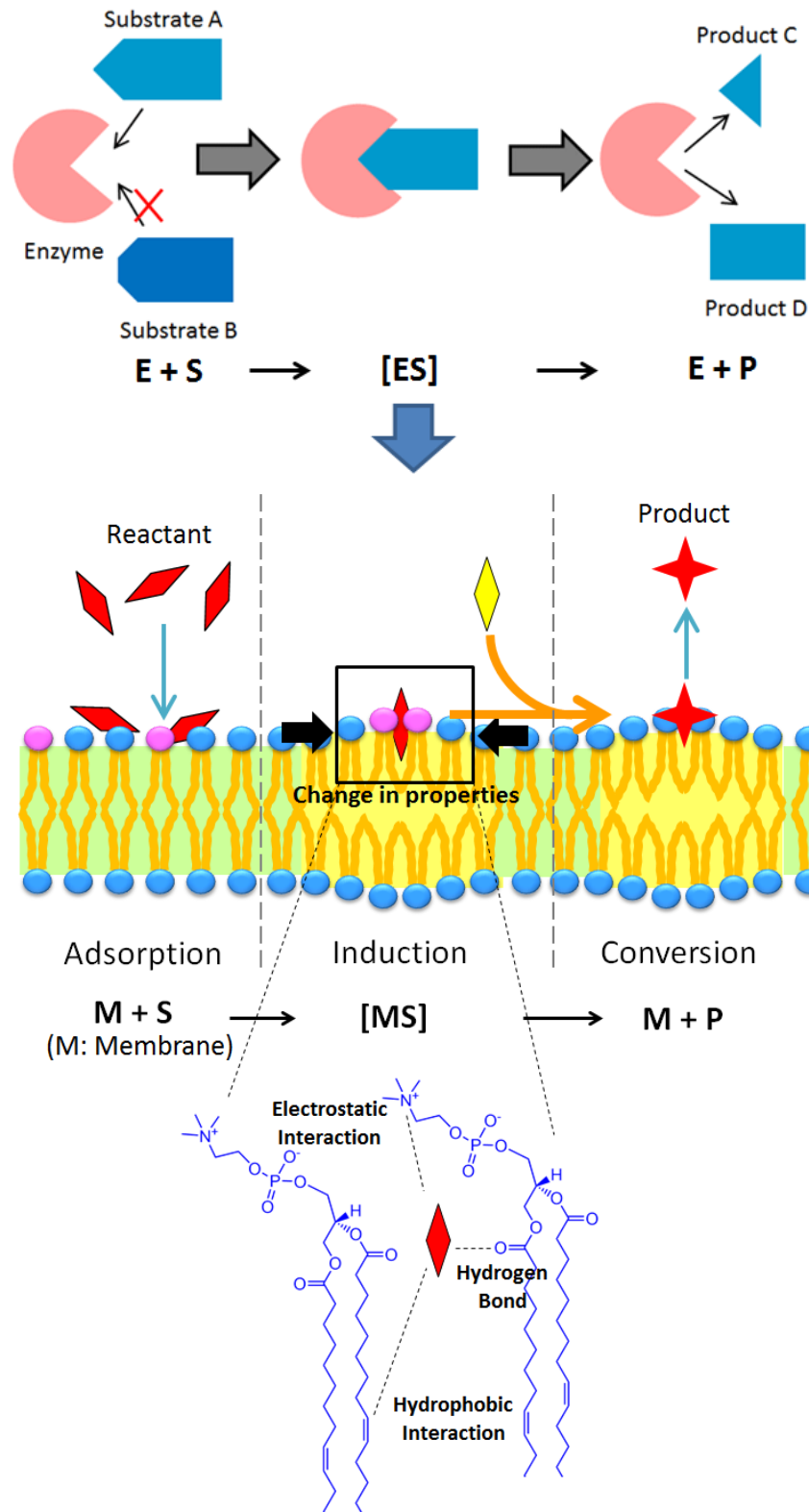


**Figure 3-8.** Schematic illustration of the enhancement of the reaction at the surface of vesicle.

In the enantioselective alkylation of amino acid derivatives, similar effects are expected. Although further analysis would be required, the change in the membrane properties for the improvement of the reaction can be assumed since multiple interactions were required for the enantioselective reaction. These series of events are relevant to the aspect of artificial enzymes, while the designed membrane surface was utilized as a platform of molecular recognition and its (enantio-)selective conversion, like as an enzymatic active center (**Fig. 3-8**). First, the adsorption of the substrate occurs, and the properties of the vesicle were varied by the interaction. Finally the reaction can proceed and is enhanced by the change in the membrane properties. Considering the reaction process, more variations in the vesicle with the variety of membrane properties would be welcome to evaluate more precisely. Especially, the self-assemblies between liquid-ordered vesicle and micelles are useful that it may achieve the high conversion and high selectivity in the alkylation reaction. The new vesicles with new physicochemical properties will be discussed in chapter 4, and further reaction mechanisms and discussions will be described in chapter 5, but the possibility of the phospholipid vesicles utilized as a platform for the enantioselective reaction was herewith proposed. It is expected that the vesicle membranes can be utilized as a strong new tool for safe and clean organic synthesis processes.



# Chapter 4

## Characterization and Evaluation of the Self-Assembly Systems

### Composed of Fully-Synthetic Amphiphiles

#### 1. Introduction

In the former chapters, the reaction processes in the aqueous media with self-assembly system were discussed. Liposomes represented the fair effect on the interfacial reaction of 1,3-dipolar cycloaddition and represented large effect on the selectivity of amino acid derivative alkylation. However, more self-assembly systems with various membrane properties are demanded to evaluate the effect of self-assembly system on the alkylation reaction, especially the self-assembly systems with membrane properties between micelles and lipid vesicles. Membrane properties of the vesicle are dependent on the chemical structure of the vesicle component, which suggest that phospholipid vesicles represent similar properties since some moieties are in common. Because the physicochemical properties are the key factors of regulating the chemical processes at the membrane surface, it is essential to prepare the vesicles with variety of membrane properties. For the objective, other materials with shorter alkyl chains and larger hydrophilic head group were attempted to form vesicles. Based on the previous reports from other scientists, cationic surfactant DDAB (dilauryldimethylammonium bromide) and anionic surfactant AOT (sodium bis(2-ethylhexyl) sulfosuccinate) were focused as a component of the vesicle membrane. AOT is usually used as an extractant or for the formation of nanoparticles; Aires-Barros *et al.* have reported the separation and purification of lipases using AOT [Aires-Barros *et al.*, 1991], and Taleb *et al.* have reported the formation of silver nanoparticles from AOT reverse micelles [Taleb *et al.*, 1997]. Similarly, DDAB is usually

carried out as a modifier of the self-assembly. DDAB can be used in the process including biological molecules such as the adsorption of DNA and the having influences on the cells [Bonincontro, *et al.*, 2008, Han,1996]. However, AOT and DDAB can self-assemble into vesicles by only dissolving them into aqueous media [Saha *et al.*, 2011, Viseu *et al.*, 2000], and expected to represent the different properties from lipid vesicles.

Other advantages of the vesicle formation by fully-synthetic surfactants such as AOT and DDAB are the cost and reusability. For the application to the industrial use, lipid vesicles were not appropriate due to its expensive cost. In addition, since the interaction between lipid molecules and reaction substrates are relatively strong, so that the additional steps for the recovery of the product would be required. Furthermore, liposomes are considered to be decomposed into lipids after the recovery process, which is the big disadvantage of liposomes for the industrial use. To reuse the lipids, additional separation process will be required since lipids do not form self-assemblies in aqueous media without the preparation of thin film. Which means, although the chemical reaction processes at the liposome surface represented the

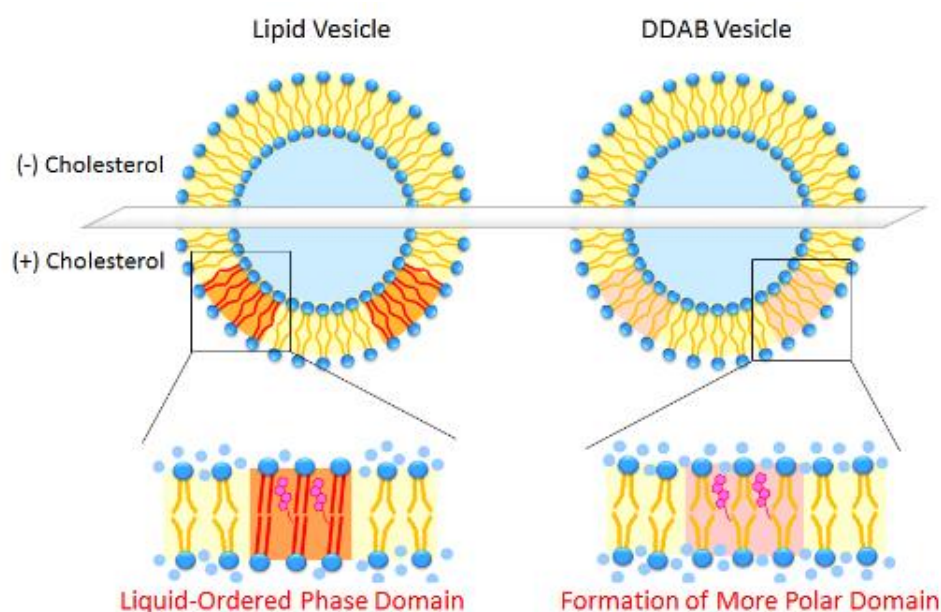


**Figure 4-1** Schematic illustration of the study in this chapter

excellent effect on the reactivity and selectivity, the process is facing a big problem to apply to the field of industry. Since AOT and DDAB can self-assemble into vesicles by only dissolving them into aqueous media, the deformation and the re-construction of the vesicles are much easier compared to the phospholipid vesicles. For example, it is required to adjust the pH and concentration of salts to construct AOT vesicle [Bergenholtz *et al.*, 1996, Sagar *et al.*, 2011, Lin, *et al.*, 2008, etc.], which indicates that the deformation and re-construction of AOT vesicles can be controlled by changing pH and concentration. In addition, critical vesicle concentrations of surfactants are relatively higher (order of millimolar) than that of phospholipids (less than micromolar order). If the concentration of surfactants can be controlled continuously by dilution and enrichment, the assembly of the surfactants can also be regulated. This finding suggests that the recovery of the product can be separated from surfactants by the deformation of vesicles, and vesicles can be reconstructed after the separation.

However, physicochemical properties of fully-synthetic surfactant vesicles such as DDAB vesicle or AOT vesicle have not been clarified yet. In this chapter, the condition for the formation of DDAB vesicle and AOT vesicle were investigated, and their surface properties were characterized (**Figure 4-1**). In relation to chapter 1, the effect of additives was also investigated to regulate the membrane surface properties similar to phospholipid membranes. The plausible interaction between vesicles and additives could be discussed with the results obtained, suggesting the general aspect of regulating the vesicle membrane.

## 2. Materials and Methods

### 2.1 Materials.

1,2-Dioleoyl-*sn*-glycero-3-phosphocholine (DOPC), 1,2-dipalmitoyl-*sn*-glycero-3-phosphocholine (DPPC), and 1,2-dioleoyl-3-trimethylammonium-propane (DOTAP, chloride salt) were purchased from Avanti Polar Lipid (Alabaster, AL, USA). AOT, *p*-aminodiphenylamine (PADPA), cholesterol, Laurdan, Prodan (*N,N*-Dimethyl-6-propionyl-2-naphthylamine), and 1,6-diphenyl-1,3,5-hexatriene (DPH) were purchased from Sigma-Aldrich (St. Louis, MO, USA). DDAB (purity>98.0%) was purchased from Tokyo Chemical Industry (Tokyo, Japan), and 1-Hexanol and other chemicals were purchased from Wako Pure Chemical (Osaka, Japan). PADPA was used after purification by recrystallization, and other chemicals were used without further purification.

### 2.2 Preparation of Vesicles.

A chloroform solution with lipids (including DDAB and AOT) was dried in a round-bottom flask by evaporation under a vacuum. The obtained thin film was dissolved in chloroform again, and the solvent was evaporated. The thin film was kept under a high vacuum for at least 3 hours, and was then hydrated with ultrapure water at room temperature. In the case of AOT vesicle, 0.1 M NaH<sub>2</sub>PO<sub>4</sub> aqueous solution was used for the hydration. The vesicle suspension was frozen at -80 °C and thawed at 50 °C to enhance the transformation of small vesicles into larger multi-lamellar vesicles (MLVs). This freeze-thaw cycle was performed five times. MLVs were used to prepare the large unilamellar vesicles by extruding the MLV suspension 11 times through two layers of polycarbonate membranes with mean pore diameters of 100 nm using an extruding device (Liposofast; Avestin Inc., Ottawa, Canada).

### **2.3 Measurement of the vesicle diameter.**

The average sizes of the vesicles were measured by dynamic light scattering (DLS) (ELS-8000, Otsuka Electronics, Osaka, Japan). The total concentrations of lipids were 1.0 mM. Each size distribution of the suspension was calculated from the result with Marquadt method.

### **2.4 Evaluation of membrane polarities.**

The emission spectra were measured by using a fluorescence spectrophotometer (FP-6500; Jasco, Tokyo, Japan) with an excitation wavelength of 340 nm after 30 min incubation at room temperature in dark, and the general polarization ( $GP_{340}$ ), the membrane polarity, was calculated as follows:

$$GP_{340} = (I_{440} - I_{490}) / (I_{440} + I_{490}),$$

where  $I_{440}$  and  $I_{490}$  represent the fluorescence intensity of Laurdan at 440 nm and 490 nm, respectively. The total concentrations of lipid and Laurdan were 1.5 mM and 15  $\mu$ M, respectively.

The fluorescent spectrum of Laurdan can be deconvoluted into two spectra by using the software Peakfit (Systat Software Inc., CA, USA): one is from ordered phase and another is from disordered phase. By calculating the area of the spectrum from ordered phase ( $A_o$ ) and the spectrum from disordered phase ( $A_d$ ), the area ratio of ordered phase and disordered phase in actual vesicle was determined.

### **2.5 Evaluation of membrane fluidity.**

The membrane fluidity ( $1/P$ ) was measured by the fluorescent probe DPH. The final concentrations of lipid and DPH were 1.5 mM and 6.0  $\mu$ M, respectively. The fluorescence polarization of DPH (Ex = 360 nm, Em = 430 nm) was measured with a fluorescent spectrophotometer (FP-6500; Jasco, Tokyo, Japan) after 30 min incubation at room temperature in dark. The sample was excited at 360 nm with vertically polarized light, and emission

intensities both perpendicular ( $I_{\perp}$ ) and parallel ( $I_{\parallel}$ ) to the excited light were recorded at 430 nm.

The fluidity ( $1/P$ ) of DPH was then calculated using the following equations:

$$1/P = (I_{\parallel} - GI_{\perp}) / (I_{\parallel} + GI_{\perp})$$

$$G = i_{\perp} / i_{\parallel}$$

where  $i_{\perp}$  and  $i_{\parallel}$  are emission the intensities, perpendicular and parallel to the horizontally polarized light, respectively, and  $G$  is the correction factor.

### 3. Results and discussions

#### 3.1 Formation of DDAB/Cholesterol vesicles and the characterization by Laurdan

DDAB molecules were known to form bilayer vesicles in aqueous media. Viseu *et al.* and Caria *et al.* have previously observed the DDAB vesicle formation by using Cryo-TEM (**Figure 4-2**) [Viseu *et al.*, 2000, Caria *et al.*, 1996], and from another point of view, Caboi *et al.* have confirmed DDAB vesicle formation by using NMR [Caboi *et al.*, 1996]. To confirm the vesicle formation by the hydration of thin film composed of DDAB and cholesterol, the self-assemblies were first characterized by DLS. **Figure 4-3** shows the size distribution of each self-assembly. The diameters of the self-assemblies were distributed from 70 nm to 200 nm, indicating the formation of vesicle structure in an aqueous solution. The size distribution of the DDAB vesicle was mono-dispersed with rather narrow width and its average diameter was estimated as  $125 \text{ nm} \pm 48 \text{ nm}$ . In the case of DDAB vesicle modified with cholesterol, a similar tendency was obtained; the size distribution was ranged between 100-200 nm and the average diameter was  $127 \text{ nm} \pm 57 \text{ nm}$ , indicating that the vesicle structure of DDAB self-assembly was still kept after the modification by cholesterol, similarly in the case of other cationic lipid (such as DOTAP). However, the width of size distribution in the above vesicles was relatively large

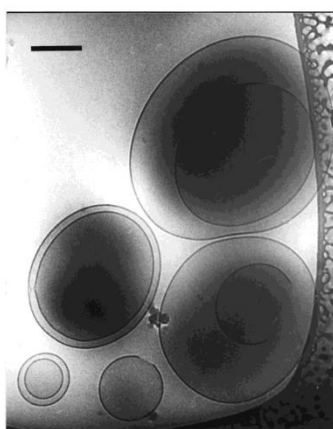


**Figure 4-2** Cryo-TEM image of DDAB vesicle. The image was taken from previous report [Viseu, 2000].

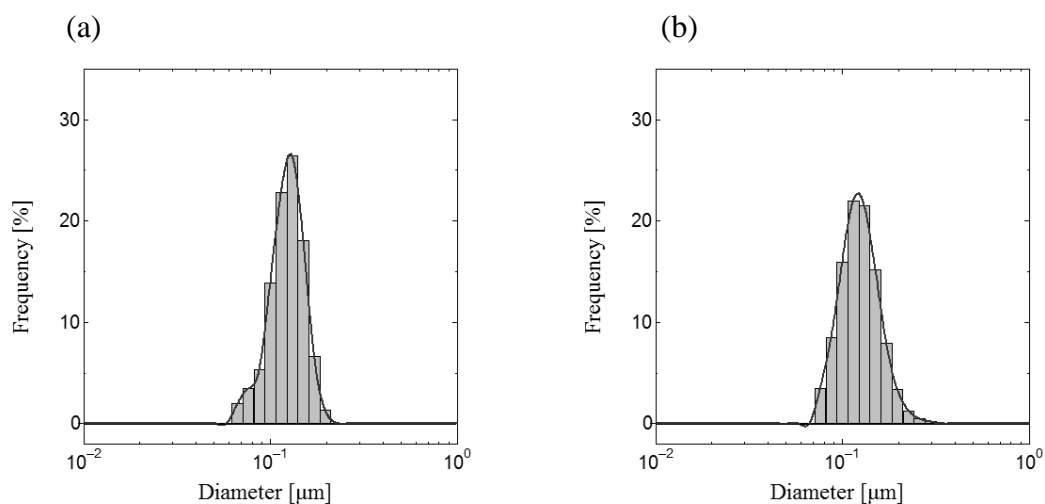


**Figure 4-3** Diameters of self-assembly analysed by DLS. (a) DDAB, (b) DDAB:Cholesterol=80:20.

in contrast to the lipid vesicles, such as DOPC liposomes. This is probably due to the higher fluidic nature of the vesicle membrane. The critical aggregation concentration (CAC) of DDAB was relatively lower than that of phospholipid vesicle (e.g. DOPC) or cationic vesicle (e.g., DOTAP). With regards to the chemical structure of DDAB, the lack of carbonyl group could decrease hydrogen bond interactions between the membrane-constituting molecules at the headgroup region. This assumption indicates that the lateral association of DDAB molecules are weak, which leads to the size distribution of DDAB vesicle during extrusion method.

To characterize the properties of DDAB vesicles, the fluorescent probe method was employed. A fluorescent probe, Laurdan, reflects the hydration environment of the self-assembly, and the fluorescent spectra of Laurdan can represent the phase state of the vesicle. **Figure 4-4** shows the typical Laurdan spectra of DDAB:cholesterol vesicles in different ratios. Within the vesicular system, the spectrum of Laurdan can be considered as the sum of two spectra; one is from Laurdan distributed at the disordered phase of the vesicle (the spectrum which shows the fluorescence peak around 450 nm) and another is from the one located at the



ordered phase (the spectrum which shows the peak around 500 nm). The deconvoluted spectra showed that disordered phase was obviously dominant in DDAB vesicle and regarded as liquid-disordered phase, and the proportion of ordered phase became larger with the increase in the ratio of cholesterol in DDAB/cholesterol vesicle. In DDAB/cholesterol=60/40 vesicle, the spectrum clearly showed both of the ordered phase and disordered phase, suggesting the heterogeneity of the membrane as in the phospholipid/cholesterol vesicles.

Not only the cationic DDAB vesicle, but also the characterization of anionic AOT vesicle was investigated for the variation of the vesicle membrane. Since AOT vesicle was already confirmed by many scientists [Bergenholtz *et al.*, 1996, Sagar *et al.*, 2011, Lin, *et al.*, 2008, etc.] and the application as a platform for chemical reaction has been reported [Junker *et al.*, Luginbühl, *et al.*, 2016], this thesis is focused on the characterization of AOT vesicle by using fluorescent probes, mainly Laurdan. In the case of AOT vesicle, cholesterol is too big to be distributed in the bilayer of AOT, so the smaller molecule 1-hexanol was used as one of the modifiers. PADPA was also carried out which is expected to interact with AOT strongly through hydrophobic interaction and electrostatic interaction. **Figure 4-5** also shows that the disordered phase is dominant in pure AOT vesicle membranes, while ordered phase dominates in vesicles composed of AOT and PADPA, for example at [AOT]/[PADPA] = 74:24. The area below the deconvoluted spectra assigned to the ordered phase ( $A_o$ ) and the one assigned to the disordered phase ( $A_d$ ) are almost the same in a vesicle suspension composed of AOT, hexanol, and PADPA at a molar ratio of 74:19:7 or in a vesicle suspension composed of AOT and aniline at a molar ratio of 87/13, suggesting the presence of heterogeneous vesicle membranes.

Area ratio values ( $A_o/A_d$ ) for various vesicle samples, including vesicles formed from phospholipids, were then calculated from the recorded and deconvoluted spectra. For DOPC liposomes (in the  $l_d$  phase at room temperature), the  $A_o/A_d$  ratio was 0.16. On the other hand, the  $A_o/A_d$  ratio for DPPC liposomes (in solid-ordered ( $s_o$ ) phase at room temperature),  $A_o/A_d$  was 6.6. In the case of [DOPC]/[DPPC] = 60/40 liposomes, which form a heterogeneous

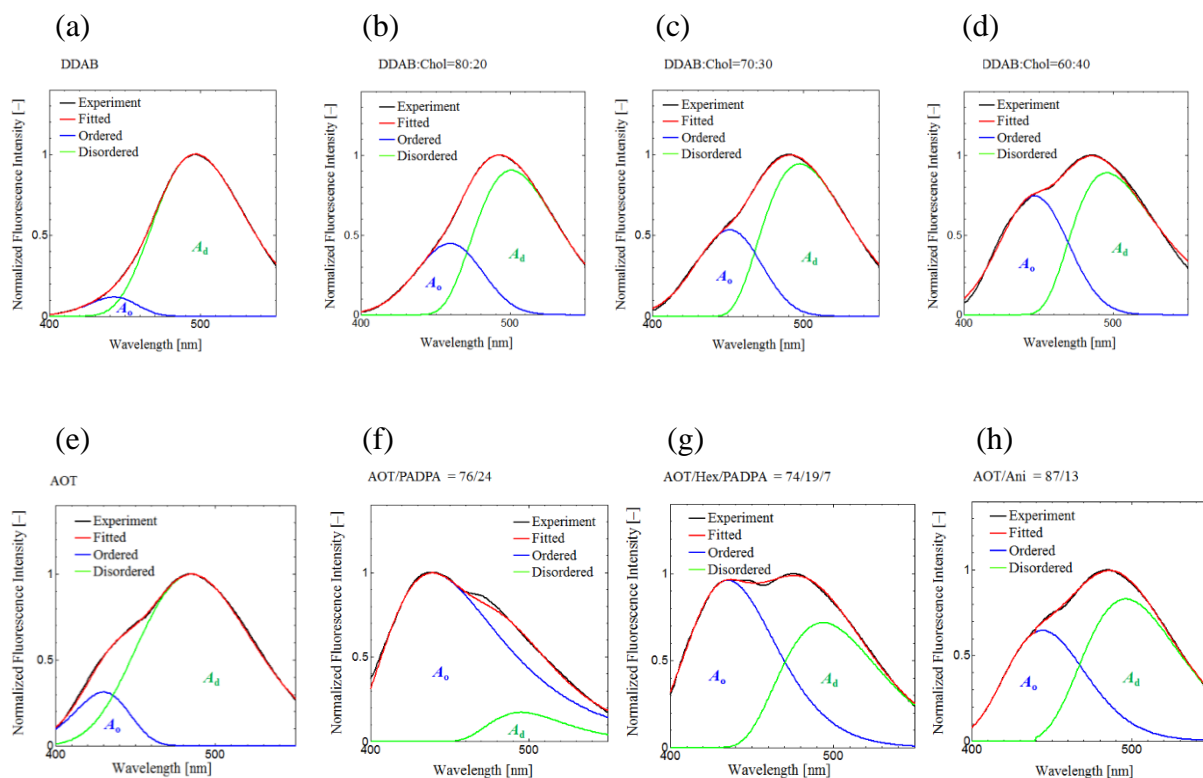


**Figure 4-4** Deconvolution of Laurdan spectra. (a) DDAB, (b) DDAB/Chol=80/20, (c) DDAB/Chol=70/30, (d) DDAB/Chol=60/40, (e) AOT, (f) AOT:PADPA=76:24, (g) AOT:hexanol:PADPA=74:19:7, (h) AOT:aniline=87:13. Each line indicates the experimental result (black), fitted line (red), the spectral fraction of ordered phase (blue), and the spectral fraction of disordered phase (green).  $A_o$  and  $A_d$  are the peak areas of the spectral fractions of ordered phases and disordered phases, respectively.

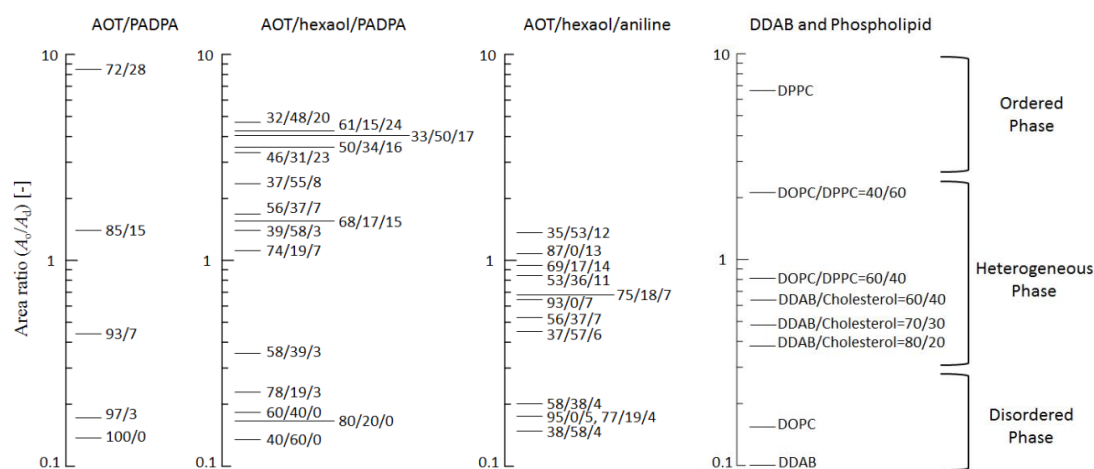


**Figure 4-5** The area ratio ( $A_o/A_d$ ) of the vesicles calculated from the area discussed in Fig. 4-4.

membrane (coexistence of  $l_d$  and  $s_o$  phases at room temperature). The  $A_o/A_d$  ratio was 0.45, which is between the values for the ordered and the disordered phases. This indicates that the  $A_o/A_d$  ratio can be taken as an indicator of the different membrane phase states. We distinguish vesicle membranes which have an ordered phase as those with  $A_o/A_d > 2.5$  (arbitrarily chosen) from vesicle membranes which are in the disordered phase ( $A_o/A_d < 0.3$ , arbitrarily chosen). In the range  $0.3 < A_o/A_d < 2.5$ , heterogeneous phases are present.

By applying this parameter to DDAB and AOT vesicles, the DDAB/cholesterol vesicles, containing  $>20\%$  cholesterol, could be regarded as heterogeneous vesicle, although these vesicles showed much more polar environment than that of conventional phospholipid vesicles. The result indicates that the effect of cholesterol that changes vesicle membrane to be more ordered could occur with DDAB vesicle similarly to that with phospholipid vesicles. In the pure AOT vesicle suspension, the  $A_o/A_d$  ratio was 0.15, confirming the disordered state of the AOT membrane. For AOT/PADPA=76/24, the membrane clearly turned into an ordered state

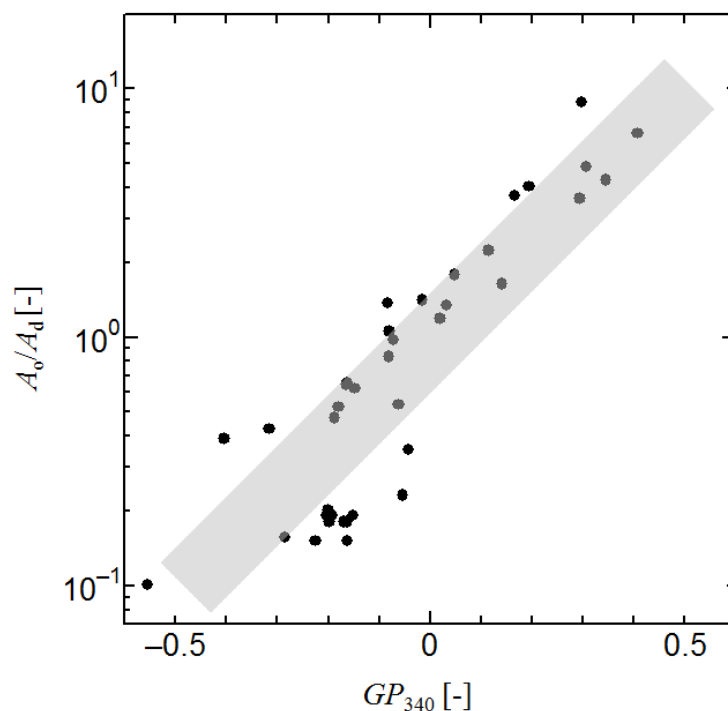


**Figure 4-6** The relationship between the area ratio ( $A_o/A_d$ ) and  $GP_{340}$  values of the vesicles.

( $A_o/A_d=8.8$ ), again in agreement with the discussion above. Moreover, the deconvolution analysis indicates that the AOT/hexanol/PADPA=74/19/7 and the AOT/aniline=87/13 vesicles have a heterogeneous membrane with intermediate  $A_o/A_d$  ratios ( $A_o/A_d=1.18$  and  $1.05$ ), *i.e.*, they contain nanosized ordered domains within a fluid membrane matrix. As a result, the addition of aniline leads to a change of the phase state of the AOT bilayer to a heterogeneous phase, but there is no indication that the phase becomes fully-ordered. One possible reason is that aniline is a too small molecule so that the weak hydrophobic interactions do not result in a drastic alteration of the membrane properties, although strong electrostatic interactions are expected to exist, so that the mobility of some of the AOT molecules is decreased (possible formation of ordered patches). On the other hand, the addition of PADPA to AOT vesicles leads to a strong ordering of the membrane. This is a result of the stronger binding of PADPA to the vesicles (electrostatic as well as hydrophobic interactions). Through the deconvolution of the Laurdan fluorescence spectra, the area and the composition of each phase state could be calculated. In addition, the values of area ratio were relating to the values of  $GP_{340}$ , which can be used to evaluate membrane polarity (**Fig. 4-6**). The values of  $GP_{340}$  reflect the hydration environment of the vesicle membrane, and the values of area ratio were used to represent the phase state of the vesicles. These two values are correlating with each other, suggesting that the phase state of the vesicles is closely related to the polarity of the vesicle membrane.

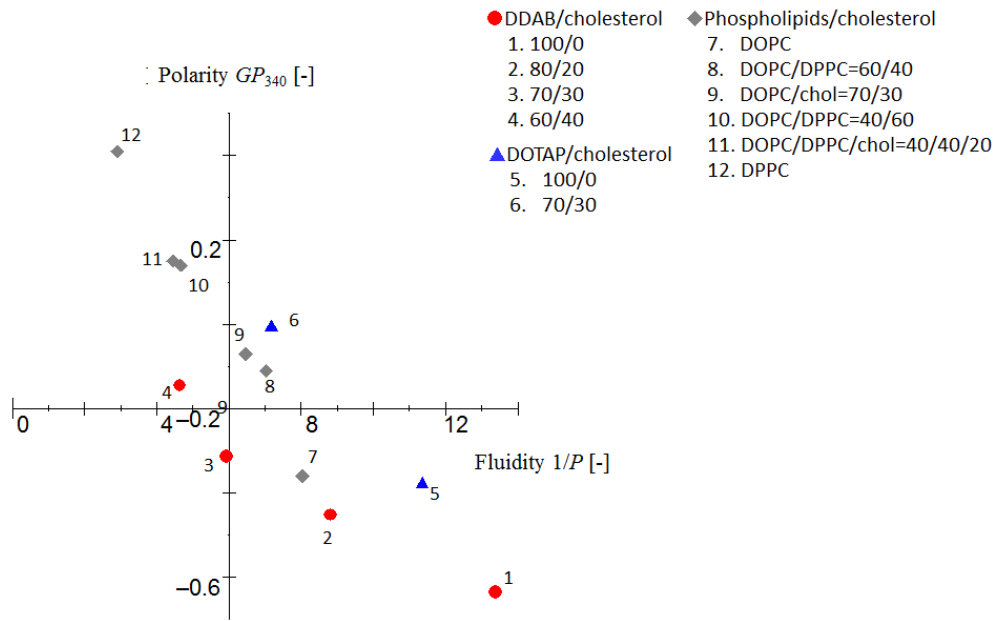
### 3.2 The interaction model of surfactants and additives

To obtain the corroborative result for the membrane properties of DDAB/cholesterol vesicles and AOT/PADPA vesicles, another fluorescent probe, DPH, was also used to analyze the membrane fluidity of the vesicles. **Figure 4-7** shows the membrane polarity and membrane fluidity of various kinds of vesicles. In this diagram,  $x$ -axis represents the membrane fluidity and  $y$ -axis represents the membrane polarity. The cross point of  $x$ - and  $y$ -axes is the threshold point of the phase transition in ordered phase and disordered phase. In this diagram, vesicles in

disordered phase are plotted in the fourth quadrant (large  $1/P$  and low  $GP_{340}$  values), in ordered phase are plotted in the second quadrant (small  $1/P$  and high  $GP_{340}$  values), and in heterogeneous phase are plotted in the first quadrant (intermediate  $1/P$  and high  $GP_{340}$  values). Based on this diagram, DDAB vesicle can be plotted on the fourth quadrant and considered to form disordered phase vesicle. It was found that DDAB vesicle showed relatively higher polarities ( $GP_{340} < -0.5$ ) and higher fluidities ( $1/P > 12$ ), even when compared to the lipid vesicles in disordered phase as well as DOPC or DOTAP vesicles. It can be also interpreted that the effect of cholesterol is different in DDAB vesicle and lipid vesicles (DOPC, DOTAP). In DOPC and DOTAP liposomes, the membrane polarities increased and membrane fluidities decreased in the same manner. On the other hand, the addition of cholesterol to DDAB vesicle resulted in a larger decrease in the fluidity and a smaller increase in the membrane polarity. In the case of AOT vesicle, apart from the observation that the addition of aniline to AOT bilayers leads to a measurable decrease in membrane fluidity, and that the addition of PADPA to the same bilayers leads to an even stronger decrease in fluidity, as discussed above, the surprising finding is that the effect of PADPA on AOT bilayers has effects which so far were only observed for vesicle membranes composed of mixtures of phospholipids or mixtures of phospholipids and cholesterol (formation of nanodomains).

The differences can be explained by the way cholesterol and lipids (including DDAB molecules) are interacting (**Fig.4-8**). It is considered that cholesterol can stiffen the vesicle through the hydrogen bonding between hydroxyl group in cholesterol and carbonyl group in phospholipids, resulting in the formation of another rigid phase known as liquid-ordered phase. However, the interaction between cholesterol and DDAB was only hydrophobic interaction due to the lack of carbonyl group. Hydrophobic interaction mainly takes place at the hydrocarbon (HC) region of the vesicle where DPH can monitor, although hydrogen bond takes place in the intermediate (IM) region where glycerol and carbonyl groups are present and Laurdan mainly monitors. Therefore, the influence to the Laurdan spectrum was significant in DOPC and

(a)



(b)

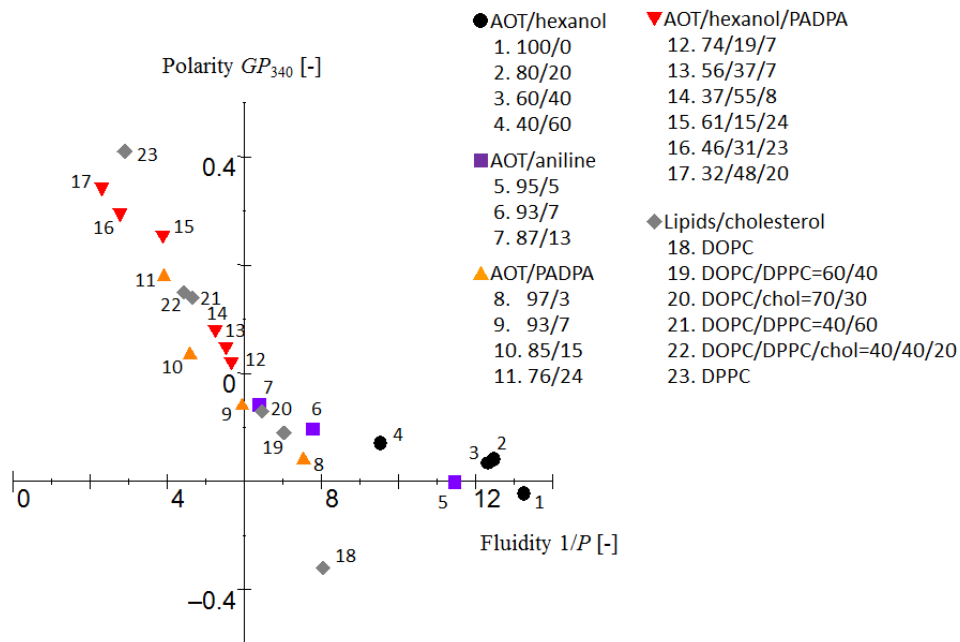


**Figure 4-7** Summary of the (a) DDAB and (b) AOT vesicle membrane fluidity and polarity changes after the addition of modifiers in comparison with phosphatidylcholine and mixed phosphatidylcholine/cholesterol membranes. The membrane polarities and fluidities were measured at room temperature.

DOTAP vesicles due to the stronger interaction (hydrogen bonding) while the hydrophobic interaction was dominant in DDAB/cholesterol vesicles. The similar effect could be observed in the AOT/PADPA vesicular system that incorporation of the protonated form of PADPA (PADPAH<sup>+</sup>) in an AOT bilayer may involve not only electrostatic but also CH- $\pi$  van der Waals interactions, which leads to the vesicle of similar properties to phospholipid/cholesterol mixture.

Furthermore, **Figure 4-7** shows another unique characteristic of DDAB vesicles. As previously mentioned, conventional vesicles composed of phospholipid and cholesterol are plotted in the first, second, and fourth quadrants in the Cartesian diagram. That is, lipid vesicles which has property of being plotted in third quadrant had not been developed. The plots of cholesterol modified DDAB vesicle appears in the third quadrant, which is considered as the new properties of vesicle. The phase state which DDAB/cholesterol vesicle formed was considered to be similar to liquid-ordered phase, but a little different (liquid-ordered-like phase). Third quadrant in **Figure 4-7** represents that the membrane fluidity is relatively low while the membrane is polar. DDAB/cholesterol=70/30 showed such a characteristic, which may be utilized as a new platform for the chemical process. For example, our previous report revealed that the hydrophobic molecules were more distributed into vesicles with polar environment than vesicles with less polar environment. However, the reaction rate of 1,3-dipolar cycloaddition was higher with the vesicles of lower polarity and fluidity. These findings suggest that the DDAB/cholesterol vesicles, which showed the characteristics of polar environment and low fluidity, have the possibility to enhance the reaction such as 1,3-dipolar cycloadditions. The membrane properties are also important for highly selective reaction, regulating the reactants within the bilayer. In summary, fully synthetic surfactant DDAB can form the heterogeneous vesicle with cholesterol, and DDAB/cholesterol vesicle can show the different characteristics as compared to conventional vesicles such as DOPC/cholesterol vesicle.

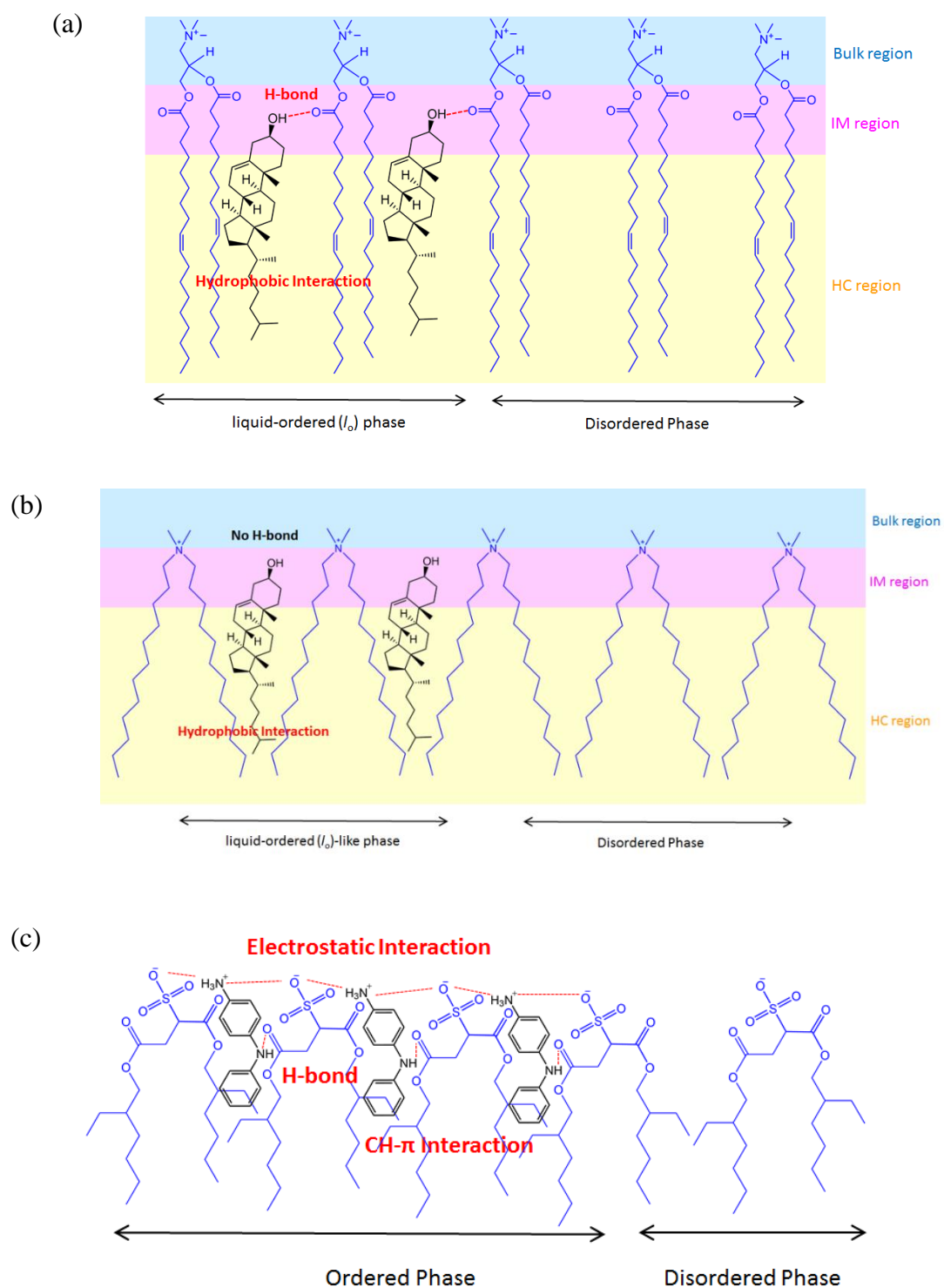


**Figure 4-7** The interaction model of (a) DOTAP and cholesterol, (b) DDAB and cholesterol, and (c) AOT and PADPA. IM region and HC region stand for intermediate region and hydrocarbon region, respectively.



#### 4. Summary

The properties of DDAB vesicle and AOT vesicle membranes were successfully characterized, resulting that their membrane properties are polar and highly fluid as compared to conventional phospholipid vesicles. The variations in the physicochemical properties of vesicles was achieved by using non-natural surfactant as a vesicle component. Focusing on the DDAB vesicle, the membrane properties could be regulated with the modification of cholesterol. DDAB/cholesterol vesicle showed the heterogeneous phase according to the experiment with fluorescent probes. Although the tendency of being heterogeneous was similar to that of phospholipid vesicles, DDAB/cholesterol vesicles also represented the big difference that the membrane polarity evaluated by Laurdan was notably high ( $GP_{340} < -0.2$ ), probably due to the lack of hydrogen bonding. The result suggested the difference in the interaction model of cholesterol against the DDAB vesicle or phospholipid vesicles.

In the case of AOT vesicle, PADPA was used as a modifier since cholesterol could not be distributed into the AOT bilayer due to its size. Upon the addition of PADPA, the membrane properties were drastically changed resulting in the changes in phase state to heterogeneous phase or even ordered phase. The interaction between AOT and PADPA including electrostatic interaction, hydrogen bond, and CH- $\pi$  interactions seems strong enough to change the phase state of vesicle. These findings suggest that the design of AOT vesicle can be achieved to be utilized in chemical reactions which do not involve PADPA as substrate.

As a whole, the “fully-synthetic” surfactant vesicles can be characterized by the addition of modifier such as cholesterol and PADPA. They are expected to be utilized as a platform for the chemical reaction similarly to the phospholipid vesicles, while at the same time, the membrane properties of these vesicles are not identical to that of phospholipid/cholesterol vesicles. The differences in the phospholipid vesicles and fully-synthetic surfactant vesicles may lead to the variation of the platform for the reaction. In other words, DDAB/cholesterol vesicles and AOT/PADPA vesicles may be favorable for a specific chemical process.

# Chapter 5

## Selective Alkylation Reaction with Vesicles Composed of Fully-Synthetic Surfactants and Comparison to Other Self-Assemblies.

### 1. Introduction

From chapter 1 through 3, it has been shown that the interfacial reaction at the surface of self-assembly can be regulated by the physicochemical properties. Other studies also have shown that the chemical process such as adsorption of substrates are depending on the properties of vesicle membrane surface. For example, Litt *et al.* have reported the stability and activity of the enzyme can be differentiated by changing the membrane properties and phase state of vesicles [Litt *et al.*, 2009]. As discussed before, one of the advantages for the reaction process at the vesicle surface is that the environment can be easily varied by changing the composition of molecules which vesicle forms. So far, this study was discussed with micellar systems, phospholipid vesicular systems, and fully-synthetic surfactant vesicular systems. Since it has been reported that the variations in membrane properties can lead to the different result in the chemical process, it is worth studying how fully synthetic surfactant vesicles can affect the reaction by used as a platform.

Based on the strategy to design the vesicle to utilize as a platform for the selective alkylation reaction discussed in chapter 3, the partitioning behavior of the reaction substrates and the changes in the membrane properties after the addition of reaction substrates were important factors. Since DDAB vesicle represented the highly-polar environment at the surface of the vesicle, the adsorption of the hydrophobic reactants and the high conversion can be expected based on the results in chapter 3. Also, DDAB vesicle can be modified with cholesterol to change its membrane properties. DDAB/cholesterol vesicles showed the unique

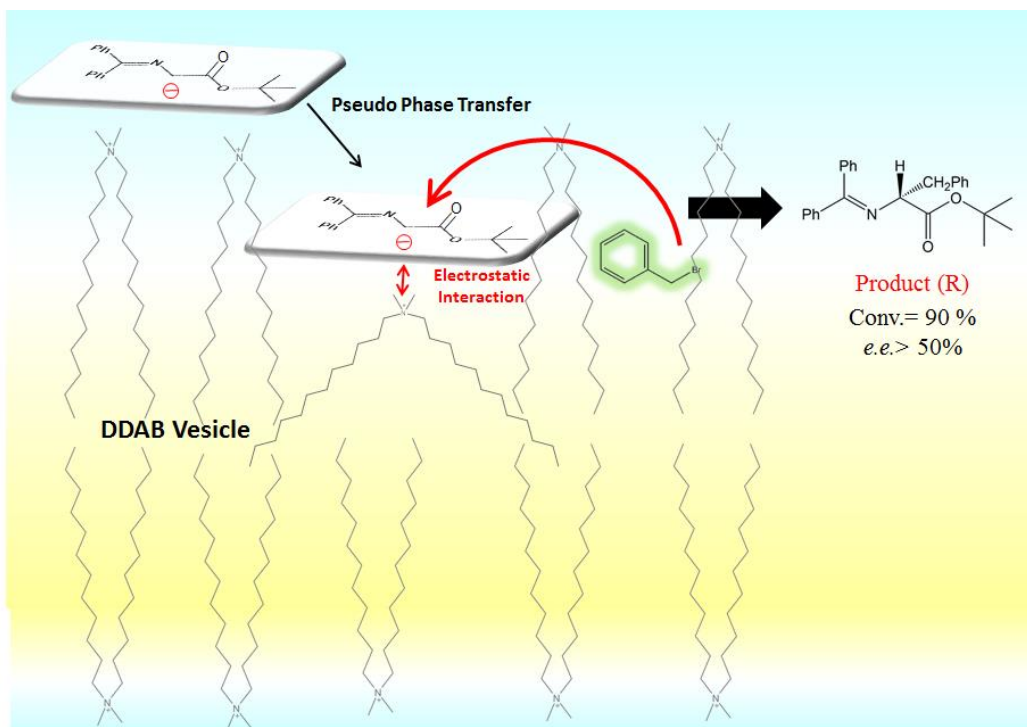


**Figure 5-1** Schematic illustration of the study in this chapter

characteristics that the vesicle membrane was ordered with higher polarity, which may be advantageous for the reaction that the higher polarity has an advantage on attracting hydrophobic molecules and ordered membrane is required for the selectivity. Furthermore, since not the chirality of the lipids but the localization of the reaction substrate was important for the selectivity, it can be expected that the vesicle composed of achiral amphiphiles also can be used for the enantioselective reaction. In this chapter, DDAB and cholesterol modified DDAB vesicle discussed in the last chapter were selected as a platform for the alkylation of amino acid derivative (**Fig. 5-1**). Comparing to the results obtained in chapter 3, the relationships between the membrane properties and reactivity were investigated. Furthermore, the different reaction mechanism models between lipid vesicles and DDAB vesicles were proposed to explain the different product obtained by these two systems. Finally, key factors of the interfacial reaction with self-assembly system were discussed, showing that it can be applied to any processes including hydrophilic-hydrophobic interface and industrial use.

## **2. Materials and Methods**

### **2.1 Materials.**

1,2-Dipalmitoyl-*sn*-glycero-3-phosphocholine (DPPC) and 1,2-dioleoyl-*sn*-glycero-3-phosphocholine (DOPC) were purchased from Avanti Polar Lipid (Alabaster, AL, USA). Cholesterol was purchased from Sigma Aldrich (St. Louis, MO, USA). Hexadecyltrimethylammonium bromide (CTAB), sodium hydroxide, and benzyl bromide were purchased from Wako Pure Chemicals (Osaka, Japan). Dilauryldimethylammonium bromide (DDAB) and *N*-(diphenylmethylene)glycine *tert*-butyl ester (DMGBE) were purchased from Tokyo Chemical Industries (Tokyo, Japan). These chemicals were used without further purification.

### **2.2 Preparation of vesicles.**

A chloroform solution containing lipids was dried in a round-bottom flask by evaporation under a vacuum. The obtained lipid thin film was dissolved in chloroform again, and the solvent was evaporated. The lipid thin film was kept under a high vacuum for at least 3 hours, and was then hydrated with distilled water at room temperature. The liposome suspension was frozen at -80 °C and thawed at 50 °C to enhance the transformation of small vesicles into larger multi-lamellar vesicles (MLVs). This freeze-thaw cycles were performed five times. MLVs were used to prepare the large unilamellar vesicles (LUVs) by extruding the MLV suspension 11 times through two layers of polycarbonate membranes with mean pore diameters of 100 nm using an extruding device (Liposofast; Avestin Inc., Ottawa, Canada).

### **2.3 Evaluation of membrane polarities.**

Laurdan is sensitive to the polarity around the molecule itself, and its fluorescence properties enable to evaluate the surface polarity of lipid membranes. The Laurdan emission spectra exhibit a red shift caused by dielectric relaxation. The emission spectra were measured

with an excitation wavelength of 340 nm, and the general polarization ( $GP_{340}$ ), the membrane polarity, was calculated as follows:

$$GP_{340} = (I_{440} - I_{490}) / (I_{440} + I_{490}),$$

where  $I_{440}$  and  $I_{490}$  represent the fluorescence intensity of Laurdan at 440 nm and 490 nm, respectively. The total concentrations of lipid (or surfactant) and Laurdan were 1 mM and 10  $\mu$ M, respectively. For CTAB micelle, the concentration of CTAB and Laurdan were 10 mM and 100  $\mu$ M due to the critical micelle concentration of CTAB ( $\sim$ 1 mM).

The fluorescence spectrum of Laurdan was deconvoluted into two spectra by using the software Peakfit (Systat Software Inc., CA, USA): one originates from the localization of Laurdan in an ordered membrane (ordered phase), and the other originates from the localization of Laurdan in a disordered membrane (disordered phase).

## 2.4 Evaluation of membrane fluidity

Fluorescent probe DPH (1,6-diphenyl-1,3,5-hexatrien) was used for evaluating membrane fluidity. The sample was excited at  $\lambda_{ex} = 360$  nm with vertically polarized light, and emission intensities both perpendicular ( $I_{\perp}$ ) and parallel ( $I_{\parallel}$ ) to the excited light were recorded at  $\lambda_{em} = 430$  nm. The fluidity ( $1/P$ ) of DPH was then calculated by using the following equations:

$$1/P = (I_{\parallel} - GI_{\perp}) / (I_{\parallel} + GI_{\perp})$$

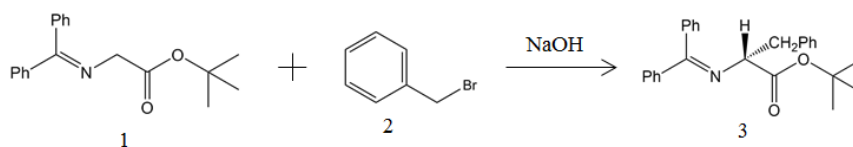
$$G = i_{\perp} / i_{\parallel}$$

where  $i_{\perp}$  and  $i_{\parallel}$  are emission intensities, perpendicular and parallel to the horizontally polarized light, respectively, and  $G$  is a correction factor. The final concentrations of lipid and DPH were 1 mM and 4  $\mu$ M, respectively.

## 2.5 Alkylation of DMGBE with benzyl bromide.

0.3 mg (1.0  $\mu$ mol) of DMGBE was dissolved in pure water, and then the aqueous solution was mixed with vesicle suspension and NaOH aqueous solution (10%) to obtain 1 mL of

reaction solution. 1.5  $\mu\text{L}$  (12  $\mu\text{mol}$ ) of benzyl bromide was finally added to initiate the reaction (Scheme 1). The reaction solution was stirred at 500 rpm in room temperature for 24 h. The total concentrations were DMGBE = 1.0 mM, benzyl bromide = 12 mM, lipid = 10 mM, NaOH = 0.3 M. In the case of micelle instead of liposomes, the aqueous solution of CTAB was added. The total concentrations were fixed to the same value to the condition of the reaction with liposomes.



**Scheme 1.** Asymmetric Reaction of DMGBE with Benzyl Bromide

1. *N*-(diphenylmethylene)glycine *tert*-butyl ester (DMGBE), 2. Benzyl bromide, 3. Product

## 2.6 HPLC measurements of reaction solution.

After the reaction was finished, the product (and reactant) were extracted to the organic solvent by using Bligh-Dyer method. In brief, the 1 mL of reaction solution was mixed with 2 mL methanol and 1 mL chloroform, resulting in homogeneous, colourless, and transparent liquid. Then 1 mL of chloroform and 1 mL pure water were added to the solution to lead to the phase separation. The centrifugation was performed (1400 rpm, 5 min) to complete the phase separation by a Tabletop Centrifuge KUBOTA 5200 (Kubota, Tokyo, Japan).

After the extraction, the organic phase was moved into round-bottom flask and chloroform was removed by evaporation. 1 mL of diethyl ether was added to the flask, and 10  $\mu\text{L}$  was taken and dissolved in 1 mL of mobile phase for HPLC analysis (Daicel Chiralpak IA, mobile phase was hexane:2-propanol = 99:1, flow rate = 0.5 mL/min). HPLC analysis was done by Waters 1515 Isocratic HPLC Pump and Waters 2489 UV/Visible Detector (Waters, Massachusetts, US) to evaluate the conversion of the reaction and the enantiomeric excess.

## 2.6 Adsorption of reactants onto vesicle.

The adsorption amounts of reactant (DMGBE) was evaluated by UV spectrophotometer (UV-1800; Shimadzu, Kyoto, Japan). The total concentration of reactant and vesicles were same as the alkylation method (DMGBE = 1.0 mM, vesicle = 12 mM, NaOH = 0.3 M). The solution was incubated for an hour in room temperature with 500 rpm stirring. The adsorption percentages were calculated from the difference in UV absorbance of the solution without and with vesicle:

$$\text{Adsorption percentage} = (A_{\text{vesicle}} - A_{\text{bulk}}) / (A_{\text{vesicle}}) \times 100,$$

where  $A_{\text{initial}}$  and  $A_{\text{filtrated}}$  represent the absorbance of the reactant in the NaOH aqueous solution and in the vesicle suspension, respectively.

### 3. Results and Discussion

#### 3.1 Evaluation of the alkylation reaction with DDAB and DDAB/cholesterol vesicles

In the chapter 3, it has been shown that the alkylation of DMGBE can be achieved (conversion > 90%) at a low enantiomeric excess (*e.e.*  $\approx$  5%) in a cetyltrimethylammonium bromide (CTAB) micelle solution, while a higher *e.e.* value (> 90%) could be obtained in a 1,2-dioleoyl-sn-glycero-3-phosphocholine (DOPC) liposome suspension. DDAB was selected as an amphiphile that can form vesicles in an aqueous solution, and possesses a tertiary ammonium group that is located on the hydrophilic side of the membrane. The alkylation of DMGBE was carried out in a suspension of DDAB vesicles, as shown in Scheme 1. This reaction showed a high conversion ( $\sim$ 90%) and medium enantioselectivity (*e.e.*  $\approx$  50%) based on a high-performance liquid chromatography (HPLC) chromatogram obtained using a chiral column (**Fig.5-2, Table 5-1**). Most importantly, the (*R*)-product was formed with the DDAB vesicles, which is same as the phase-transfer catalyst, while the (*S*)-product was formed in the presence of the DOPC liposomes. When the DDAB vesicles were modified with 20% cholesterol, the *e.e.* value increased as compared to that of unmodified DDAB vesicles, reaching approximately 80%. The reactants, such as DMGBE and benzyl bromide, were added stepwise to the DDAB vesicle solution in different orders to confirm the partitioning of reactants into the DDAB vesicle membrane. The insertion of benzyl bromide into the DDAB vesicle membrane prior to the addition of DMGBE resulted in the formation of the (*S*)-product with an *e.e.* value that reached  $\sim$ 70%. These results indicate that benzyl bromide can be oriented in the deeper region of the DDAB vesicle membrane and could react with the DMGBE molecule at the outer surface of the membrane. The conformation of DMGBE during its interaction with the DDAB vesicle membrane should differ from that with the DOPC liposome membrane, considering the results obtained in chapter 3.



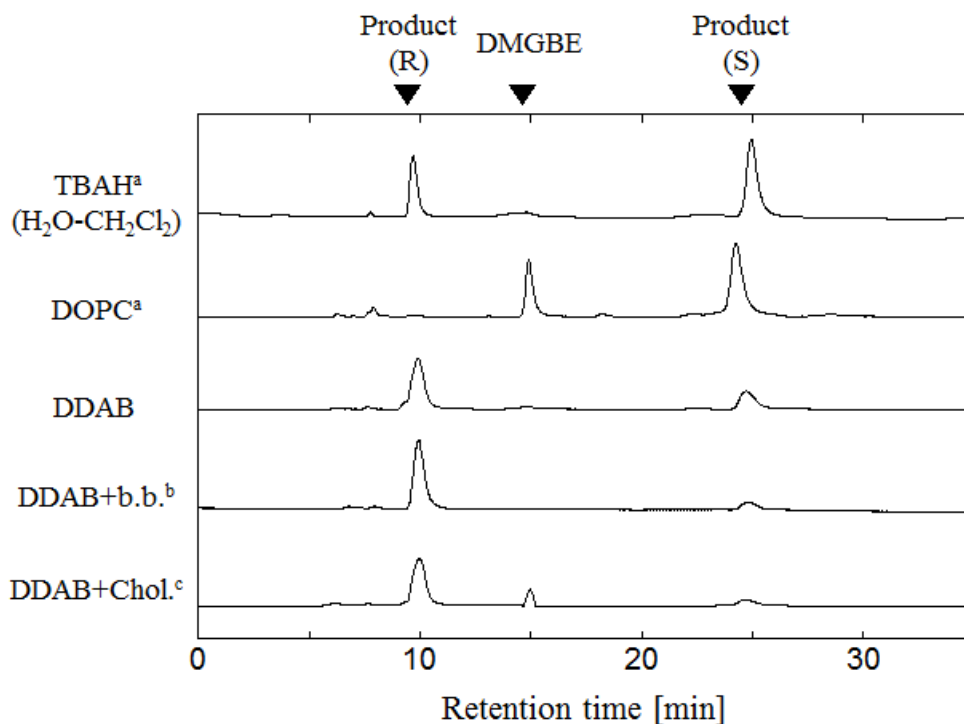


**Figure 5-2** HPLC chart of the reaction with each vesicle. [a] From our previous report; see Ref 18 for detailed information. [b] b.b.=benzyl bromide. Benzyl bromide was initially added and mixed with the vesicle suspension, and then incubated for 1 h. The reaction was initiated by adding NaOH (aq) and DMGBE. [c] Chol.=cholesterol. The vesicle composition was DDAB:Cholesterol=80:20.

**Table 5-1** Alkylation of amino acid derivative using various kinds of amphiphiles

Entry	Amphiphile	Conversion (%)	<i>e.e.</i> ((S)-(R) %)
1	DDAB (vesicle)	90	-49
2	DDAB:Chol = 80:20 (vesicle)	87	-77
3 <sup>a</sup>	DDAB (vesicle)	88	-56
4	CTAB (micelle)	95	5
5	DOPC (liposome)	62	97

[a] Benzyl bromide was initially added and mixed with the vesicle suspension, and then incubated for 1 h. The reaction was initiated by adding NaOH (aq) and DMGBE.

### 3.2 The effects of the membrane polarities on the reaction system.

The physicochemical properties of the membrane are important to the outcome of a reaction on the membrane of either a vesicle or a liposome. The surface properties of various self-assemblies were analyzed by using the previously reported method to investigate the differences between the DOPC liposomes, CTAB micelles, and DDAB vesicles. Fluorescent probes, such as Laurdan and 1,6-diphenyl-1,3,5-hexatriene (DPH), have been used to evaluate the membrane polarity and fluidity, respectively. The spectrum of Laurdan is strongly related to the hydration environment of the Laurdan embedded in the membrane: the spectrum of Laurdan is blue-shifted when its environment is dehydrated. The surface characteristics of the self-assembling system can therefore be distinguished from others by analyzing the fluorescence spectra of Laurdan. Laurdan shows a peak at 440 nm when embedded in vesicles with a solid ordered ( $s_o$ ) phase; at 490 nm when in vesicles with a liquid-disordered ( $l_d$ ) phase, and at 505 nm for micelles. **Figure 5-3** shows the fluorescence spectra of Laurdan embedded in a typical liposome (vesicle), micelle, and a DDAB vesicle. The fluorescence spectrum of Laurdan in the presence of DDAB vesicle indicates that the DDAB membrane has quite different characteristics from those of a micelle, showing it to be more hydrated than typical  $l_d$  phase vesicles. The membrane polarity can be analyzed in detail by calculation of its  $GP_{340}$  values (**Fig. 5-4**); vesicles in  $s_o$  phase (such as DPPC liposome) showed high  $GP_{340}$  value of  $\sim 0.4$ , while the  $GP_{340}$  values were about  $-0.3$  for  $l_d$  phase vesicles, such as DOPC liposomes (**Fig. 5-4 (a)**). The  $GP_{340}$  value for a micelle was much lower ( $GP_{340} < -0.7$ ), indicating that the micelle surface is a hydrated environment. The DDAB vesicles also showed low  $GP_{340}$  value ( $GP_{340} \sim -0.6$ ), indicating that the DDAB vesicle also forms a highly hydrated environment, as found in micelles. These results were also proved by the evaluation of the membrane fluidity, which was analyzed by a fluorescent probe DPH (**Fig. 5-4 (b)**). The membrane fluidity ( $1/P$ ) of the DDAB vesicles was much higher than that of conventional vesicles (such as the DOPC liposomes). The addition of benzyl bromide to DDAB vesicle

caused the fluorescent spectrum of Laurdan and the value of  $GP_{340}$  to be varied (Fig. 2 (b) and (c)) while the addition of benzyl bromide to the DOPC liposome did not change its membrane properties. The membrane of the DDAB vesicle changed to a more “ordered” structure through its interaction with benzyl bromide, indicating that the hydrophobic molecules, used as reaction substrates, can change the membrane properties of the DDAB vesicles. In addition, the modification of the DDAB vesicle membrane with cholesterol also resulted in a similar variation of the membrane as seen for benzyl bromide. These findings indicate that the membrane properties of the DDAB vesicles can be regulated by the addition of hydrophobic

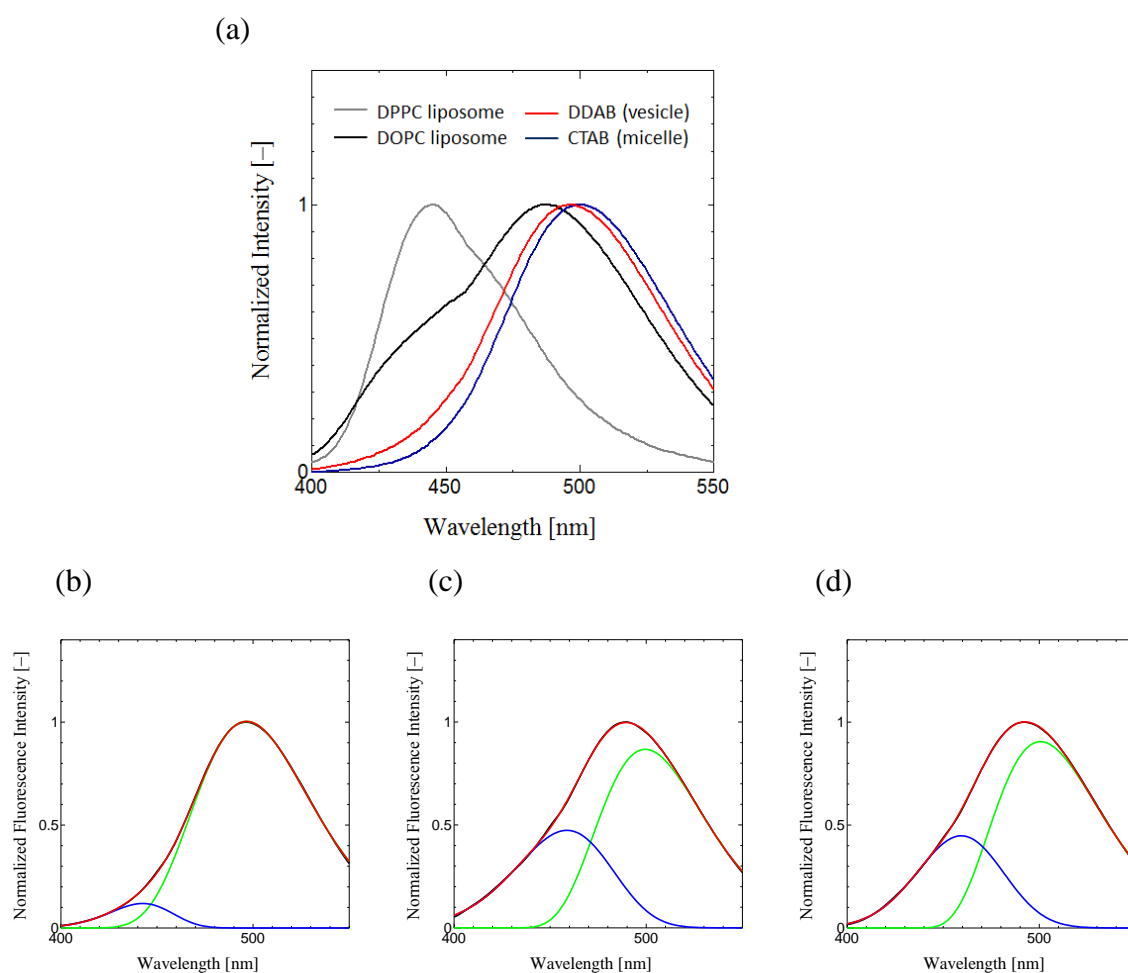


**Figure 5-3** (a) Fluorescent spectra of Laurdan embedded in each self-assembly system. (b) DDAB vesicle (c) DDAB vesicle + benzyl bromide (d) DDAB:Cholesterol=80:20 vesicle. Each line indicates the experimental result (black), fitted line (red), the spectral fraction of ordered phase (blue), and the spectral fraction of disordered phase (green).

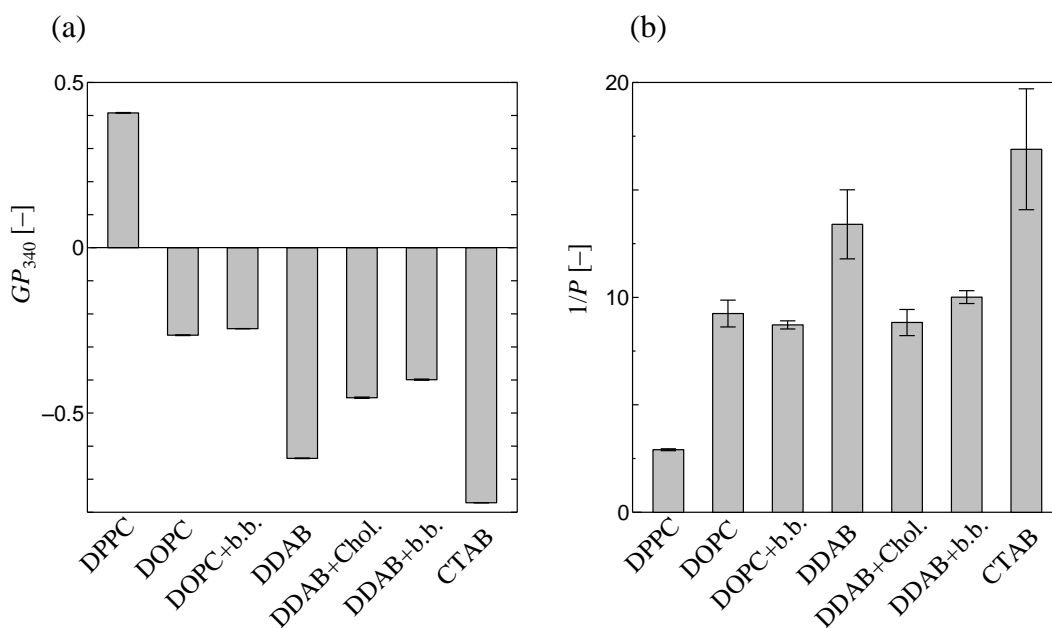


**Figure 5-4** Properties of self-assembly system. b.b.=benzyl bromide, Chol.=Cholesterol. DOPC+b.b. and DDAB+b.b. shows the  $GP_{340}$  values after the addition of 1.2 equivalent of benzyl bromide. Composition of DDAB+Chol. vesicle was DDAB:Cholesterol=80:20. (a) Polarity ( $GP_{340}$ ) of each self-assembly system. See materials and methods for the condition of the experiments and the calculation of the values. (b) Fluidity ( $1/P$ ) of each self-assembly system evaluated by DPH.

molecules. However, the DDAB vesicles modified with either benzyl bromide or cholesterol had more polar environments than those were found for the liposomes, indicating that DDAB vesicles formed a different platform to that formed by liposomes. This finding explains the observed variation in the enantioselectivity of reaction using these platforms.

The dependence of the enantioselective alkylation of DMGBE on the membrane properties of the self-assemblies was studied by direct comparison of the obtained results (**Fig. 5-5**). The conversion values were plotted against the  $GP_{340}$  values, showing an approximately linear relationship (**Fig. 5-5(a)**). It can be clearly seen that the self-assembling systems that showed lower (more negative)  $GP_{340}$  values could enhance the conversion in the reaction. The reason

for this enhancement is probably related to the adsorption of the reactants onto the surface (membrane) of the self-assembling system. Our previous reports have shown that the self-assembly systems with higher polarity (lower  $GP_{340}$  values) could attract a greater number of hydrophobic substrates. The adsorption behavior of the reactants was also investigated in this study. It was found that a greater quantity of reactants was adsorbed onto the self-assemblies with lower  $GP_{340}$  values (**Fig. 5-5 (a)**). The adsorption of DMGBE was strongly related to the conversion, indicating that the interaction between DMGBE and self-assembly was an important factor for the reaction. Although the *e.e.* values were low ( $\sim 5\%$ ) in the presence of systems with lower- $GP_{340}$  values, such as CTAB micelles, some

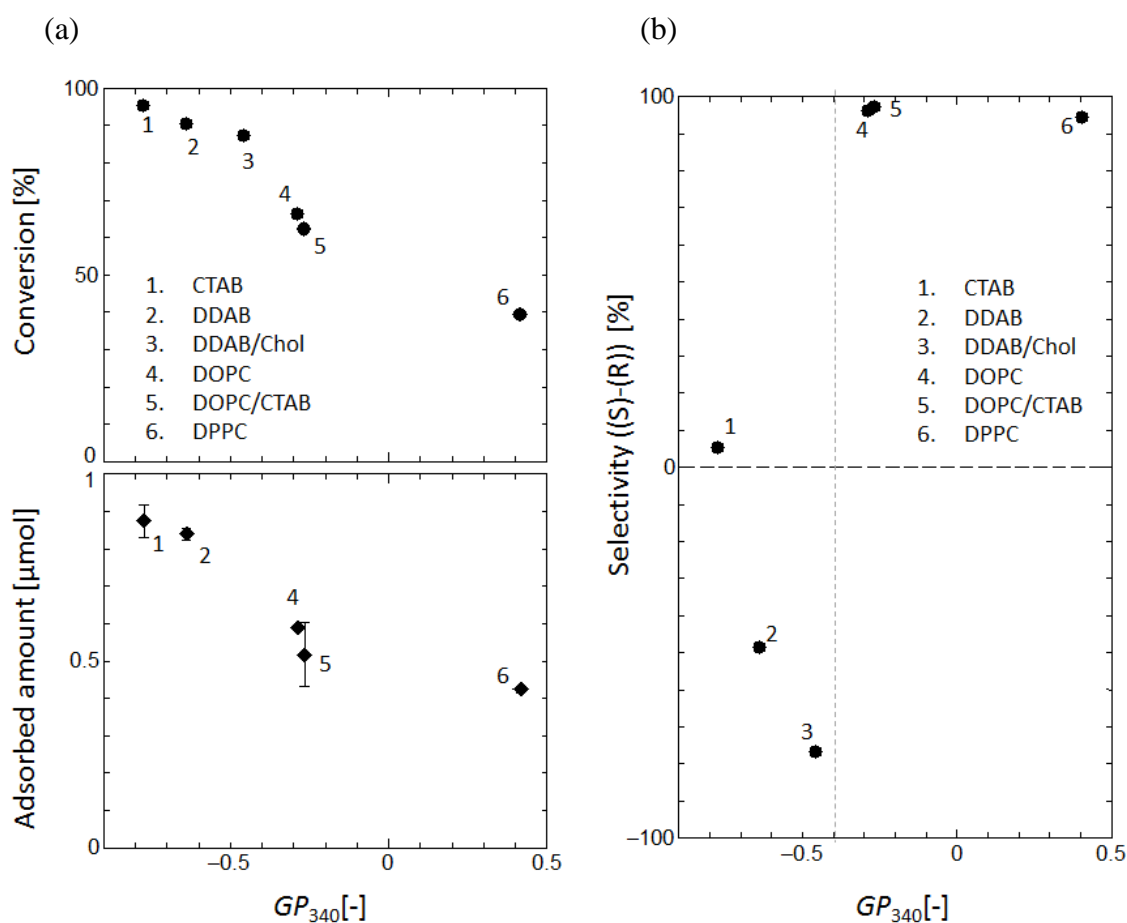


**Figure 5-5** The effects of polarity on the reaction and adsorption of the reactants onto self-assembly systems. (a) top: conversion of the reaction, bottom: adsorption amount of DMGBE. (b) *e.e.* values of the product.

liposomes that showed higher  $GP_{340}$  values achieved high enantioselectivity (*e.e.*~90%, **Fig. 5-5 (b)**). The conversion and enantioselectivity were, respectively, suppressed and increased to some extent when benzyl bromide was inserted into the DDAB vesicle prior to DMGBE addition. This effect was probably because of the associated change in the  $GP_{340}$  value. These findings reveal the importance of the properties of self-assembling systems in highly effective reactions at the surface of self-assemblies.

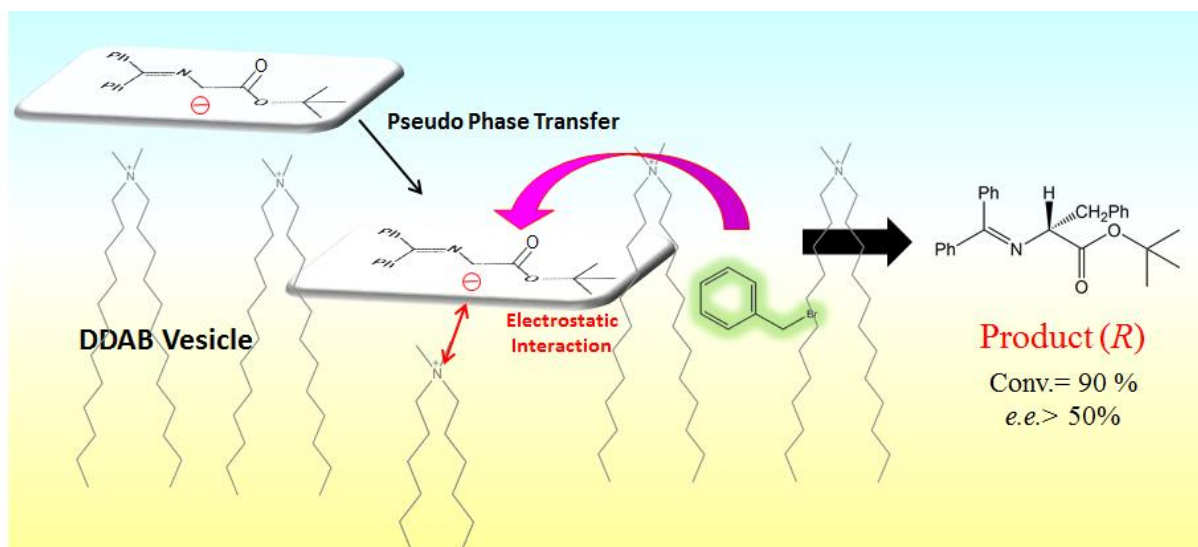
### **3.3 Plausible reaction model of the reaction with DDAB vesicle and comparison to the reaction with phospholipid vesicles.**

We suggest that the reaction model for the enantioselective alkylation at the surface of self-assemblies is also related to the membrane properties and the chemical structures of the reactants and amphiphiles. As previously reported in phase transfer catalysis, *Si* face of DMGBE tends to interact and be covered by the hydrophobic region of the catalyst which resulted in producing (*R*)-form enantiomers [Kitamura *et al.*, 2005]. By applying this tendency to DDAB vesicle system, *Si* face of DMGBE is facing towards the hydrophobic region of DDAB vesicle and hindered by the hydrophobic interaction and electrostatic interaction between DDAB and DMGBE. By forming DDAB-DMGBE complex, the complex shows high hydrophobicity based on its chemical structure, the complex can enter into deeper area of DDAB vesicle to form stronger hydrophobic interaction (**Fig. 5-6**). As a result, benzyl bromide only can react with the *Re* face of DMGBE, which can produce (*R*)-form of the product. This simple interaction between DDAB and DMGBE could be supported by the time required to accomplish the reaction. It took only a short time (within a few hours) to finish the reaction, which is much shorter compared to the reaction with DOPC liposome. DOPC and DMGBE might form complicated reaction intermediate via multiple forces such as (i) electrostatic interaction, (ii) hydrophobic interaction, and (iii) hydrogen bond of both molecules at the interface. In our previous report, multiple interaction is suggested to be induced in the case of

chiral adsorption of L-amino acids on the phospholipid membrane surface, where induction time are needed to obtain the “mature” interactions at the liposome surface [Ishigami *et al.*, 2015]. Similarly, the multiple interactions between DMGBE and DOPC molecules are thought to be rather complicated and, therefore, it could require more than several hours to form appropriate reaction intermediate to obtain chiral (*S*-form) product (**Fig. 5-6 (b)**). The difference in interaction were considered to vary the covered plain face of DMGBE due to the tilted assembly of DOPC, which resulted in the production of opposite enantiomer to each other.

By the modification of cholesterol to DDAB vesicle, the value of  $GP_{340}$  increased as mentioned in the former chapter, which relates to the packing density of the vesicle. The steric hindrance for benzyl bromide to attack the *Si* face of DMGBE became larger because the packing density of DDAB was increased by the presence of cholesterol. This effect of cholesterol lead to the enhanced enantioselectivity of the reaction. In general, the properties of the self-assembling system can regulate the conversion and enantioselectivity of interfacial alkylation reactions at the surface of the assembly.

(a)



(b)

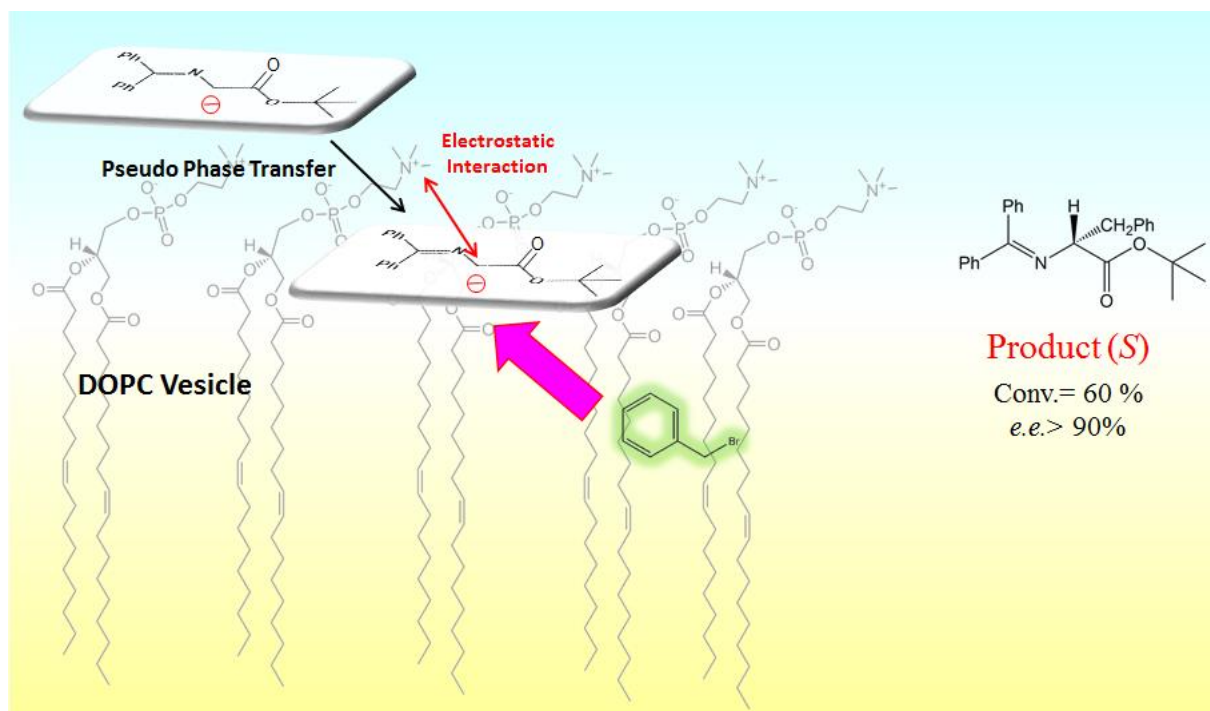


**Figure 5-6** Plausible interaction and reaction model of DMGBE and benzyl bromide with (a) DDAB vesicle, (b) DOPC vesicle.



#### 4. Summary

Bilayer vesicles composed of fully-synthetic surfactants with quaternary ammonium moieties could be used for the asymmetric alkylation of amino acid derivatives. As mentioned in previous chapters, the adsorption ratio, the conversion, and the selectivity were related to the membrane properties, particularly the membrane polarities. The adsorption amount increased with the decrease in the  $GP_{340}$  value, indicating that the exposure of the hydrophobic interior is important to withdraw hydrophobic molecules, and the enrichment effect can lead to the high conversion of the reaction. On the other hand, the selectivity (*e.e.*) increased with the increase in the  $GP_{340}$  value. This result suggests that the highly-ordered surface to regulate the interaction is required for the enantioselective reaction. DDAB/cholesterol vesicle could show the reasonable platform for the reaction which can achieve high conversion (conv. ~ 90 %) and moderate enantioselectivity (*e.e.* ~ 70 %).

Interestingly, the enantiomer produced in this reaction is opposite to each other in the reaction with phospholipid vesicles and DDAB vesicles. The difference can be explained by the interaction mechanism between vesicles and DMGBE. As it was shown in the interaction model, the quaternary ammonium moiety of DDAB interact with the *Si*-face of DMGBE and quaternary ammonium moiety of phospholipid such as DOPC interact with the *Re*-face of DMGBE considering the hydrophobic interaction.

As a conclusion, the alkylation of the amino acid derivative can be regulated by the membrane properties and chemical structure of the vesicle (**Fig. 5-7**). Based on the results obtained, the self-assembly systems can be distinguished by the  $GP_{340}$  values, and the type of the self-assembly is one important factor to regulate the reaction. The micelles showed unique characteristics that the reaction conversions or yields are strongly dependent on the adsorption ratio of the reaction substrates. The reaction process with micelles, one should consider and design the surface so that the substrates can be enriched at the surface of the micelles. On the other hand, the most important factor in the reaction at the surface of vesicle membranes is the

interaction between substrates and the vesicles, which can be evaluated by the variation in  $GP_{340}$  values. Both of the conversion and enantioselectivity can be regulated by the interactions; therefore, it was found to consider and expect the interaction between substrates and vesicles. Now it is expected that an interfacial enantioselective reaction could be regulated by adjusting the membrane properties of vesicles by changing the vesicle components, providing a new and clean process for asymmetric synthesis.

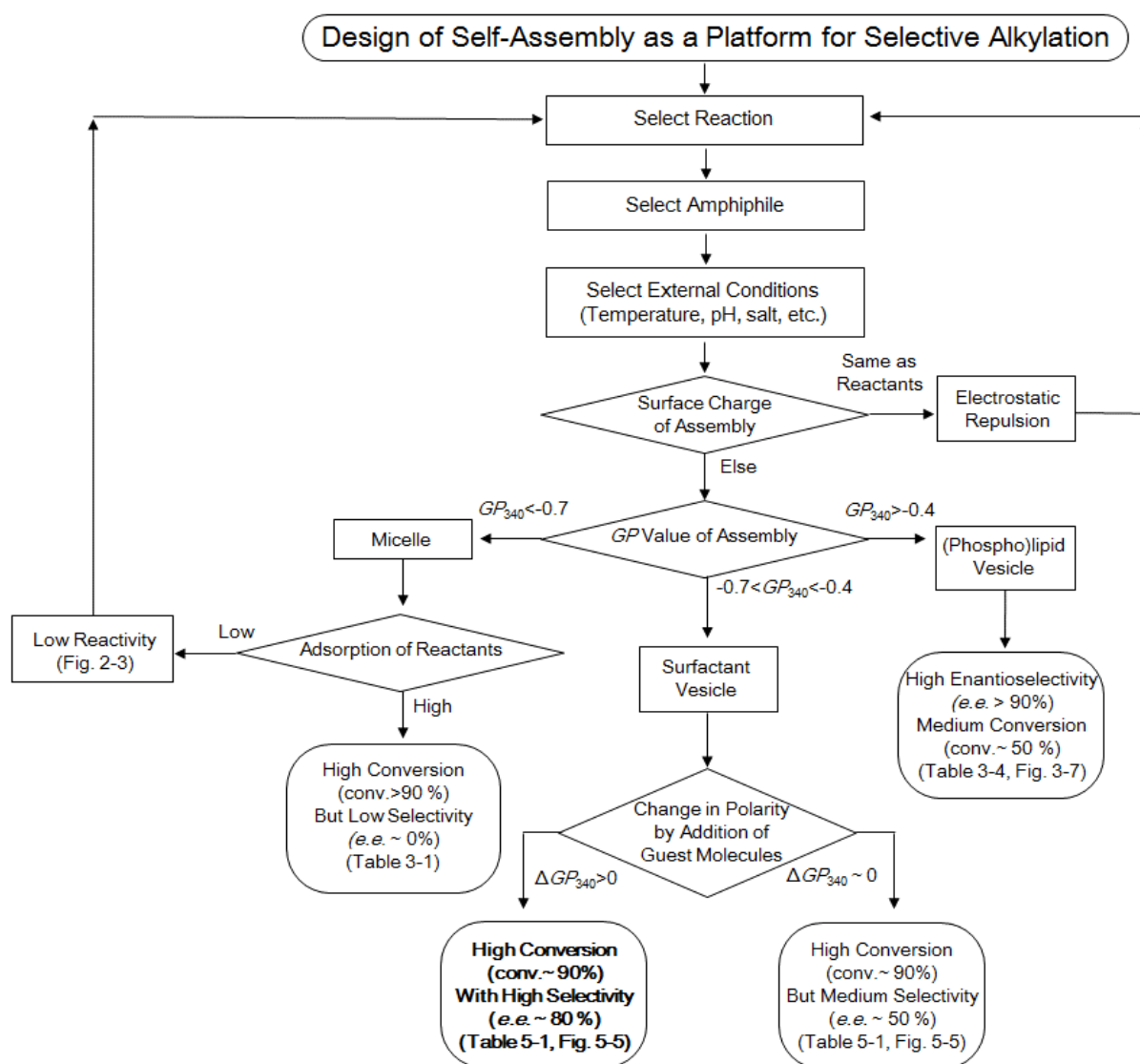


**Figure 5-7** Scheme for the design of self-assembly systems as a platform for alkylation.

## General Conclusion

The methodology to design the various vesicle membrane for the improvement of the interfacial reaction was established. Based on the previous findings, (model-)biomembranes could be utilized for the platform to regulate and recognize biomolecules. Although the hydrophilic-hydrophobic interface has also been focused as a platform for the chemical processes including the chemical reactions, the previous studies had not clarified the influence of physicochemical properties of the interface on the reaction. Not only the reaction rate, yield, or selectivity of the reaction, but also the partitioning behavior of the substrates and the interactions could be regulated by the variation of the hydrophilic- hydrophobic interface of self-assembly systems.

In chapter 1, the method to analyze the micro-environment of vesicles and the partitioning behavior of the reaction substrates onto vesicle membrane were examined. The partitioning of the substrates could be regulated by the differences in the membrane properties of the vesicles, and the result showed that the electrostatic interaction was an essential factor to regulate the partitioning behaviors. The micro-polarity and micro-viscosity of the vesicle membrane evaluated by using two fluorescent probes, Laurdan and DPH, before and after the partitioning of substrates were also analyzed, resulting in the dehydration of the vesicle membrane by the partitioning of hydrophobic molecules. The dehydration of the vesicle membrane also lead to the increase in micro-viscosity, showing that the properties of the vesicle membrane could be varied by the addition of hydrophobic molecules. It has been proposed that the interaction between vesicles and substrates could be controlled by changing its membrane properties.

In chapter 2, 1,3-dipolar cycloaddition of BNO and EMI was carried out as a model reaction in the variety of the dielectric environment. The new parameter was introduced to evaluate the value of relative dielectric constant ( $\epsilon'$ ) to refer the environment formed by self-

assembly systems to the various solvents. In the water/1,4-dioxane systems, the reaction rates were low and decreased linearly with the increase in the value of  $\varepsilon'$  while the largest reaction rate at the certain  $\varepsilon$  value ( $\varepsilon' \sim 25$ ) was observed with the self-assembly systems. The reaction rate was found to be strongly influenced by the adsorption ratio of the reaction substrates, resulting that the cationic DOTAP vesicle, which showed the highest adsorption ratio of BNO, also represented the highest reaction rates. However, normalized reaction rates at the vesicle surface per number of BNO adsorbed was relatively low with cationic vesicle compared to zwitterionic vesicle, suggesting that the strong interactions between vesicles and substrates was not always positive for the reaction. These findings have shown that the reaction rate at the surface of self-assembly system could be enhanced by two factors: enrichment effect and the environment effect. Therefore, it is important to design the vesicle membrane surface to obtain high adsorption ratio and reactivity.

In chapter 3, the enantioselective alkylation of amino acid derivative, another reaction which required not only the yield but also the selectivity, was carried out. When the reaction was conducted in two-solvent system (aqueous-organic two phase system) or micellar system, the high conversion was obtained but the product was racemic. With phospholipid vesicles, significantly high enantioselectivity (*e.e.* >95 %) was obtained although the conversion was decreased as compared with micellar systems. For the enantioselective recognition and reaction, it has been reported that the three interactions are required to regulate the molecules, suggesting that three interactions (electrostatic interaction, hydrogen bond, and hydrophobic interaction) between substrates and phospholipid molecules were occurred hierarchically in the lipid bilayer. Considering about the fundamental self-assembly design as a platform for the alkylation reaction, it is important to regulate the adsorption ratio of the reaction substrates and the environment which vesicles form. The adsorption ratio can be regulated by considering the chemical properties of substrates (charge, hydrophobicity, etc.) and the membrane properties of vesicles (surface charge, polarity, etc.). The variations in the membrane properties by the

addition of substrates play an important role on regulating the environment at the surface of vesicles. The enrichment effect and the interaction between substrates and vesicles to change membrane properties were found to be an important factor for the high conversion and high selectivity in the interfacial reaction.

In chapter 4, the non-natural (“fully-synthetic”) surfactants, DDAB and AOT, were employed to form vesicles in order to have more variety on the physicochemical properties of vesicle membrane. The conditions for the formation of DDAB vesicles and AOT vesicles and their surface properties were investigated, resulting in the different properties from conventional phospholipid vesicles. Furthermore, by the addition of hydrophobic modifiers such as cholesterols, the phase states of the vesicles were varied, as observed in the conventional phospholipid/cholesterol vesicular system. However, DDAB/Cholesterol vesicles resulted in the formation of polar heterogeneous phase, which could not be observed in the phospholipid/cholesterol vesicles, indicating that the non-natural surfactant vesicles can provide hydrophilic-hydrophobic interface with new unique properties.

In chapter 5, the enantioselective alkylation was discussed again with DDAB and DDAB/cholesterol vesicles, and the effect of the hydrophilic-hydrophobic interface properties on the reaction was investigated. The alkylation reaction with DDAB vesicle resulted in the high conversion (~90%) and medium enantioselectivity (*e.e.* ~50%). By comparing the reaction with various self-assembly systems, the values of conversion and enantioselectivity were found to depend on the membrane polarity. The self-assembly system of polar environment (lower  $GP_{340}$  values) could attract more reactants to the surface of the assembly, resulting in the enrichment of the reactants and the high conversion. On the other hand, highly-ordered self-assembly system (higher  $GP_{340}$  values) such as vesicles could regulate the multiple interactions within the reactants and lipid molecules, leading to the high enantioselectivity. The most significant difference in the reaction with DDAB vesicle and phospholipid vesicle was that the enantiomer obtained was opposite from each other. The obtained results indicated the difference

in the interaction model that phospholipids could block the *Re* face of the substrates while DDAB blocked the *Si* face considering their chemical structure and the possible interaction models. These findings suggested the importance of the design about the vesicle membrane for the effective chemical reactions.

The bases of the vesicle membrane designs for the selective chemical reaction was finally established based on the analysis of membrane properties, partitioning behavior of substrates, and plausible interaction models. These findings are expected to contribute to the approach for the chemical reaction process at the hydrophilic-hydrophobic interface to produce fine chemicals and new materials effectively.

## **Suggestions for Future Works**

### **(1) Further Investigation on the Design of Vesicles as a Platform for the Chemical Reactions by Regulating the External Conditions.**

To optimize the reaction condition, the changes in external conditions such as pH, temperature, salt concentration, etc. should be included. At the same time, the regulation of the vesicle membrane properties is important since the properties can be varied by the changes in external conditions. Therefore, the design of the vesicles considering the influence of external condition would be required for the practical use of vesicle membrane as a platform for chemical reactions. Not only the vesicle membrane properties, but also the interaction between vesicle and substrates can be affected. For the better yield and selectivity, the influence of pH, temperature, and salt concentration should be investigated systematically by the methodology of fluorescent probes to measure the membrane properties and analyze the interaction.

### **(2) Use of Nano-Domains on the Vesicle Membrane for the Improvement of Chemical Processes.**

In the previous studies, there have been many reports that nano-domains on the vesicle membrane could regulate the adsorption of the substrates or the activity of the enzymes at the surface of vesicles. In this study, localization of the reaction substrates in vertical direction (from the surface to the interior of the vesicles) could be regulated, but not in the horizontal direction. By the formation and the control of the nano-domains on the vesicles, the localization of the substrates in horizontal direction can be expected, which can lead to the larger enrichment effect of the substrates. The reactivity also can be varied by utilizing the nano-domains that the nano-domains show the different properties from the homogeneous vesicle membrane.

### **(3) Expansion of the Target Reactions and the Scale-up of the Reaction Process to Be Widely Used.**

One of the biggest problems about the reactions in aqueous media and the reactions utilizing the self-assembly system is the limitation of the reaction which can be applied. Only a few of the catalysts which can work in aqueous media have been reported, and the most of the reaction which have been reported are related to the aldol reaction or Michael addition. The application to the various reaction system is demanded, which may be achieved by the regulation of physicochemical properties. Also, as a whole process, the possibility of the application to Industrial use is an important factor. The reactions in the vesicle suspension tend to be difficult to be used in industry due to mainly two difficulties. One is the small relative surface area compared to micellar system and two-solvent systems so that only small amount of the product can be obtained. Another is the problems in extraction due to the strong interaction between vesicles and substrates. In this study, the reaction system with vesicles had been utilized, but it may be beneficial to investigate the regulation of the hydrophilic-hydrophobic interface of micelles or two-solvent system based on the methodology of regulating physicochemical properties of vesicle membranes. The design of hydrophilic-hydrophobic interface should be the key factor of improving the reaction.



## Nomenclatures

$A$	= absorbance of UV-Vis light	[a.u.]
$A_o$	= area of Laurdan spectrum from ordered phase	[-]
$A_d$	= area of Laurdan spectrum from disordered phase	[-]
$A_o/A_d$	= area ratio of ordered phase and disordered phase	[-]
$C_m$	= concentration of adsorbent on liposome membranes	[mM]
$C_w$	= concentration of adsorbent in water	[mM]
$D$	= distribution ratio in emulsion phase	[-]
$G$	= correction factor	[-]
$GP_{340}$	= general polarization calculated at exciting light at 340 nm	[-]
$k$	= observed reaction rate of 1,3-dipolar cycloaddition	[s <sup>-1</sup> ]
$k_{rel}$	= relative reaction rate compared to the rate in water	[s <sup>-1</sup> ]
$k_L$	= reaction rate at pseudo-interphase of self-assembly	[s <sup>-1</sup> ]
$k_w$	= reaction rate of 1,3-dipolar cycloaddition in water	[s <sup>-1</sup> ]
$NF_{340}$	= Non-polar factor calculated at exciting light at 340 nm	[-]
$1/P$	= membrane fluidity	[-]
$r$	= anisotropy of DPH	[-]
$\epsilon'$	= relative dielectric constant	[-]
$\eta_{DPH}$	= micro-viscosity of self-assembly system	[cP]

## List of Abbreviation

AOT	Sodium bis(2-ethylhexyl) sulfosuccinate
b.b.	Benzyl bromide
BINAP	2,2'-bis(diphenylphosphino)-1,1'-binaphthyl
BNO	Benzonitrile oxide
BO	Benzaldoxime
cac	critical aggregate concentration
Chol	Cholesterol
cmc	critical micelle concentration
CTAB	Cetyltrimethylammonium bromide
cvc	critical vesicle concentration
DBSA	Dodecylbenzenesulfonic acid
DDAB	Dilauryldimethylammonium bromide
DLS	Dynamic light scattering
DMGBE	N-(diphenylmethylene)glycine tert-butyl ester
DODAB	Diocetyltrimethylammonium bromide
DOPC	1,2-Dioleoyl- <i>sn</i> -glycero-3-phosphocholine
DOTAP	1,2-Dioleoyl-3-trimethylammonium-propane
DPH	1,6-Diphenyl-1,3,5-hexatriene
DPPC	1,2-Dipalmitoyl- <i>sn</i> -glycero-3-phosphocholine
DPTAP	1,2-Dipalmitoyl -3-trimethylammonium-propane
DSPC	1,2-Distearoyl- <i>sn</i> -glycero-3-phosphocholine
EMI	<i>N</i> -Ethylmaleimide
<i>e.e.</i>	Enantiomer excess

Em	Emission wavelength
Ex	Excitation wavelength
FMO	Frontier molecular orbital
HPLC	High-performance liquid chromatography
$l_d$	Liquid disordered
$l_o$	Liquid ordered
LUV	Large unilamellar vesicle
Laurdan	6-Lauroyl-2-dimethylamino naphthalene
MLV	Multilamellar vesicle
NMR	Nuclear magnetic resonance
PADPA	<i>p</i> -Aminodiphenylamine
POPC	1-Palmitoyl-2-oleoyl- <i>sn</i> -glycero-3-phosphocholine
Pro	Proline
PTC	Phase transfer catalysis
SDS	Sodium dodecyl sulfate
$s_o$	Solid ordered
TBAH	Tetrabutylammonium hydrogensulfate
TEM	Transmission electron microscope
TNS	6-( <i>p</i> -toluidino)naphthalene-2-sulfonate
$T_m$	Phase transition temperature
UV-vis	Ultraviolet-visible

## References

- Aires - Barros, M.R.; Cabral, J.M.S. Selective Separation and Purification of Two Lipases from *Chromobacterium Viscosum* Using AOT Reversed Micelles, *Biotech. Bioeng.*, **1991**, *38*, 1302-1307.
- Alkindi, A.S.; Al-Wahaibi, Y. M.; Muggeridge, A.H. Physical Properties (Density, Excess Molar Volume, Viscosity, Surface Tension, and Refractive Index) of Ethanol + Glycerol, *J. Chem. Eng. Data*, **2008**, *53*, 2793-2796.
- Anyarambhatla, G. R.; Needham, D. Enhancement of the Phase Transition Permeability of DPPC Liposomes by Incorporation of MPPC: a New Temperature-Sensitive Liposome for Use with Mild Hyperthermia. *J. Liposome Res.* **1999**, *9*, 491-506.
- Barnier Quer, C.; Elsharkawy, A.; Romeijin, S.; Kros, A.; Jiskoot, W. Cationic Liposomes as Adjuvants for Influenza Hemagglutinin: More Than Charge Alone. *Eur. J. Pharm. Biopharm.* **2012**, *81*, 294-302.
- Benchouk, W.; Mekelleche, S. M.; Silvi, B.; Aurell, M. J.; Domingo, L. R. Understanding the Kinetic Solvent Effects on the 1,3-Dipolar Cycloaddition of Benzonitrile N-oxide: a DFT study. *J. Phys Org Chem.* **2011**, *24*, 611-618.
- Benjamin, I. Chemical Reactions and Solvation at Liquid Interfaces: A Microscopic Perspective. *Chem. Rev.* **1996**, *96*, 1449-1475.
- Bergenholtz, J.; Wagner, N.J. Formation of AOT/Brine Multilamellar Vesicles. *Langmuir* **1996**, *12*, 3122-3126.
- Blaedel, W.J.; Kissel, T. R.; Boguslaski, R.C. Kinetic Behavior of Enzymes Immobilized in Artificial Membranes. *Anal. Chem.*, **1972**, *44*, 2030-2037.

- Bonincontro, A.; Falivene, M.; La Mesa, C.; Risuleo, G.; Peña, M.R. Dynamics of DNA adsorption on and release from SDS-DDAB Cat - Anionic vesicles: A multitechnique study, *Langmuir*, **2008**, *24*, 1973-1978.
- Boyle, N. A.; Janda, K. D. Formats for Combinatorial Synthesis: Solid-phase, Liquid-Phase and Surface. *Curr. Opin. Chem. Bio.* **2002**, *6*, 339-346.
- Breslow, R. Biomimetic Chemistry and Artificial Enzymes: Catalysis by Design. *Acc. Chem. Res.*, **1995**, *28*, 146-153.
- Breslow, R.; Overman, L. E. An "Artificial Enzyme" Combining a Metal Catalytic Group and a Hydrophobic Binding Cavity. *J. Am. Chem. Soc.*, **1970**, *92*, 1075-1077.
- Buchanan, M.; Arrault, J.; Cates, M.E. Swelling and Dissolution of Lamellar Phases: Role of Bilayer Organization. *Langmuir* **1998**, *14*, 7371-7377.
- Caboi, F.; Monduzzi, M. Didodecyldimethylammonium Bromide Vesicles and Lamellar Liquid Crystals. A Multinuclear NMR and Optical Microscopy Study, *Langmuir*, **1996**, *12*, 3548-3556.
- Caria, A.; Khan, A. Phase Behavior of Catanionic Surfactant Mixtures: Sodium bis(2-ethylhexyl) Sulfosuccinate - Didodecyldimethylammonium Bromide - Water System, *Langmuir*, **1996**, *12*, 6282-6290.
- Chatterjee, A.; Maiti, D. K.; Bhattacharya, P. K. Water Exclusion Reaction in Aqueous Media: Nitrene Formation and Cycloaddition in a Single Pot. *Org. Lett.* **2003**, *5*, 3967-3969.
- Chomczynski, P.; Sacchi, N. Single-step Method of RNA Isolation by Acid Guanidinium Thiocyanate-Phenol-Chloroform Extraction, *Anal. Biochem.*, **1987**, *162*, 156-159.
- Darbre, T.; Reymond, J.-L. Peptide Dendrimers as Artificial Enzymes, Receptors, and Drug-Delivery Agents. *Acc. Chem. Res.*, **2006**, *39*, 925-934.
- De Vries, J. G.; Lefort L. The Combinatorial Approach to Asymmetric Hydrogenation: Phosphoramidite Libraries, Ruthenacycles, and Artificial Enzymes. *Chem. Eur. J.*, **2006**, *12*, 4722-4734.

- Demir, A.S.; Sesenoglu, O.; Eren, E.; Hosrik, B.; Pohl, M.; Janzen, E.; Kolter, D.; Feldann, R.; Dunkelmann, P.; Muller, M. Enantioselective Synthesis of  $\alpha$ -Hydroxy Ketones via Benzaldehyde Lyase-Catalyzed C-C Bond Formation Reaction. *Adv. Synth. Catal.*, **2002**, *344*, 96-103.
- Dieck, H. A.; Heck, R. F. Organophosphinepalladium Complexes as Catalysts for Vinylic Hydrogen Substitution Reactions, *J. Am. Chem. Soc.* **1974**, *96*, 1133.
- Ediz, O.; Tabakci, M.; Memon, S.; Yilmaz, M.; Roundhill, D. M. A Convenient Approach towards the Synthesis of a "Proton Switchable" Chromium(VI) Extractant Based on Calix[4]arene. *Supramol. Chem.* **2004**, *16*, 199-204.
- Engberts J. B. F. N.; Fernández, E.; García-Río, L.; Leis, J. R. Water in Oil Microemulsions as Reaction Media for a Diels-Alder Reaction between *N*-Ethylmaleimide and Cyclopentadiene. *J. Org. Chem.* **2006**, *71*, 6118-6123.
- Frantz, D. E.; Fassler, R.; Tomooka, C. S.; Carreira, E. M. The Discovery of Novel Reactivity in the Development of C-C Bond-Forming Reactions: In situ Generation of Zinc Acetylides with  $Zn^{II}/R_3N$ . *Acc. Chem. Res.*, **2000**, *33*, 373-381.
- Ghosh, O.; Miller, C. A. Liquid-Crystalline and Microemulsion Phase Behavior in Alcohol-Free Aerosol-OT/Oil/Brine Systems. *J. Phys. Chem.*, **1987**, *91*, 4528-4535.
- Glueck, S. M.; Pirker, M.; Nestl, B. M.; Ueberbacher, B. T.; Larissegger-Schnell, B.; Csar, K.; Hauer, B.; Stuermer, R.; Kroutil, W.; Faber, K. Biocatalytic Racemization of Aliphatic, Arylaliphatic, and Aromatic  $\alpha$ -Hydroxycarboxylic Acids, *J. Org. Chem.*, **2005**, *70*, 4028-4032.
- Gothelf, K. V.; Jorgensen, K. A. Asymmetric 1,3-Dipolar Cycloaddition Reactions. *Chem. Rev.* **1998**, *98*, 863-909.
- Grillo, I.; Kats, E. I.; A. R. Muratov, A. R. Formation and Growth of Anionic Vesicles Followed by Small-Angle Neutron Scattering. *Langmuir*, **2003**, *19*, 4573-4581.

- Gröger, H.; Wilken, J. The Application of L-Proline as an Enzyme Mimic and Further New Asymmetric Syntheses Using Small Organic Molecules as Chiral Catalysts. *Angew. Chem. Int. Ed.* **2001**, *40*, 529-532.
- Guo, Z.; Hauser, N.; Moreno, A.; Ishikawa, T.; Walde, P. AOT Vesicle as Templates for the Horseradish Peroxidase-Triggered Polymerization of Aniline. *Soft Matter* **2011**, *7*, 180-193.
- Hamasaka, G.; Uozumi, Y.; Cyclization of Alkynoic Acids in Water in the Presence of a Vesicular Self-Assembled Amphiphilic Pincer Palladium Complex Catalyst. *Chem. Commun.* **2014**, *50*, 14516-14518.
- Han, K. An Efficient DDAB-Mediated Transfection of Drosophila S2 Cells, *Nucl. Acid. Res.*, **1996**, *24*, 4362-4363.
- Hashimoto, T.; Maruoka, K. Recent Development and Application of Chiral Phase-Transfer Catalysis. *Chem. Rev.* **2007**, *107*, 5656-5682.
- Hayashi, K.; Shimanouchi, T.; Kato, K.; Miyazaki, T.; Nakamura, A.; Umakoshi, H. Span80 Vesicles have a More Fluid, Flexible and "Wet" Surface Than Phospholipid Liposomes. *Colloids Surf. B* **2011**, *87*, 28-35.
- Hayashi, T.; Hisaeda, Y. New Functionalization of Myoglobin by Chemical Modification of Heme-Propionates. *Acc. Chem. Res.*, **2002**, *35*, 35-43.
- Hayashi, Y.; Sumiya, T.; Takahashi, J.; Gotoh, H.; Urushima, T.; Shoji, M. Highly Diastereo- and Enantioselective Direct Aldol Reactions in Water. *Angew. Chem. Int. Ed.* **2006**, *45*, 958-961.
- Hirose, Y.; Kariya, K.; Nakanishi, Y.; Kurono, Y.; Achiwa, K. Inversion of Enantioselectivity in Hydrolysis of 1,4-Dihydropyridines by Point Mutation of Lipase PS, *Tetrahedron Lett.*, **1995**, *36*, 1063-1066.
- Huisgen, R. The Concerted Nature of 1,3-Dipolar Cycloadditions and the Question of Diradical Intermediates. *J. Org. Chem.* **1976**, *41*, 403-419.

- Jia, C.; Piao, D.; Oyamada, J.; Lu, W.; Kitamura, T.; Fujiwara, Y. Efficient Activation of Aromatic C-H bonds for Addition to C-C Multiple Bonds. *Science*, **2000**, *287*, 1992-1995.
- Junker, K.; Luginbuhl, S.; Schuttel, M.; Bertschi, L.; Kissner, R.; Schuler, L. D.; Rakvin, B.; Walde, P. Efficient Polymerization of the Aniline Dimer *p*-Aminodiphenylamine (PADPA) with *Trametes Versicolor* Laccase/O<sub>2</sub> as Catalyst and Oxidant and AOT Vesicles as Templates. *ACS Catal.* **2014**, *4*, 3421-3434.
- Junker, K.; Zandomenighi, G.; Guo, Z.; Kissner, R.; Ishikawa, T.; Kohlbrecher, J.; Walde, P. Mechanistic Aspects of the Horseradish Peroxidase-Catalysed Polymerisation of Aniline in the Presence of AOT Vesicles as Templates. *RSC Adv.* **2012**, *2*, 6478-6495.
- Jurkiewicz, P.; Olżyńska, A.; Langner, M.; Hof, M. Headgroup Hydration and Mobility of DOTAP/DOPC Bilayers: A Fluorescence Solvent Relaxation Study, *Langmuir*, **2006**, *22*, 8741-8749.
- Kawano, S.; Horikawa, M.; Yasohara, Y.; Hasegawa, J. Microbial Enantioselective Reduction of Acetylpyridine Derivatives, *Biosci. Biotechnol. Biochem.*, **2003**, *67*, 809-814.
- Keinan, E., Hafeli, E.K., Seth, K.K., Lamed, R. Thermostable Enzymes in Organic Synthesis. 2. Asymmetric Reduction of Ketones with Alcohol Dehydrogenase from *Thermoanaerobium brockii*, *J. Am. Chem. Soc.*, **1986**, *108*, 162-169.
- Kepczynski, M.; Lewandowska, J.; Witkowska, K.; Kedracka-Krok, S.; Mistrikova, V.; Bednar, J.; Wydro, P.; Nowakowska, M. Bilayer Structures in Dioctadecyldimethylammonium Bromide/Oleic Acid Dispersions, *Chem. Phys. Lipids*, **2011**, *164*, 359-367.
- Kepczynski, M.; Jamroz, D.; Wytrwal, M.; Bednar, J.; Rząd E.; Nowakowska, M. Interactions of a Hydrophobically Modified Polycation with Zwitterionic Lipid Membranes. *Langmuir* **2012**, *28*, 676-688.
- Khursan, S. L.; Samarkina, A. B. Effect of Methanol on the Regioselectivity and Reaction Rate of 1,3-Dipolar Cycloaddition of Methyl diazoacetate to Methyl Acrylate and Butane-1. *J. Mol. Struct.* **2010**, *959*, 35-41.



- Kirschning, A.; Solodenko, W.; Mennecke, K. Combininf Enabling Techniques in Organic Synthesis: Continuous Flow Processes with Heterogenized Catalysts. *Chem. Eur. J.* **2006**, *12*, 5972-5990.
- Kitamura, M.; Tokunaga, M.; Ohkuma, T.; Noyori, R. Asymmetric Hydrogenation of 3-Oxo Carboxylates Using BINAP-Ruthenium Complexes: (*R*)-(-)-Methyl 3-Hydroxybutanoate, *Org. Syn.*, **2003**, *1*.
- Kobayashi, S.; Flow “Fine” Synthesis: High Yielding and Selective Organic Synthesis by Flow Methods. *Chem. Asian J.*, **2016**, *11*, 425-436.
- Kofoed, J.; Reymond, J.-L. Dendrimers as Artificial Enzymes. *Curr. Opin. Chem. Biol.*, **2005**, *9*, 656-664.
- Kokubo, M.; Ogawa, C.; Kobayashi, S.; Lewis Acid Catalysis in Water with a Hydrophilic Substrate: Scandium-Catalyzed Hydroxymethylation with Aqueous Formaldehyde in Water. *Angew. Chem. Int. Ed.* **2008**, *47*, 6909-6911.
- Krei, G.A.; Hustedt, H. Extraction of Enzymes by Reverse Micelles, *Chem. Eng. Sci.*, **1992**, *47*, 99-111
- Kumar, A.; Bhakuni, V. Enantioselective Epoxidation Using Liposomised *m*-Chloro-Perbenzoic Acid (LIP MCPBA). *Tetrahedron Lett.* **1996**, *37*, 4751-4754.
- Kumar, A.; Gupta, M.K.; Kumar, M.; Saxena, D. Micelle Promoted Multicomponent Synthesis of 3-Amino Alkylated Indoles via a Mannich-Type Reaction in Water, *RSC Advances*, **2013**, *3*, 1673-1678.
- Kunishima, M.; Yamamoto, K.; Watanabe, Y.; Hioki, K.; Tani, S. Unusual Rate Enhancement of Bimolecular Dehydrocondensation to Form Amides at the Interface of Micelles of Fatty Acid Salts. *Angew. Chem. Int. Ed.* **2005**, *44*, 7254-7257.
- Li, J.; Tang, Y.; Wang, Q.; Li, X.; Cun, L.; Zhang, X.; Zhu, J.; Li, L.; Deng, J. Chiral Surfactant-Type Catalyst for Asymmetric Reduction of Aliphatic Ketones in Water. *J. Am. Chem. Soc.* **2012**, *134*, 18522-18525.

- Lin, C.; Zhao, J.; Jiang, R. Nile Red Probing for the Micelle-to-Vesicle Transition of AOT in Aqueous Solution. *Chem. Phys. Lett.* **2008**, *464*, 77-81.
- Lin, Y.; Li, Z.; Chen, Z.; Ren, J.; Qu, X. Mesoporous Silica-Encapsulated Gold Nanoparticles as Artificial Enzymes for Self-Activated Cascade Catalysis. *Biomaterials*, **2013**, *34*, 2600-2610.
- Lipkowitz, K.B.; Cavanaugh, M.W.; Baker, B.; O'Donnell, M.J. Theoretical Studies in Molecular Recognition: Asymmetric Induction of Benzophenone Imine Ester Enolates by the Benzylcinchoninium Ion. *J. Org. Chem.* **1991**, *56* (17), 5181-5192.
- List, B.; Lerner, R. A.; Barbas, C. F. Proline-Catalyzed Direct Asymmetric Aldol Reactions. *J. Am. Chem. Soc.* **2000**, *122*, 2395-2396.
- Litt, J.; Padala, C.; Asuri, P.; Vutukuru, S.; Athmakuri, K.; Kumar, S.; Dordick, J.; Kane, R.S. Enhancing Protein Stability by Adsorption onto Raftlike Lipid Domains. *J. Am. Chem. Soc.* **2009**, *131*, 7107-7111.
- Luginbühl, S.; Bertschi, L.; Willeke, M.; Schuler, L. D.; Walde, P. How Anionic Vesicles Steer the Oligomerization of Enzymatically Oxidized *p*-Aminodiphenylamine (PADPA) toward a Polyaniline Emeraldine Salt (PANI-ES)-Type Product. *Langmuir*, **2016**, *32*, 9765-9779.
- Ma, Y.; Zhuang, Y.; Xie, X.; Wang, C.; Wang, F.; Zhou, D.; Zeng, J.; Cai, L. The Role of Surface Charge Density in Cationic Liposome-Promoted Dendritic Cell Maturation and Vaccine-Induced Immune Responses. *Nanoscale* **2011**, *3*, 2307-2314.
- Makino, K.; Yamada, T.; Kimura, M.; Oka, T.; Ohshima, H., Kondo, T. Temperature- and Ionic Strength-Induced Conformational Changes in the Lipid Head Group Region of Liposomes as Suggested by Zeta Potential Data. *Biophys. Chem.* **1991**, *41*, 175-183.
- Makino, R.; Yamazaki, I. Effects of 2,4-Substituents of Deuterobemin upon Peroxidase Functions: 1. Preparation and Some Properties of Artificial Enzymes. *J. Biochem.*, **1972**, *72*, 655-664.

- Manabe, K.; Iimura, S.; Sun, X. -M.; Kobayashi, S. Dehydration Reactions in Water. Brønsted Acid-Surfactant-Combined Catalyst for Ester, Ether, Thioether, and Dithioacetal Formation in Water. *J. Am. Chem. Soc.* **2002**, *124*, 11971-11978.
- Marlau, M. L.; Mejia, M. del P.; Nguyen, S. T.; Hupp, J. T. Artificial Enzymes Formed through Directed Assembly of Molecular Aquare Encapsulated Epoxidation Catalysts. *Angew. Chem. Int. Ed.*, **2001**, *40*, 4239-4242.
- Mase, N.; Nakai, Y.; Ohara, N.; Yoda, H.; Takabe, K.; Tanaka, F.; Barbas III, C. F. Organocatalytic Direct Asymmetric Aldol Reactions in Water. *J. Am. Chem. Soc.* **2006**, *128*, 734-735.
- Miyaura, N.; Yamada, K.; Suzuki, A. A New Stereospecific Cross-Coupling by the Palladium-Catalyzed Reaction of 1-Alkenylboranes with 1-Alkenyl or 1-Alkynyl Halides, *Tetrahedron Letters*, **1979**, *20*, 3437-3440.
- Nanda, V.; Koder, R. L. Designing Artificial Enzymes by Intuition and Computation. *Nat. Chem.*, **2010**, *2*, 15-24.
- Nájera, C.; Sansano, J. M. Catalytic Enantioselective 1,3-Dipolar cycloaddition Reaction of Azomethine Ylides and Alkenes: The Direct Strategy to Prepare Enantioenriched Highly Substituted Proline Derivatives. *Angew. Chem. Int. Ed.* **2005**, *44*, 6272-6276.
- O'Donnell, M. J. The Enantioselective Synthesis of  $\alpha$ -Amino Acids by Phase-Transfer Catalysis with Achiral Schiff Base Esters. *Acc. Chem. Res.* **2004**, *37*, 506-517.
- O'Donnell, M.J.; Bennett, W.D.; Wu, S. The Stereoselective Synthesis of  $\alpha$ -Amino Acids by Phase-Transfer Catalysis. *J. Am. Chem. Soc.* **1989**, *111*, 2353-2355.
- Ooi, T.; Kameda, M.; Maruoka, K. Molecular Design of a C<sub>2</sub>-Symmetric Chiral Phase-Transfer Catalyst for Practical Asymmetric Synthesis of  $\alpha$ -amino acids. *J. Am. Chem. Soc.* **1999**, *121*, 6519-6520.

- Otto, S.; Engberts, J. B. F. N.; Kwak, J. C. T. Million-Fold Acceleration of a Diels-Alder Reaction due to Combined Lewis Acid and Micellar Catalysis in Water. *J. Am. Chem. Soc.* **1998**, *120*, 9517-9525.
- Pan, X.; Lu, C.; Nie, J.; Chen, Z.; Yang, G.; Dong, N.; Shi, J. Asymmetric Domino Michael–Aldol Reactions Catalyzed by Recyclable PEG Supported Chiral Primary Aminoalcohol and Primary–Secondary Diamine Catalysts in Water. *Catal. Commun.* **2014**, *53*, 72-76.
- Panja, S.; Mohapatra, P. K.; Tripathi, S. C.; Gandhi, P. M.; Janardan, P. Role of Organic Diluents on Am(III) Extraction and Transport Behaviour Using *N,N,N',N'*-Tetraoctyl-3-Oxapentanediamide as the Extractant. *J. Membr. Sci.* **2012**, *403*, 71-77.
- Parasassi, T.; De Stasio, G.; Ravagnan, G.; Rusch, R. M.; Gratton, E. Quantitation of Lipid Phases in Phospholipid Vesicles by the Generalized Polarization of Laurdan Fluorescence. *Biophys. J.* **1991**, *60*, 179–189.
- Pence, H. E.; Williams, A. ChemSpider: an Online Chemical Information Resource. *J. Chem. Edu.* **2010**, *87*, 1123-1124.
- Perez-Casas, S.; Castillo, R.; Castas, M. Effect of Alcohols in AOT Reverse Micelles. A Heat Capacity and Light Scattering Study. *J. Phys. Chem. B.* **1997**, *101*, 7043-7054.
- Pinaka, A.; Vougioukalakis, G. C.; Dimotikali, D.; Yannakopoulou, E.; Chankvetadze, B.; Papadopoulos, K. Green Asymmetric Synthesis:  $\beta$ -Amino Alcohol-Catalyzed Direct Asymmetric Aldol Reactions in Aqueous Micelles. *Chirality* **2013**, *25*, 119-125.
- Pires, M.J.; Aires-Barros, M. R.; Cabral, J. M. S. Liquid-liquid Extraction of Proteins with Reversed Micelles, *Biotech. Progress*, **1996**, *12*, 290-301.
- Pramanik, R.; Das, P. K.; Bagchi, S. Fluorescence Anisotropy of Ketocyanine Dyes in Homogeneous and Heterogeneous Media. Estimation of Micellar Microviscosity. *Phys. Chem. Chem. Phys.*, **2000**, *2*, 4307-4311.
- Rispens, T.; Engberts, J. B. F. N. A Kinetic Study of 1,3-Dipolar Cycloadditions in Micellar Media. *J. Org. Chem.* **2003**, *68*, 8520-8528.

- Rispens, T.; Engberts, J. B. F. N. Micellar Catalysis of Diels-Alder Reactions: Substrate Positioning in the Micelle. *J. Org. Chem.* **2002**, *67*, 7369-7377.
- Ruiz, F.-J.; Rubio, S.; Pérez-Bendito, D. Water-Induced Coacervation of Alkyl Carboxylic Acid Reverse Micelles: Phenomenon Description and Potential for the Extraction of Organic Compounds, *Anal. Chem.*, **2007**, *79*, 7473-7484.
- Sagar, G. H.; Bellare, J. R. Estimation of Mechanical Strength of Unilamellar and Multilamellar AOT/Water Vesicles and Their Rupture Using Micropipet Aspiration. *J. Phys. Chem. B* **2011**, *113*, 13805-13810.
- Saha, R.; Verma, P. K.; Mitra, R. K.; Pal, S. K. Structural and Dynamical Characterization of Unilamellar AOT Vesicles in Aqueous Solutions and Their Efficacy as Potential Drug Delivery Vehicle. *Colloids Surf., B* **2011**, *88*, 345-353.
- Shiraishi, Y.; Inoue, T.; Hirai, T. Local Viscosity Analysis of Triblock Copolymer Micelle with Cyanine Dyes as a Fluorescent Probe, *Langmuir*, **2010**, *26*, 17505-17512.
- Shirakawa, S.; Maruoka, K. Recent Developments in Asymmetric Phase-Transfer Reactions. *Angew. Chem. Int. Ed.* **2013**, *52*, 4312-4348.
- Solde, L.; Ferstl, W.; Loebbecke, S.; Maggi, R.; Malmassari, C.; Sartori, G.; Yada, S. Use of Immobilized Organic Base Catalysts for Continuous-Flow Fine Chemical Synthesis. *J. Catal.*, **2008**, *258* 289-295.
- Souillart, L.; Cramer, N. Highly Enantioselective Rhodium(I)-Catalyzed Carbonyl Carboacylations Initiated by C-C Bond Activation. *Angew. Chem. Int. Ed.*, **2014**, *53*, 9640-9644.
- Starks, C. M. Phase-Transfer Catalysis. I. Heterogeneous Reactions Involving Anion Transfer by Quaternary Ammonium and Phosphonium Salts. *J. Am. Chem. Soc.* **1971**, *93*, 195-199.
- Stephen, A.; Hashmi, K.; Schwarz, L.; Choi, J.-H.; Frost, T.M. A New Gold-Catalyzed C-C Bond Formation. *Angew. Chem. Int. Ed.*, **2000**, *39*, 2285-2288.

- Stsiapura, V. I.; Maskevich, A. A.; Kuzmitsky, V. A.; Uversky, V. N.; Kuznetsova, I. M.; Turoverov, K. K. Thioflavin T as a molecular rotor: Fluorescent properties of thioflavin T in solvents with different viscosity, *J. Phys. Chem. B*, **2008**, *112*, 15893-15902.
- Suga, K.; Tanabe, T.; Tomita, H.; Shimanouchi, T.; Umakoshi, H. Conformational Change of Single-Stranded RNAs Induced by Liposome Binding, *Nucl. Acids Res.* **2011**, *39*, 8891-8900.
- Suga, K.; Tanabe, T.; Umakoshi, H. Heterogeneous Cationic Liposomes Modified with 3b-{N-[(N',N'-dimethylamino)ethyl]carbamoyl}cholesterol Can Induce Partial Conformational Changes in Messenger RNA and Regulate Translation in An Escherichia Coli Cell-Free Translation System. *Langmuir* **2013**, *29*, 1899-1907.
- Suga, K.; Umakoshi, H. Detection of Nano-Sized Ordered Domains in DOPC/DPPC and DOPC/Ch Binary Lipid Mixture Systems of Large Unilamellar Vesicles Using a TEMPO Quenching Method. *Langmuir*, **2013**, *29*, 4830–4838.
- Taleb, A.; Petit, C.; Pileni, M. P. Synthesis of Highly Monodisperse Silver Nanoparticles from AOT Reverse Micelles: A Way to 2D and 3D Self-Organization, *Chem. Mater.*, **1997**, *9*, 950-959
- Tang, W.; Zhang, H.; Wang, L.; Qian, H. Antimicrobial Peptide Isolated from Ovalbumin Hydrolysate by Immobilized Liposome-Binding Extraction, *Eur. Food Res. Tech.*, **2013**, *237*, 591-600.
- Thankachan, A. P.; Asha, S.; Sindhu, K. S.; Anilkumar, G. An Overview of Zn-Catalyzed Enantioselective Aldol Type C-C Bond Formation. *RSC Adv.*, **2015**, *5*, 62179-62193.
- Tuan, L. Q.; Umakoshi, H.; Shimanouchi, T.; Kuboi, R. Liposome-Recruited Activity of Oxidized and Fragmented Superoxide Dismutase, *Langmuir* **2008**, *24*, 350-354.

- Uchiyama, S.; Matsumura, Y.; de Silva, A. P.; Iwai, K. Fluorescent Molecular Thermometers Based on Polymers Showing Temperature-Induced Phase Transitions and Labeled with Polarity-Responsive Benzofurazans *Anal. Chem.*, **2003**, *75*, 5926-5935.
- Ueoka, R.; Matsumoto, Y.; Yoshino, T.; Watanabe, N.; Omura, K.; Murakami, Y. Remarkable Steric Control for the Enantioselective Cleavage of Amino Acid Esters. *Chem. Lett.* **1986**, *15*, 1743-1746.
- Umakoshi, H.; Morimoto, K.; Yasuda, N.; Shimanouchi, T.; Kuboi, R. Development of Liposome-Based Mimics of Superoxide Dismutase and Peroxidase Based on the "LIPOzyme" Concept. *J. Biotechnol.* **2010**, *147*, 59-63.
- Van Mersbergen, D.; Wijnen, J. W.; Engberts, J. B. F. N. 1,3-Dipolar cycloadditions of Benzonitrile Oxide with Various Dipolarophiles in Aqueous Solutions. A Kinetic Study. *J. Org. Chem.* **1998**, *63*, 8801-8805.
- Villa, C.C.; Correa, N.M.; Silber, J.J.; Moyano, F.; Falcone, R.D. Singularities in the Physicochemical Properties of Spontaneous AOT-BHD Unilamellar Vesicles in Comparison with DOPC vesicles. *Phys. Chem. Chem. Phys.* **2015**, *17*, 17112-17121.
- Viparelli, P.; Alfani, F.; Cantarella, M. Models for Enzyme Superactivity in Aqueous Solutions of Surfactants. *Biochem. J.* **1999**, *344*, 765-773.
- Viseu, M.I.; Edwards, K.; Campos, C. S.; Costa, S. M. B. Spontaneous Vesicles Formed in Aqueous Mixtures of Two Cationic Amphiphiles, *Langmuir*, **2000**, *16*, 2105-2114.
- Walde, P.; Umakoshi, H.; Stano, P.; Mavelli, F. Emergent Properties Arising from the Assembly of Amphiphiles, *Chem. Comm.*, **2014**, *50*, 10177-10197.
- Wang, C.; Jia, G.; Zhou, J.; Li, Y.; Liu, Y.; Lu, S.; Li, C. Enantioselective Diels-Alder Reactions with G-quadruplex DNA-Based Catalysts. *Angew. Chem. Int. Ed.* **2012**, *52*, 9352-9355.
- Wang, F.; Wen, M.; Feng, K.; Liang, W.-J.; Li, X.-B.; Chen, B.; Tung, C.-H.; Wu, L.-Z. Amphiphilic Polymeric Micelles as Microreactors: Improving the Photocatalytic Hydrogen Production of the [FeFe]-Hydrogenase Mimic in Water. *Chem. Commun.* **2016**, *52*, 457-460.

- Wang, Q.; Yang, Z.; Zhang, X.; Xiao, X.; Chang, C. K.; Xu, B.; A Supramolecular-Hydrogel-Encapsulated Hemin as an Artificial Enzyme to Mimic Peroxidase. *Angew. Chem. Int. Ed.*, **2007**, *46*, 4285-4289.
- Wentworth Jr., P.; Janda, K. D. Liquid-Phase Chemistry: Recent Advances in Soluble Polymer-Supported Catalysts, Reagents and Synthesis. *Chem. Commun.* **1999**, *19*, 1917-1924.
- Wojciechowski, K.; Bitner, A.; Warszynski, P.; Zubrowska, M. The Hofmeister Effect in Zeta Potentials of CTAB-Stabilized Toluene-in-Water Emulsions. *Colloid. Surface. A* **2011**, *376*, 122-126.
- Zhou, H.; Yang, Q.; Wang, X. Spectrometric Study on the Binding of Curcumin with AOT: Effect of Micelle-to-Vesicle Transition. *Food Chemistry*, **2014**, *161*, 136-141.



## List of Publications

### [Papers]

1. Fumihiko Iwasaki, Keishi Suga, Dai Kondo, Hiroshi Umakoshi, Partitioning of Hydrophobic Molecules to Liposome Membrane Can Induce Variations of their Micro-Polarity and Micro-Viscosity. *Solvent Extr. Res. Dev., Jpn.*, **2015**, 22, 79-85.
2. Fumihiko Iwasaki, Keishi Suga, Hiroshi Umakoshi, Pseudo-Interphase of Liposome Promotes 1,3-Dipolar Cycloaddition Reaction of Benzonitrile Oxide and N-Ethylmaleimide in Aqueous Solution. *J. Phys. Chem. B*, **2015**, 119, 9772-9779.
3. Fumihiko Iwasaki, Keishi Suga, Yukihiro Okamoto, Hiroshi Umakoshi, Liposomes Can Conduct Enantioselective C-C bond formation of an  $\alpha$ -Amino Acid Derivative in Aqueous Media. *ACS Omega*, **2017**, 2, 91-97.
4. Fumihiko Iwasaki, Keishi Suga, Yukihiro Okamoto, Hiroshi Umakoshi, Characterization of DDAB/Cholesterol Vesicles and Its Comparison with Lipid/Cholesterol Vesicles. *J. Nanosci. Nanotech.*, **2017**, DOI: 10.1166/jnn.2017.14252.
5. Fumihiko Iwasaki, Keishi Suga, Yukihiro Okamoto, Hiroshi Umakoshi, Enantioselective C-C Bond Formation Enhanced by Self-Assembly of Achiral Surfactants. *ACS Omega*, in press.

### [Related Papers]

1. Sandra Luginbuhl, Fumihiko Iwasaki, Elizabeth Chirackal Verkey, Hiroshi Umakoshi, Peter Walde, A Novel Role of Vesicles as Templates for the Oxidation and Oligomerization of N-Phenyl-1,4-phenylenediamine by Cytochrome c. *Helvetica Chimica Acta*, in press.
2. Fumihiko Iwasaki, Sandra Luginbuhl, Keishi Suga, Peter Walde, Hiroshi Umakoshi, Fluorescent Probe Study of the AOT Vesicle Membrane and Their Alteration upon Addition of Aniline or the Aniline Dimer p-Aminodiphenylamine (PADPA). *Langmuir*, **2017**, DOI: 10.1021/acs.langmuir.6b04480

### [International Conference / Symposium]

1. Fumihiko Iwasaki, Keishi Suga, Hiroshi Umakoshi, Adsorptive Behavior of Substrates and Regulation of Cycloaddition using Cationic Liposome. Next Symposium "Membranome" for "Bio-Inspired Chemical Engineering", Osaka, Japan, September (2013)

2. Fumihiko Iwasaki, Keishi Suga, Yukihiro Okamoto, Hiroshi Umakoshi, Design of "bio-inspired mambrane" as a platform for molecular recognition and conversion. The 10th International Congress on Membranes and Membrane Processes, Suzhou, China, July (2014)
3. Fumihiko Iwasaki, Keishi Suga, Yukihiro Okamoto, Hiroshi Umakoshi, Design of Liposome Membrane as a Platform for Recognition of Hydrophobic Molecules and Their Conversion. 10th Int'l Conference on Separation Science and Technology, Nara, Japan, October (2014)
4. Fumihiko Iwasaki, Keishi Suga, Yukihiro Okamoto, Hiroshi Umakoshi, Design of Liposome Membrane as a Platform for Recognition of Hydrophobic Molecules and Their Conversion. The 1st International Symposium on Interactive Materials Science Cadet Program, Osaka, Japan, November (2015)
5. Fumihiko Iwasaki, Keishi Suga, Yukihiro Okamoto, Hiroshi Umakoshi, Evaluation and Control of Chemical Reaction on Surface of Self-Assembly. International Symposium on Engineering Science, Singapore, May (2015)
6. Fumihiko Iwasaki, Keishi Suga, Yukihiro Okamoto, Hiroshi Umakoshi, Design of Phospholipid Bilayer Membranes as a Platform for Chemical Reactions in Water. The 21th Symposium of Young Asian Biochemical Engineers' Community, Chuncheon, Korea, October (2015)
7. Fumihiko Iwasaki, Keishi Suga, Yukihiro Okamoto, Hiroshi Umakoshi, Liposome membrane can act as a platform for organic synthesis. Pacifichem 2015, Hawaii, United States, December (2015)
8. Fumihiko Iwasaki, Keishi Suga, Yukihiro Okamoto, Hiroshi Umakoshi, Characterization of AOT Vesicle as a Platform for Interfacial Reaction. The 10th Conference of Aseanian Membrane Society, Nara, Japan, July (2016)

**[Article / Review]**

1. Fumihiko Iwasaki, Variations in the Micro-Polarity and Micro-Viscosity of the Surface of Liposome Membrane Induced by the Partitioning of Hydrophobic Molecules (in Japanese), *Bunri Gijutsu*, **2014**, *44*, 5.
2. Fumihiko Iwasaki, Characterization of Alcohol Modified AOT Vesicle Membrane and Its Application to the Polymerization of PADPA (in Japanese), *Membrane*, **2016**, *41*, 4.

## Acknowledgements

The author is greatly indebted to Prof. Dr. Hiroshi Umakoshi (Division of Chemical Engineering, Graduate School of Engineering Science, Osaka University), for his excellent guidance and helpful advice and supports throughout this work. The author is thankful to Prof. Dr. Koichiro Jitsukawa, Prof. Dr. Nobuyuki Matsubayashi, Prof. Dr. Norikazu Nishiyama (Division of Chemical Engineering, Graduate School of Engineering Science, Osaka University) for a number of valuable comments and suggestions during the completion of this thesis. The author would like to offer my special thanks to Assist. Prof. Dr. Keishi Suga (Division of Chemical Engineering, Graduate School of Engineering Science, Osaka University) for a huge support on my research. The author also would like to offer special thanks Assoc. Prof. Dr. Yukihiro Okamoto, Assoc. Prof. Dr. Tomoo Mizugaki (Division of Chemical Engineering, Graduate School of Engineering Science, Osaka University), and Assoc. Prof. Dr. Toshinori Shimanouchi (Division of Environmental Science, Graduate School of Environmental and Life Science, Okayama University), and for his valuable comments, and helpful advises. The author would like to express one's thankfulness to Ms. Keiko Fukumoto for her kind support during this work.

The author would like to show my greatest appreciation to Prof. Dr. R. Kuboi, Prof. Dr. K. Ohgaki, Prof. Dr. Y. Inoue, (Honored Professor of Osaka University). The author is thankful to Prof. Dr. M. Taya, Prof. Dr. Y. Okano, Prof. Dr. M. Nakano, Prof. Dr. T. Hirai, Prof. Dr. S. Sakai, and all the staff of Division of Chemical Engineering, Graduate School of Engineering Science, Osaka University for their kind cooperation during my research.

The author wishes to thank for Prof. Dr. P. Walde (Institute for Polymer, ETH, Zurich), Prof. Dr. B. Higgins (Department of Chemical Engineering and Materials Science, University of California, Davis), Prof. Dr. P. Alexandridis (Department of Chemical Engineering, University at Buffalo), Prof. Dr. Ho-Sup Jung (Department of Mechanical and Aerospace Engineering, Seoul National University), Prof. Dr. S. Ichikawa (Graduate School of Life and Environmental Sciences, University of Tsukuba), Prof. Dr. H. Nakamura (Department of Chemical Engineering, National Institute of Technology, Nara College), Prof. Dr. M. Konno (Department of Applied Chemistry, Tohoku University) for their comments and suggestions during this work. The author is grateful for the advice given by Assoc. Prof. Dr. A. Heyden (Department of Chemical Engineering, University of South Carolina), Assoc. Prof. Dr. K. Kato (Department of Materials Science and Biotechnology, Graduate School of Science and Engineering, Ehime University), Assoc. Prof. Dr. K. Shiomori (Department of Applied Chemistry, University of Miyazaki), Assoc. Prof. Dr. D. Nagao (Department of Applied Chemistry, Tohoku University), Assoc. Prof. Dr. M. Yoshimoto (Department of Applied Molecular Bioscience, Yamaguchi University), Assoc. Prof. Dr. S. Morita (Department of Material Science, Wakayama National College of Technology), Assist. Prof. Dr. N. Yoshimoto (Graduate School of Medicine, Yamaguchi University), Assist. Prof. Dr. H. Ishii (Tohoku University), Assist. Prof. Dr. K. Hayashi (National Institute of Technology), Dr. V. T. Huong (Hanoi National University of Education), Dr. H. Sugaya (Toray Industries, inc.), Dr. Y. Yamada (Kao corporation).

Special thanks are given to following colleagues for their experimental collaboration: T. Ishigami, S. Tanaka, T. Tatsui, T. Yokoi, J. Chinzaka, T. Hinoyama, N. Maruyama, K. Sugita, M. Hirose, M. Kiriishi, D. Kondo, Y. Takaya, Y. Kaneko, T. Bando, T. Katsura, S. Taguchi, K. Goshima, A. Hamasaki, M. Kota, Y. Tsujimoto, T. Yoshida, B. T. Tham, Y. Kishi, K. Akizaki, Y. Higashie, T. Ikeda, N. Watanabe, R. Matsuba, Y. Mine, Y. Otsuka, Y. Shinozuka, S. Sugisaki, A. Tauchi, D. Wada, J. Han, K. Midogochi, R. Ito, T. Wakita, Y. Ooe, R. Kawakami, R. Kawakami, R. Nishino, K. Yoshida, K. Tanimura, M. S. Chern, C. Lishi, C. Tran, A. Ajaikumar, R. Wakerlin, M. F. Salim, Y.-C. Lai, and all the member in Bio-Inspired Chemical Engineering Laboratory. The author also would like to show appreciation to S. Luginbuhl, A. Kuchler, X. Sun, E. C. Verkey, and all the members in the group of polymer chemistry, Department of Materials, ETH Zurich for kind helps during my research stay in ETH Zurich.

The author would like to thank his parents Nobuhiko Iwasaki and Yuka Iwasaki and his brother and sister Masashi Iwasaki and Yuki Iwasaki for their continuous encouragements and kind support throughout this work.

The author gratefully acknowledges the financial support of this work by the fellowship of the Japan Society for the Promotion of Science (JSPS).